Prog. Aerospace Sci. Vol. 26, pp. 1–77, 1989.
Printed in Great Britain.

0376–0421/89 $0.00 + 0.50

ESTIMATION OF AIRCRAFT AERODYNAMIC PARAMETERS FROM FLIGHT DATA

VLADISLAV KLEIN

The George Washington University JIAFS/NASA LaRC, Hampton, VA 23665-5225, U.S.A.

(*Received 18 July 1988*)

Abstract—Several ways for obtaining aerodynamic parameters of an aircraft from flight data are presented with the emphasis on present problem areas. The paper starts with a brief description of data analysis from steady measurements. Then, a concept of system identification applied to aircraft is introduced with a discussion of various steps in this procedure. This is followed by a formulation of a mathematical model of an aircraft with aerodynamic forces and moments approximated either by polynomials or splines. The main part contains a rather detailed treatment of two more often used techniques for parameter estimation. The first method is based on linear regression which can be extended to a stepwise regression for model structure determination and to data handling procedure, known as data partitioning. The second technique applies the maximum likelihood principle to measured data. In this part, mainly the output error estimation method is considered. The problem of near linear relationship among measured time histories is mentioned in a separate section together with some diagnostic measures and two estimation techniques dealing with this problem. Because of a renewed interest in the frequency domain analysis, one section of the paper is devoted to this problem. All the methods explained in the paper are demonstrated in several examples using real flight data.

CONTENTS

NOTATION 1
1. INTRODUCTION 3
2. ANALYSIS OF DATA FROM STEADY MEASUREMENTS 4
   2.1. Basic relationships from the theory of static longitudinal stability and control 4
   2.2. Interpretation of flight test data 6
   2.3. Accuracy of estimated derivatives 10
   2.4. Examples 11
3. SYSTEM IDENTIFICATION APPLIED TO AIRCRAFT 12
   3.1. Design of an experiment 15
   3.2. Data compatibility check 19
   3.3. Model structure determination and parameter estimation 21
   3.4. Model verification 24
4. MATHEMATICAL MODEL OF AN AIRCRAFT 24
5. LINEAR REGRESSION USED IN PARAMETER ESTIMATION AND MODEL STRUCTURE DETERMINATION 28
   5.1. Least squares estimates 29
   5.2. Stepwise regression 30
   5.3. Data partitioning 32
   5.4. Examples 34
6. MAXIMUM LIKELIHOOD METHOD FOR PARAMETER ESTIMATION 45
   6.1. System with process noise 47
   6.2. Output error method 53
   6.3. Examples 55
7. DATA COLLINEARITY AND BIASED ESTIMATION 58
   7.1. Principal components regression 64
   7.2. Mixed estimation 65
   7.3. Example 65
8. PARAMETER ESTIMATION IN FREQUENCY DOMAIN 68
   8.1. Example 71
9. CONCLUDING REMARKS 75
ACKNOWLEDGEMENTS 75
REFERENCES 75

NOTATION

Only the main and the most frequently used symbols which have a global use are introduced. Some of these symbols may have another local meaning. The other symbols are explained in the body of the paper and in Figs 1 and 2.

A—system matrix
$a_{x,y,z}$—longitudinal, lateral and vertical accelerations, g units or m/s^2
B—control matrix
b—wing span
C, D—transformation matrices in the output equation
C_{h_e}—elevator hinge-moment coefficient
C_L—lift coefficient
$C_{l,m,n}$—rolling-, pitching-, and yawing-moment coefficient
$C_{X,Y,Z}$—longitudinal-, lateral-, and vertical-force coefficient
Cov$\{\cdot\}$—covariance matrix
$\bar{c}$—wing mean aerodynamic chord, m
E$\{\cdot\}$—expected value
g—acceleration due to gravity, m/s^2
H—matrix of sensitivities
J—cost function
M—Fisher information matrix
m—mass, kg
N—number of data points
n—number of unknown parameters
p, q, r—roll, pitch, and yaw rates, rad/s or deg/s
S—wing area, m^2
s—standard error
s^2—estimated variance
T—thrust, N
t—time, s
u—output vector
V—airspeed, m/s
$V_{x,y,z}$—longitudinal-, lateral-, and vertical-airspeed components, m/s
$\bar{V}$—tail volume, $S_t l / S\bar{c}$
v—measurement-noise vector
w—process-noise vector
X—matrix of independent variables
x—(a) state vector
(b) independent variable in regression equation
Y—vector of dependent variables
y—(a) output vector
(b) dependent variable in regression equation
z—vector of measured outputs
α—angle of attack, rad or deg
β—sideslip angle, rad or deg
δ_a, δ_e, δ_r—aileron, elevator, and rudder deflections, rad or deg
δ_c, δ_f, δ_s—canard, flaperon and strake deflections, rad or deg
ε—(a) equation error
(b) downwash angle, rad or deg
ϕ, θ, ψ—roll, pitch, and yaw angles, rad or deg
θ—vector of unknown parameters
v—residual
ρ—air density, kg/m^3
σ^2—variance of measurement noise
ω—vector of angular velocities
$\tilde{\omega}$—skew symmetric matrix of angular velocities

Subscripts

0—initial conditions
t—tail
v—vane
w—wing-body

Superscripts

T—transpose matrix
-1—inverse matrix

Abbreviations

LS—least squares
ML—maximum likelihood
MSE—mean square error
MSR—modified stepwise regression
PRESS—prediction sum of squares
SVD—singular value decomposition

Aerodynamic derivatives referenced to a system of body axes (see Fig. 1).

$$C_{a_q} = \frac{\partial C_a}{\partial \frac{q\bar{c}}{2V}}, \quad C_{a_\alpha} = \frac{\partial C_a}{\partial \alpha}, \quad C_{a_\delta} = \frac{\partial C_a}{\partial \delta}$$

for $a = L$, X, or Z and $\delta = \delta_e$, δ_c, δ_f, or δ_s

$$C'_{m_q} = \frac{\partial C_m}{\partial \frac{q\bar{c}}{2V}}, \quad C'_{m_\alpha} = \frac{\partial C_m}{\partial \alpha}, \quad C'_{m_{\delta_e}} = \frac{\partial C_m}{\partial \delta_e}, \quad C_{m_{\dot{\alpha}}} = \frac{\partial C_m}{\partial \frac{\dot{\alpha}\bar{c}}{2V}}$$

C_{m_q}, C_{m_α}, and $C_{m_{\delta_c}}$ defined by Eq. (4.6).

$$C_{a_p} = \frac{\partial C_a}{\partial \frac{pb}{2V}}, \quad C_{a_r} = \frac{\partial C_a}{\partial \frac{rb}{2V}}, \quad C_{a_\beta} = \frac{\partial C_a}{\partial \beta}$$

$$C_{a_{\delta_a}} = \frac{\partial C_a}{\partial \delta_a}, \quad C_{a_{\delta_r}} = \frac{\partial C_a}{\partial \delta_r} \quad \text{for } a = Y, l, \text{ or } n.$$

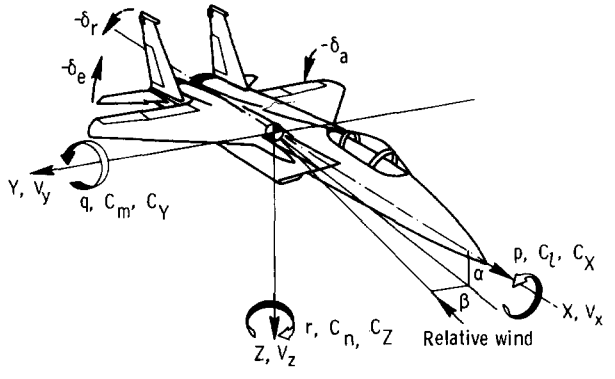

FIG. 1. Model characterization.

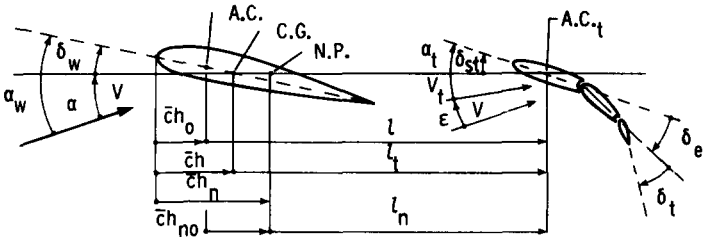

FIG. 2. Some geometrical characteristics of an aircraft.

1. INTRODUCTION

During the last several years computational methods and wind-tunnel testing have been refined in such a way that they can provide in many instances comprehensive data about aerodynamic characteristics of an aircraft. There are still, however, several reasons why the determination of aerodynamic parameters from flight data forms a very important part of flight test data analysis. They include:

1. requirements for better understanding of theoretical predictions and wind-tunnel testing and the possibility of deeper understanding of aerodynamic phenomena and their relationship to aircraft stability and control,
2. robustness of wind-tunnel data for actual flight environments,
3. requirements for better stability augmentation and flight control systems,
4. requirements for simulators which need to be a more accurate representation of the aircraft in all flight regimes.

In the past only limited information about aircraft aerodynamics was obtained from measurements in steady symmetric and turning flights. One of the first approaches for obtaining static and dynamic parameters from flight data was given by Milliken[52] in 1947. He used frequency response data and a simple semi-graphical method for the analysis. Four years later Greenberg[22] and Shinbrot[64] established more general and rigorous ways for determining aerodynamic parameters from transient maneuvers. In these reports they introduced parameter estimation methods based on the application of ordinary and non-linear least squares.

Improvements in aircraft parameter estimation techniques came in the late sixties and early seventies because of the availability of digital computers and progress in the new technical discipline known as system identification. Based upon both developments researchers are now able to determine from one test run the model structure of aerodynamic equations and to estimate all or almost all parameters involved, together with their accuracies. At the same time the accuracy of measured data is also estimated so that the data can be used in the analysis with a corresponding level of confidence. If necessary, there is a possibility to separate the measurement noise in the output variables from external disturbances to the system caused by gust wind effects or modeling errors. The identification techniques give the opportunity of including in the analysis the prior knowledge of aircraft parameters obtained from wind-tunnel measurements and/or previous flight measurements. The identification methods also provide a tool for obtaining more accurate data by reconstructing some output variables and estimating bias errors in measured data. Finally, system identification approach to data analysis addresses a problem of an optimal input form used for excitation of aircraft maneuvers which can lead to more accurate parameter estimates.

Substantial contributions in the field of aircraft identification were made by several authors in Refs 20, 25, 28, 51, 65 and 66. Besides these contributions the merits of NASA as an organization should be mentioned as well. In this establishment the new techniques of system identification have found very positive acceptance and applications to many different

types of aircraft. The other two organizations, NATO Advisory Group for Aerospace Research and Development (AGARD) and American Institute for Aerospace and Aeronautics (AIAA) have also played very constructive roles in the exchange of information and results, and in the education of aeronautical engineers and researchers in the area of aircraft identification and parameter estimation, as follows from Refs 2 and 3, and numerous papers presented at various meetings organized by both agencies.

The purpose of this paper is to continue in informing the aeronautical research community about the estimation of aircraft aerodynamic parameters from flight data with the emphasis on present problem areas. They include parameter estimation in high angle-of-attack flight regimes and identification of a highly augmented, sometimes inherently unstable aircraft. The substantial part of the paper is taken from reports and papers written by the author himself or in cooperation with his students and researchers at NASA Langley Research Center. The paper starts with a brief description of data analysis from steady measurements. Then, a concept of system identification applied to aircraft is introduced with a discussion of various steps in this procedure. This is followed by a formulation of a mathematical model of an aircraft with aerodynamic forces and moments approximated either by polynomials or splines. The main part contains a rather detailed treatment of two more often used techniques for parameter estimation. The first method is based on linear regression which can be extended for model structure determination. Because in the linear regression the time does not appear explicitly, the measured data points can be arranged in arbitrary order. This led to a data handling procedure, known as data partitioning, which can enable the analyst to obtain more detailed information about aircraft aerodynamics. The second technique applies the maximum likelihood principle to measured data. In this part mainly the output error estimation method is considered. The problem of near linear relationship among measured time histories (data collinearity) is mentioned in a separate section together with some diagnostic measures and techniques dealing with collinear data. These techniques belong to a relatively new class of biased estimation methods. Because of a renewed interest in the frequency domain analysis, one section of the paper is devoted to this problem. All the methods explained in the paper are demonstrated in several examples using real flight data. The paper is completed by concluding remarks.

2. ANALYSIS OF DATA FROM STEADY MEASUREMENTS

In this section a method for obtaining aerodynamic derivatives from steady symmetric flights is described. Basic relationships between aerodynamic coefficients and control variables are summarized and their utilization for the design of an experiment and the analysis of measured data is discussed. A general theory of static longitudinal stability and control was developed by Gates and Lyon.[18] Both authors also indicated in Ref. 19 a technique for the estimation of the static and c.g. margin, and aerodynamic characteristics of the horizontal tail from flight measurements. These results were extended in Ref. 35 to the estimation of longitudinal static stability and control derivatives and to the estimation of tail contribution to the damping derivatives. The accuracy of estimated aerodynamic derivatives is discussed in terms of the resulting standard errors or a bound on the systematic errors. The process of estimating aerodynamic derivatives is then demonstrated in two examples.

2.1. Basic Relationships From the Theory of Static Longitudinal Stability and Control

The basic relationship from the theory of static longitudinal stability and control are formulated with the following assumptions:

(1) At a given speed and Mach number C_L, C_m, C_{L_t} and C_{h_e} are linear functions of the angle-of-attack, elevator deflection and trim tab deflection,
(2) all the coefficients mentioned in assumption (1) are undetermined functions of the speed,

(3) the equilibrium conditions of $C_R V^2 = \text{constant}$ for the steady flights is simplified as $C_L V^2 = \text{constant}$,
(4) the lift and pitching moment of the whole aircraft are composed of the wing–body and tail contributions.

The non-dimensional lift and pitching moment equations for the whole aircraft have the form

$$C_L = C_{L_w} + \frac{S_t}{S} C_{L_t} \tag{2.1}$$

$$C_m = C_{m_{w0}} + C_{L_w}(h - H_0) - \frac{S_t l_t}{S\bar{c}} C_{L_t}. \tag{2.2}$$

Introducing

$$A_1 = \frac{\partial C_{L_t}}{\partial \alpha_t},\ A_2 = \frac{\partial C_{L_t}}{\partial \delta_e},\ A_3 = \frac{\partial C_{L_t}}{\partial \delta_t}$$

similarly B_1, B_2, B_3 as the derivatives of C_{h_e} with respect to the same variables, $B_0 = C_{h_e}$ where $\alpha_t = \delta_e = \delta_t = 0$, and using the linearity assumption, the coefficients C_{L_t} and C_{h_e} can be expressed as

$$C_{L_t} = A_1 \alpha_t + A_2 \delta_e + A_3 \delta_t \tag{2.3}$$

and

$$C_{h_e} = B_0 + B_1 \alpha_t + B_2 \delta_e + B_3 \delta_t \tag{2.4}$$

where the angle-of-attack at the tail is

$$\alpha_t = \alpha_w \left(1 - \frac{d\varepsilon}{d\alpha}\right) + \delta_{st} - \delta_w - \varepsilon_0. \tag{2.5}$$

Substituting Eqs (2.1), (2.3), and (2.5) into (2.2), the equation for C_m is modified as

$$C_m = C_{m_{w0}} + C_L(h - H_0) - V_T \left[C_L \frac{A_1}{A}\left(1 - \frac{d\varepsilon}{d\alpha}\right) + A_1(\delta_{st} - \delta) + A_2 \delta_e + A_3 \delta_t \right], \tag{2.6}$$

where

$$V_T = \frac{\bar{V}}{1+F} = \frac{1}{1+F}\frac{S_t l}{S\bar{c}} \tag{2.7}$$

$$F = \frac{S_t}{S}\frac{A_1}{A}\left(1 - \frac{d\varepsilon}{d\alpha}\right) \tag{2.8}$$

$$\delta = \delta_w + \varepsilon \quad \text{and} \quad A = (\partial C_L / \partial \alpha)_{\text{no tail}}.$$

The static margin stick-fixed is defined as

$$K_n = -\frac{dC_m}{dC_L} = -\frac{\partial C_m}{\partial \alpha}\frac{d\alpha}{dC_L} + \frac{V}{2C_L}\frac{\partial C_m}{\partial V}. \tag{2.9}$$

The derivative of Eq. (2.6) may be written as

$$K_n = (H_0 - h)\Psi_1 + \Psi_0, \tag{2.10}$$

where Ψ_1 and Ψ_0 are functions of C_L. A possible form of these functions is given in Ref. 18.

The neutral point stick-fixed is defined as $h_n = h$, for which $K_n = 0$. Therefore

$$h_n = H_0 + \frac{\Psi_0}{\Psi_1}$$

and then

$$h_n - h = H_n = \frac{K_n}{\Psi_1}, \tag{2.11}$$

where H_n is the so-called c.g. margin.

In the simplified theory where the values of A_1, A_2 and A_3 are independent of V

$$\Psi_1 = 1 \quad \text{and} \quad \Psi_0 = V_T \frac{a_1}{a}\left(1 - \frac{\partial \varepsilon}{\partial \alpha}\right)$$

and, consequently, $H_n = K_n$.

From Eq. (2.6) the elevator deflection required to maintain the steady-state flight is given as

$$\delta_e = \frac{1}{V_T A_2}\left\{C_{m_{wo}} + C_L(h - H_0) - V_T\left[C_L \frac{A_1}{A}\left(1 - \frac{d\varepsilon}{d\alpha}\right) + A_1(\delta_{st} - \delta) + A_3 \delta_t\right]\right\}. \tag{2.12}$$

The variation of elevator angle to the lift coefficient at trim for δ_t = constant must provide a pitching moment to balance the rate of change of pitching moment with the lift coefficient at δ_e = constant. Then, from Eq. (2.6)

$$\left(\frac{dC_m}{dC_L}\right)_{\delta_e = \text{constant}} = V_T A_2 \left(\frac{d\delta_e}{dC_L}\right)_{C_m = 0}$$

and, therefore

$$\frac{d\delta_e}{dC_L} = \frac{-K_n}{V_T A_2}. \tag{2.13}$$

Substituting Eq. (2.4) into (2.6), the expression for the stick-free trim curve is obtained as

$$C_{h_e} = \frac{B_2}{V_T^* A_2}\left\{C_{m_{wo}} - C_L(h - H_0) - V_T^*\left[C_L \frac{\bar{A}_1}{A}\left(1 - \frac{d\varepsilon}{d\alpha}\right) + \bar{A}_1(\delta_s - \delta) + \bar{A}_3 \delta_t\right]\right\}, \tag{2.14}$$

where

$$V_T^* = \frac{\bar{V}}{1 + F^*}$$

$$F^* = \frac{S_t}{S}\frac{\bar{A}_1}{A}\left(1 - \frac{d\varepsilon}{d\alpha}\right)$$

$$\bar{A}_1 = A_1 - A_2 \frac{B_1}{B_2}$$

$$\bar{A}_3 = A_3 - A_2 \frac{B_1}{B_2}.$$

The static margin with stick-free is defined as the value of $-dC_m/dC_L$ where the elevator is initially trimmed and is subsequently free. The expression for it can be found from Eqs (2.4) and (2.6). Similar to the stick-fixed case, the expression for neutral point stick-free and the corresponding c.g. margin can be developed.

2.2. Interpretation of Flight Test Data

The elevator effectiveness, stick-fixed static margin and c.g. margins can be determined from measured trim curves, $\delta_e(C_L)$, at two different c.g. positions with fixed tailplane and trim tab settings. Using Eq. (2.12) and formulating the increment $\Delta\delta_e$ due to change Δh, the

elevator effectiveness is obtained as

$$V_T A_2 = \frac{\Delta h}{\Delta \delta_e} C_L. \tag{2.15}$$

The static margin can be obtained from Eq. (2.13).

The increment in the static margin due to Δh can be expressed from Eq. (2.10) as

$$\Delta K_n = \Psi_1 \Delta h. \tag{2.16}$$

Combination of Eqs (2.13), (2.15), and (2.16) yields

$$\Psi_1 = \frac{C_L}{\Delta \delta_e} \Delta \left(\frac{d\delta_e}{dC_L} \right). \tag{2.17}$$

Then, from Eq. (2.11) and (2.17) the c.g. margin is given as

$$H_n = \frac{\Delta h}{\Delta \left(\frac{d\delta_e}{dC_L} \right)} \frac{d\delta_e}{dC_L}. \tag{2.18}$$

In Fig. 3, two possible results from measurement of $\delta_e(C_L, h)$ are schematically illustrated. In the first case there is no speed effect on the lines with the intersection on the δ_e-axis. The derivative dC_m/dC_L remains constant within the given C_L range and there is no difference between the static and c.g. margin, as follows from Eqs (2.13) and (2.18).

In the second case the speed effect is present. The measured relationships are non-linear and their tangents for a given C_L do not intersect on the δ_e-axis. The derivative dC_m/dC_L varies with the speed, consequently K_n is different from H_n. It should be emphasized, however, that the non-linear behavior of $\delta_e(C_L)$ does not necessarily mean different values for K_n and H_n. Only the tangents at a given C_L could distinguish this difference provided that during the measurement δ_{st} and δ_t were set at fixed values.

Estimation of Stability and Control Derivatives. For development of expressions for the estimation of stability and control derivatives from trim curves and $C_L(\alpha)$-curve, the simplified approach will be taken. It will be assumed that the coefficients of linearity in Eqs (2.3) and (2.4), and the values of A and H_0 are constant. These coefficients will be replaced by small letters, $a_1, a_2, \ldots, a, h_0$, assumed constant.

Differentiating Eq. (2.6) with respect to δ_e gives

$$\frac{\partial C_m}{\partial \delta_e} = \frac{\partial C_L}{\partial \delta_e} \left[h - h_0 - V_T \frac{a_1}{a} \left(1 - \frac{\partial \varepsilon}{\partial a} \right) \right] - V_T a_2. \tag{2.19}$$

Because

$$\frac{\partial C_L}{\partial \delta_e} = \frac{S_t}{S} \frac{\partial C_{L_t}}{\partial \delta_e}$$

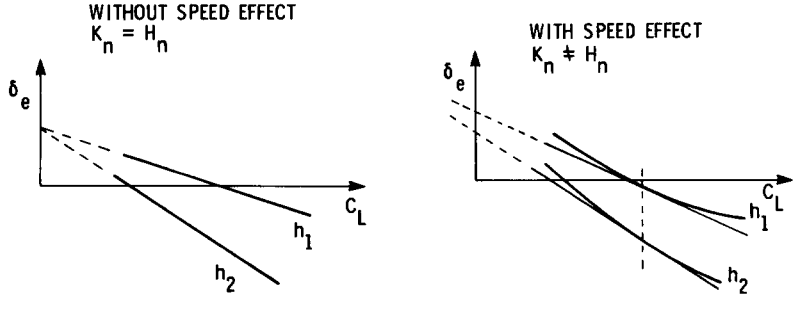

FIG. 3. Illustration of typical measured trim curves at two different c.g. positions with and without speed effect.

then from Eq. (2.2)

$$\frac{\partial C_m}{\partial \delta_e} = -\frac{\partial C_L}{\partial \delta_e}\frac{l_t}{\bar{c}} \tag{2.20}$$

From Eqs (2.19) and (2.20) the expressions for two control derivatives follow as

$$C'_{m_{\delta_e}} = \frac{-V_T a_2}{1-\frac{\bar{c}}{l_t}H_n} \tag{2.21}$$

and

$$C_{L_{\delta_e}} = -\frac{\bar{c}}{l_t}C'_{m_{\delta_e}}. \tag{2.22}$$

The derivative C_{L_α} can be determined from the slope of measured relationship $C_L(\alpha, \delta_e)$. In steady flight

$$\begin{aligned} C_L(\alpha=0)+C_{L_\alpha}\alpha+C_{L_{\delta_e}}\delta_e &= C_{L_{trim}} \\ C_m(C_L=0)+C'_{m_\alpha}\alpha+C'_{m_{\delta_e}}\delta_e &= 0. \end{aligned} \tag{2.23}$$

Solving (2.23) for $C_{L_{trim}}$ and differentiating with respect to α yields

$$C_{L_\alpha} = \frac{dC_L}{d\alpha} + \frac{C_{L_{\delta_e}}}{C'_{m_{\delta_e}}}C'_{m_\alpha}, \tag{2.24}$$

where the value of $dC_L/d\alpha$ represents the slope of the trimmed polar curve, whereas C_{L_α} is the slope of the basic curve $C_L(\alpha)$ for $\delta = 0$.

Differentiation of Eq. (2.6) with respect to α gives

$$\frac{\partial C_m}{\partial \alpha} = \frac{\partial C_L}{\partial \alpha}\left[h - h_0 - V_T\frac{a_1}{a}\left(1-\frac{\partial \varepsilon}{\partial \alpha}\right)\right]. \tag{2.25}$$

For $\partial C_m/\partial\alpha = 0$ there is $h = h_n$ and

$$h_n = h_0 + V_T\frac{a_1}{a}\left(1-\frac{\partial \varepsilon}{\partial \alpha}\right). \tag{2.26}$$

Then, from Eqs (2.25) and (2.26)

$$C'_{m_\alpha} = -C_{L_\alpha}H_n. \tag{2.27}$$

Estimation of Tail Contribution of Damping Derivatives. If the measured trim curves are available at two values of h and δ_{st}, then it is possible to estimate the tail contribution to the derivatives C'_{m_q} and $C'_{m_{\dot{\alpha}}}$. These contributions are usually approximated as

$$(C'_{m_q})_t = -2a_1\frac{S_t}{S}\left(\frac{l_t}{\bar{c}}\right)^2, \tag{2.28}$$

and

$$(C'_{m_{\dot{\alpha}}})_t = -2a_1\frac{S_t}{S}\left(\frac{l_t}{\bar{c}}\right)^2\frac{\partial \varepsilon}{\partial \alpha}, \tag{2.29}$$

and are, therefore, determined by two aerodynamic characteristics a_1 and $\partial\varepsilon/\partial\alpha$.

Considering the increment $\Delta\delta_e$ due to $\Delta\delta_{st}$ it follows from Eq. (2.12) that

$$\frac{A_1}{A_2} = -\frac{\Delta\delta_e}{\Delta\delta_{st}}. \tag{2.30}$$

For the explicit determination of A_1, however, the value of the modified tail volume V_T must be known. As indicated by Eq. (2.7), the value of V_T not only depends on geometrical characteristics but also on the aerodynamic ones which are not known in advance.

To remove this disadvantage, a new expression for V_T will be developed. As indicated by Eq. (2.25), the c.g. margin is given by the expression

$$H_n = h_0 - h_n + V_T \frac{a_1}{a}\left(1 - \frac{\partial \varepsilon}{\partial \alpha}\right),$$

from which

$$\frac{a_1}{a} = \frac{h_n - h_0}{\frac{S_t}{S}\frac{l}{\bar{c}}\left(1 - \frac{\partial \varepsilon}{\partial \alpha}\right)}(1+F). \tag{2.31}$$

Then Eqs (2.8) and (2.31) give

$$F = \frac{\bar{c} h_{n0}}{l_n}, \tag{2.32}$$

where the distance $\bar{c}h_{n0}$ and l_n are shown in Fig. 2. Now, for the estimates of F and V_T, the aerodynamic center of an aircraft without tail must be found first.

A possibility for this is given by the measured trim curves $\delta_e(C_L, h, \delta_{st})$ and $C_{h_e}(C_L, h, \delta_{st})$. From Eqs (2.12) and (2.14) the following expression can be developed

$$\left(\frac{\Delta \delta_e}{\Delta C_{h_e}}\right)_{\Delta \delta_{st} = \text{constant}} \times \left(\frac{dC_{h_e}}{dC_L}\right)_{h=h_0} + \left(\frac{d\delta_e}{dC_L}\right)_{h=h_0} = 0 \tag{2.33}$$

where $\Delta\delta_e$ and ΔC_{h_e} are the increments due to $\Delta\delta_{st}$. The increment $\Delta\delta_{st}$ is a difference in tail setting for the measurement of both trim curves. Having found the slopes of the trim curves for several (at least two) values of h, and using Eq. (2.33), the value of h_0 can be obtained. When the estimates of F and a_1 are known, the slope of the downwash angle at the tail can also be estimated. From Eqs (2.1) and (2.8)

$$\frac{\partial \varepsilon}{\partial \alpha} = 1 - \frac{F}{1+F}\frac{S}{S_t}\frac{C_{L_\alpha}}{a_1}. \tag{2.34}$$

Estimation of Speed Effect on C_L and C_m. The consideration of the speed effect on the coefficient C_L and C_m can formally include the high-speed effects and also a phenomenon which has nothing to do with high speed, the effect of slipstream or jets.

Assuming the speed effect, $C_L = C_L(\alpha, V)$ and

$$\frac{dC_L}{d\alpha} = C_{L_\alpha} - \frac{V}{2C_L}\frac{\partial C_L}{\partial V}\frac{dC_L}{d\alpha}. \tag{2.35}$$

From Eqs (2.9) and (2.35) the static margin can be expressed as

$$K_n = k_V H_n + \frac{V}{2C_L}\frac{\partial C_m}{\partial V}, \tag{2.36}$$

where

$$k_V = 1 + \frac{V}{2C_L}\frac{\partial C_L}{\partial V}. \tag{2.37}$$

Then, from Eq. (2.36)

$$\frac{\partial C_m}{\partial V} = \frac{2C_L}{V}(K_n - k_V H_n). \tag{2.38}$$

This relationship indicates that the value of the derivative $\partial C_m/\partial V$ can be found as a difference between the estimates of K_n and H_n provided this difference is significant with respect to the accuracy of measured trim curves.

The effect of $\partial C_L/\partial V$ is usually neglected. It can be pronounced at transonic speeds or on aircraft with strong propeller effects on C_L. The estimate of the derivative $\partial C_L/\partial V$ might also be obtained from steady-state measurements.

Considering $C_L(\alpha, V, \delta_e)$, then the differential dC_L is given as

$$dC_L = C_{L_\alpha}\, d\alpha + C_{L_{\delta_e}}\, d\delta_e + \frac{\partial C_L}{\partial V}\, dV.$$

From this expression it follows that

$$\frac{\partial C_L}{\partial V} = \frac{2C_L}{V}\left[\frac{d\alpha}{dC_L}\left(\frac{dC_L}{d\alpha}\right)_V - 1\right] \tag{2.39}$$

and

$$\frac{dC_L}{d\alpha} = \frac{dC_L}{dV}\frac{dV}{d\alpha} \approx -\frac{C_L}{V}\left[\left(\frac{dV}{d\alpha}\right)_{H_1} + \left(\frac{dV}{d\alpha}\right)_{H_2}\right], \tag{2.39}$$

where H_1 and H_2 indicate two different altitudes. Then

$$\left(\frac{dC_L}{d\alpha}\right)_V \approx \frac{C_{L_2} - C_{L_1}}{\alpha_2 - \alpha_1}. \tag{2.40}$$

This approach is schematically shown in Fig. 4.

2.3. Accuracy of Estimated Derivatives

For the assessment of the developed procedure the accuracy of the estimated aerodynamic derivatives should be determined. The formula for the derivative estimates are algebraic expressions containing, in general, known constants, and directly or indirectly measured quantities. The resulting errors can be, therefore, determined by the application of the 'law of propagation of errors'.

Considering a functional relationship

$$w = f(x, y), \tag{2.41}$$

where the estimates of the mean values $\hat{x}$ and $\hat{y}$, and their variances $s^2(\hat{x})$ and $s^2(\hat{y})$ are known. Then, for the uncorrelated measurements of x and y, the variance of $\hat{w}$ is given as

$$s^2(\hat{w}) \approx \left(\frac{\partial f}{\partial x}\right)^2_{x=\hat{x}} s^2(\hat{x}) + \left(\frac{\partial f}{\partial y}\right)^2_{y=\hat{y}} s^2(\hat{y}). \tag{2.42}$$

The overall systematic error of $\hat{w}$ cannot be determined. There is, however, at least a possibility for finding a bound on this error. For the functional relationship, Eq. (2.41), a bound $|\Delta w|$ for the systematic error in $\hat{w}$ can be approximated as

$$|\Delta w| \approx \left|\left(\frac{\partial f}{\partial x}\right)_{x=\hat{x}} \Delta x\right| + \left|\left(\frac{\partial f}{\partial y}\right)_{y=\hat{y}} \Delta y\right|, \tag{2.43}$$

assuming that the systematic errors of Δx and Δy are small. This formula usually gives

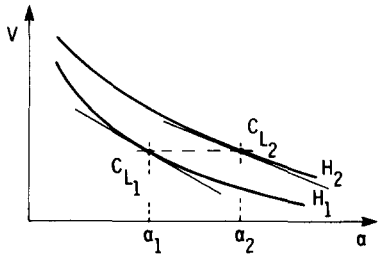

FIG. 4. Scheme for the estimation of $\partial C_L/\partial V$ derivative.

conservative estimates because it ignores a possibility that the systematic errors in measured data might have different signs and, therefore, some of these errors can cancel each other to a certain extent.

Equations (2.42) and (2.43) can also be used for the specification of the accuracy of measured data, if a specified accuracy of the aerodynamic derivatives is to be achieved.

2.4. Examples

The substantial part of the technique for the estimation of aerodynamic derivatives from steady-state measurement is demonstrated in two examples.[35] In the first example the measured data from a light, single engine, low wing aircraft with all-movable tail was used for the estimation of the static aerodynamic derivatives and the damping derivatives due to tail. In the second example, only the aerodynamic center of an aircraft without tail and the rate of downwash angle at the tail were determined from the flight data from a light, twin engine, low wing aircraft.

Example 2.1. The aircraft used in the experiment had the following characteristics

$$m = 1074 \text{ kg} \quad \bar{c} = 1.62 \text{ m}$$
$$S = 14.9 \text{ m}^2 \quad l_t = 4.2 \text{ m (for } h = 0.2125)$$
$$S_t = 2.32 \text{ m}^2 \quad \bar{c}h_0 = 0.308 \text{ m}.$$

The measured and fitted $C_L(\alpha)$ and $\delta_e(C_L)$ curves are presented in Fig. 5 and Fig. 6. From these measurements the average value of $V_T a_2$ was found equal to 1.1173, the stick-fixed

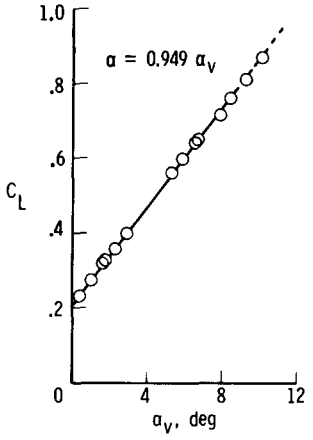

FIG. 5. Measured and fitted lift coefficient against angle-of-attack. Single engine aircraft.

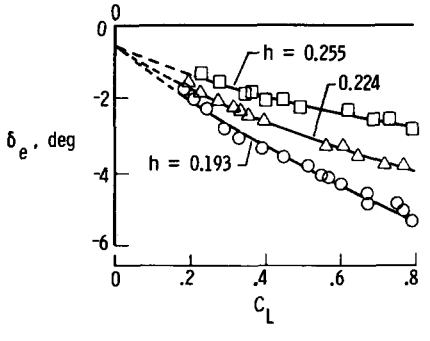

FIG. 6. Measured and fitted elevator deflection against lift coefficient. Single engine aircraft.

neutral point $h_n = 0.309$, and the slope of the $C_L(\alpha)$ line equal to 4.08. The static stability and control derivatives were determined from Eqs (2.21), (2.22), (2.24), and (2.27). For the estimation of C_{m_q} due to tail, it was assumed that $a_1 = a_2$. The value of h_0 was estimated from the geometrical characteristics of the aircraft. Then, the tail volumes were calculated from Eqs (2.7) and (2.32) as $\bar{V} = 0.4075$, $F = 0.062$, $V_T = 0.3837$. Using Eq. (2.28) and the value for $a_1 = 2.91$, the value of damping derivative ($C'_{m_{qt}}$) became -6.1.

The estimated derivatives and their standard errors are summarized in Table 1 and compared with the maximum likelihood estimates from transient maneuvers.[13] The maximum likelihood estimates and their standard errors are the sample values from eight repeated runs for the same flight conditions. The comparison indicates very good agreement in the C_{L_α} values. The pitching moment derivatives agree reasonably well if the large errors of these derivatives from the steady-state data are taken into consideration. The large standard errors mentioned are due to inaccurate measurements of the trim curves, as indicated by the scatter of measured points in Fig. 6.

Example 2.2. The main aircraft characteristics were

$$m = 1480 \text{ kg} \qquad S_e = 1.28 \text{ m}^2$$

$$S = 17.09 \text{ m}^2 \qquad \bar{c} = 1.48 \text{ m}$$

$$S_t = 3.31 \text{ m}^2 \qquad l_t = 4.81 \text{ m (for } h = 0.228).$$

The measured and fitted stick-fixed and stick-free trim curves are presented in Fig. 7 and Fig. 8. These data were measured at idle power in the 'saw-tooth' flights for three values of the c.g. positions and two tailplane settings. In Fig. 9 the slopes $\mathrm{d}\delta_e/\mathrm{d}C_L$ and $\mathrm{d}C_{h_e}/\mathrm{d}C_L$ which, multiplied by the ratio

$$(\Delta\delta_e/\Delta C_{h_e})_{\Delta\delta_{st} = \text{constant}}$$

are plotted as a function of h. The plotted points were fitted by straight lines and the correction for the unbalanced elevator was applied. The intersection of the two lines is the solution of Eq. (2.33) and gives the estimate of the aerodynamic center of the aircraft without the tail as $h_0 \approx 0.21$. This graphical solution indicates that a small inaccuracy in the data might have a large effect on the position of the intersection and thus on the accuracy of the h_0 estimate.

For the known value of h_0 it was possible to find the value of the parameter $F = 0.075$. Further, from the $\delta_e(C_L)$ measurement the quantities $V_T a_2 = 1.241$ and $a_1/a_2 = 1.437$ were determined. Finally, from the measured $C_L(\alpha)$ curve the derivative $C_{L_\alpha} = 5.09$ was found. Then, using Eq. (2.34), the rate of change of the downwash angle at the tail was estimated. The estimated values of h_0 and $\partial\varepsilon/\partial\alpha$ are compared with those determined from geometrical characteristics using diagrams.[1]

Characteristics	Flight data	Reference 1
h_0	0.21	0.182
$\partial\varepsilon/\partial\alpha$	0.39	0.365

The above results indicate the feasibility of the estimation of both characteristics from the steady data using only measured trim curves and $C_L(\alpha)$ curve. The accuracy assessment of these characteristics, however, will need more detailed comparison with the theoretical and wind-tunnel values.

3. SYSTEM IDENTIFICATION APPLIED TO AIRCRAFT

System identification has been developed as a strategy and technique for establishing the properties of a dynamic system by the measurement of its input and output time histories. One of the first definitions of system identification was given by Zadeh[71] as "Identification

TABLE 1. COMPARISON OF ESTIMATED AERODYNAMIC DERIVATIVES FROM STEADY-STATE AND TRANSIENT FLIGHT DATA. SINGLE ENGINE AIRCRAFT

	Steady-state data		Transient data	
Derivative	Mean value	Standard error	Mean value	Standard error
C_{L_α}	4.22	0.11	4.32	0.15
$C_{L_{\delta_e}}$	0.448	0.087	0.583	0.054
C'_{m_α}	−0.407	0.090	−0.461	0.011
$C'_{m_{\delta_e}}$	−1.16	0.23	−1.51	0.14
C'_{m_q}	−6.7*	—	−7.7	1.3

*$C'_{m_q} \approx 1.1(C'_{m_q})_t$.

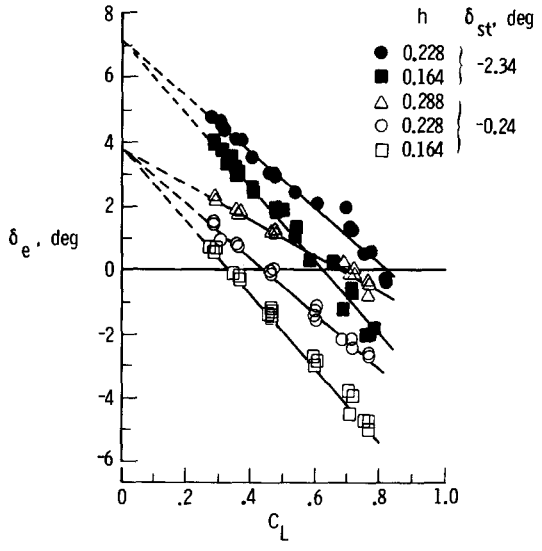

FIG. 7. Measured and fitted elevator deflection against lift coefficient. Twin engine aircraft.

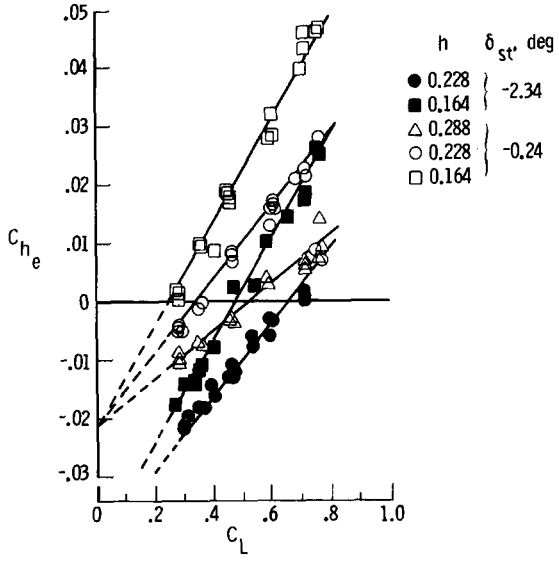

FIG. 8. Measured and fitted elevator hinge moment coefficient against lift coefficient. Twin engine aircraft.

is the determination, on the basis of input and output, of a system within a specified class of systems to which the system under test is equivalent."

During the development of system identification several different approaches and methods have been proposed and tested. Their review may be found in a survey paper by

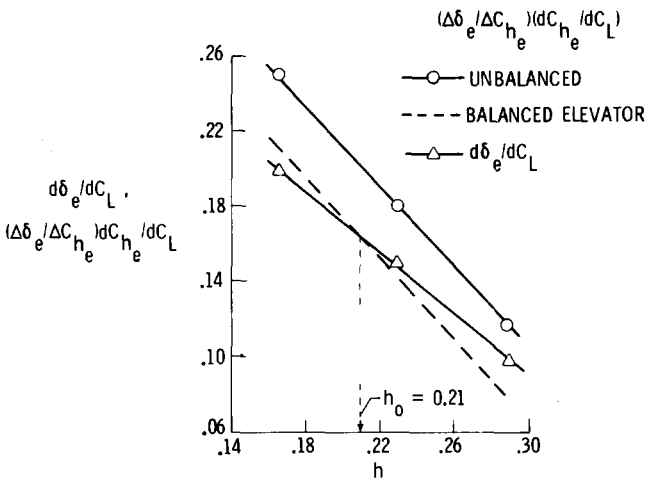

FIG. 9. Estimation of neutral point of an aircraft without tail from measured trim curves. Twin engine aircraft.

Astrom and Eykhoff.[5] When system identification is applied to an aircraft as a dynamic system the equations governing its motion are postulated and the measurements of its input and output variables are given. The equations of motion include the force and moment equations

$$m\dot{V}+m\tilde{\omega}V=F(\theta) \tag{3.1}$$

$$I\dot{\omega}+\tilde{\omega}I\omega=G(\theta), \tag{3.2}$$

and a set of kinematic equations relating the Euler angles and angular velocities. In these equations the vectors F and G represent external forces and moments and θ are parameters which specify aerodynamic characteristics of the aircraft. The aircraft identification can be stated as the determination, from input and output measurements, of a structure of F and G and estimation of parameters θ in F and G. In many practical cases the aerodynamic forces and moments are approximated by linear terms in their Taylor series expansion, a well known approach leading to stability and control derivatives. Then, the structure of F and G is known and aircraft identification is reduced to a parameter estimation problem.

A general approach to aircraft identification is shown in Fig. 10 in the form of a block diagram. Various steps in the procedure include the design of an experiment, measured data compatibility check, model structure determination and parameter estimation, and model verification. A brief description of these steps follows.

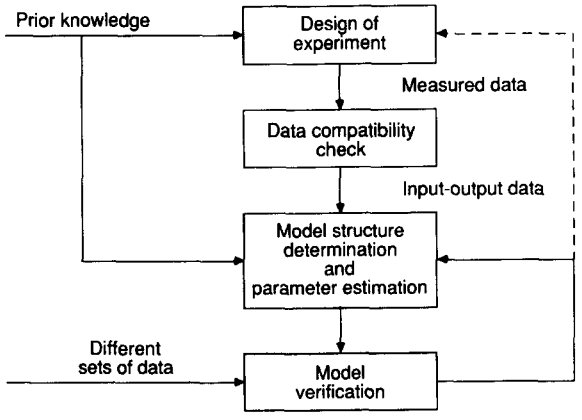

FIG. 10. Block diagram of aircraft identification procedure.

3.1. Design of an Experiment

Design of an experiment includes a selection of an instrumentation system and specification of the aircraft configuration, flight conditions and maneuvers for system identification. The instrumentation system is primarily required to measure the time histories of input and output variables. The input variables are represented by control surface deflections, sometimes completed by stick and pedal deflections and corresponding forces. The output variables include air data (airspeed, sideslip and angle-of-attack), angular velocities, linear and angular accelerations, and attitude (Euler) angles. In addition to these variables, quantities defining flight conditions and configurations are also measured. These quantities may include outside temperature for the evaluation of air density and fuel consumption for the estimation of airplane center-of-gravity (c.g.) position, weight and inertias.

The application of non-steady flight techniques and system identification methodology places special demands on the characteristics of an instrumentation system, namely on its accuracy and resolution. The accuracy, expressed in % of full scale reading of an instrument, of an order 0.1% is usually required for the measurement of linear accelerations, angular rates and control surface deflections, accuracy 0.02% for the measurement of airspeed and incidence angles. The remaining variables should be measured with the accuracy of 0.5% to 1.0%. The resolution, defined as the maximum difference of output step change as the input is continuously varied over the input range of the device and expressed in % of full scale output, is required to be 0.006% which means at least 14 bit binary for a digital instrumentation system.

The sampling rate varies between 20 to 100 samples/s and the above information requires about 40 channels to be recorded. The other requirements may include an easy access to all components and transducers for calibration, repair and replacement, the possibility to calibrate the entire measuring channel rather than separate components, and the possibility for pre- and post-flight check of some points of calibration curves. Detailed discussion of flight test instrumentation for airplane identification can be found in Ref. 11, and the example of an advanced instrumentation system for the measurement of transient maneuvers in Ref. 70. Characteristics of an analog instrumentation system used in the measurements of unsteady maneuvers of a general aviation aircraft[37] are summarized in Table 2 and Table 3. Table 2 contains measured quantities in the study, transducers and static characteristics of corresponding channels. The dynamic characteristics are presented in Table 3 in terms of natural frequencies, damping ratios and equivalent time constants.

The second critical part of an experiment design is the specification of the input forms which are to be used in the excitation of maneuvers suitable for parameter estimation and model structure determination. Since the first efforts of applying parameter estimation techniques to aircraft flight test data, many different forms of control inputs have been used. It was recognized that the shape of an input signal could influence the accuracy of estimated parameters from dynamic flight measurements, see Refs 13 and 54. Following the experience with data analysis and some engineering judgement, basic requirements for input signals have emerged. They can be summarized as:

(a) The input form should be selected in agreement with the mathematical model representing the aircraft under test. For example, an input for the longitudinal short-period model with linear stability and control derivatives should not cause aircraft motion where the assumptions of constant airspeed and linear aerodynamic model are not valid.
(b) The power of an input signal should be distributed uniformly over a wide frequency range. In Fig. 11 taken from Ref. 57, power spectral densities of three inputs are presented. It can be seen that the power spectral density of multiple input is a relatively wide band, whereas the doublet excites a particular band at a higher frequency. By changing the duration of the doublet the peak of the power spectral density can be shifted to lower or higher frequencies. The step input contains energy only at low frequencies. For that reason it is unsuitable for parameter estimation.
(c) The input form should be as simple as possible such that it can be realized by the pilot.

TABLE 2. CHARACTERISTICS OF THE INSTRUMENTATION SYSTEM

Quantity measured	Transducer	Range (*)	Static sensitivity (†)	Resolution (‡)	rms measurement error	
					Unit	Percent of full range
Longitudinal acceleration (g units)		−1 to 1	2.54	0.001	0.0046	0.23
Lateral acceleration (g units)	Servo accelerometer	−1 to 1	2.48	0.001	0.0050	0.25
Vertical acceleration (g units)		−3 to 6	0.56	0.001	0.0050	0.06
Rolling velocity (deg/s)		−102 to 102	0.025	0.12	0.20	0.10
Pitching velocity (deg/s)	Rate gyro	−29 to 29	0.088	0.032	0.19	0.33
Yawing velocity (deg/s)		−29 to 29	0.084	0.034	0.080	0.14
Roll angle (deg)	Vertical gyro	−90 to 90	0.028	0.10	0.077	0.04
Pitch angle (deg)		−87 to 87	0.029	0.098	0.092	0.05
Angle-of-attack (deg)	Flow direction	−12 to 27	0.127	0.029	0.027	0.07
Angle of sideslip (deg)	velocity sensor	−29 to 32	0.124	0.018	0.019	0.03
Right aileron angle (deg)		−23 to 10	0.147	0.0020	0.019	0.06
Left aileron angle (deg)	Control position	−10 to 25	0.142	0.0020	0.0061	0.02
Stabilator angle (deg)	transducer	−16 to 3	0.263	0.010	0.0037	0.02
Rudder angle (deg)		−31 to 28	0.084	0.011	0.0091	0.02
Airspeed (m/s)	Pressure transducer	0 to 75	0.067	0.037	0.89	1.2
Altitude (m)	Altimeter	−150 to 2900	0.0016	—	—	—
Air temperature (°C)	Thermometer	−18 to 38	0.089	—	—	—

* Working range of the channel.
† Obtained as volts per pertinent unit.
‡ Referred to a reading from the digitized tape.

TABLE 3. DYNAMIC CHARACTERISTICS OF THE INSTRUMENTATION SYSTEM

Quantity measured	Natural frequency (Hz)	Damping ratio	Equivalent time constant (s)
Longitudinal acceleration (g units)	402	1.58	0.0012
Lateral acceleration (g units)	216	1.10	0.0016
Vertical acceleration (g units)	921	1.58	0.0005
Rolling velocity (deg/s)			
Pitching velocity (deg/s)	27	0.64	0.0075
Yawing velocity (deg/s)			
Angle of sideslip (deg)	(*)	(*)	
Angle-of-attack (deg)	23	0.085	0.0012

* At V = 50 m/s.

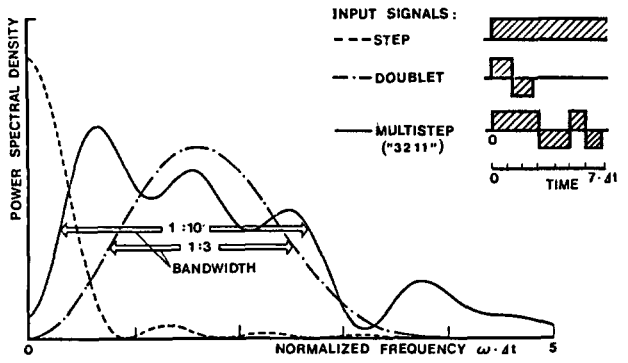

FIG. 11. Frequency domain comparison of various input signals. (Reproduced from Ref. 57.)

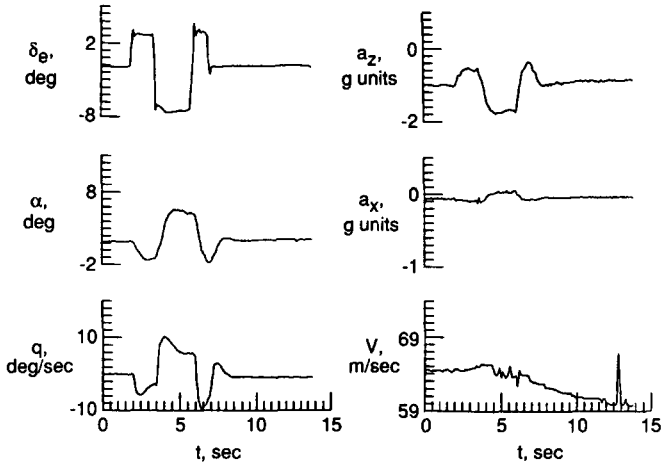

FIG. 12. Measured time histories of input and output variables in longitudinal maneuver.

Figures 12 and 13 show time histories of input and output variables used in estimation of stability and control derivatives of an executive aircraft. In Fig. 12 the short period motion of the aircraft was excited by a combination of several elevator pulses. In Fig. 13 a combination of rudder and aileron deflections was used in the lateral maneuver. The following two figures are an example of large amplitude maneuvers of a general aviation aircraft used for model structure determination and parameter estimation.[39] Figure 14 presents the input and output variables for a longitudinal motion. The input variables for the maneuver shown in Fig. 15 were the aileron and rudder deflection whereas the elevator

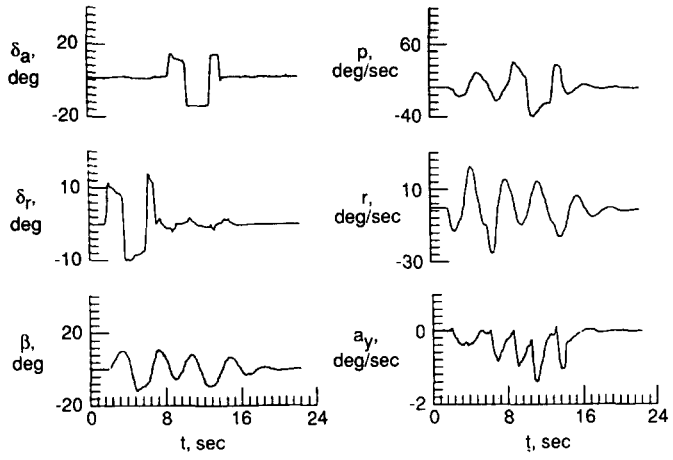

FIG. 13. Measured time histories of input and output variables in lateral maneuver.

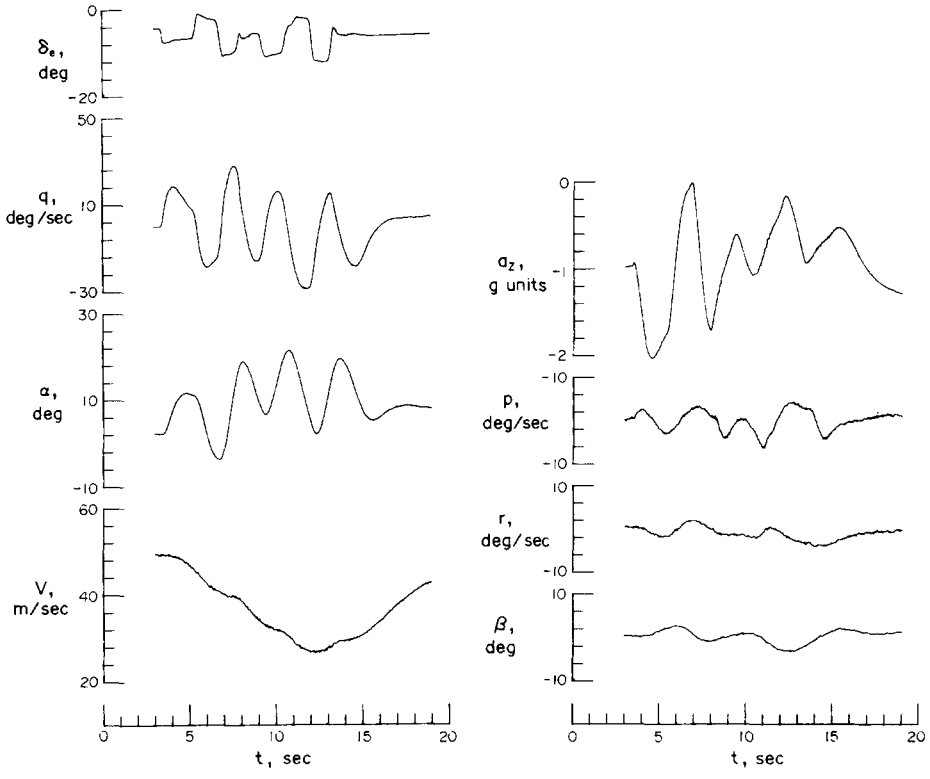

FIG. 14. Measured time histories of input and output variables in longitudinal large-amplitude maneuver.

deflection remained almost constant. The resulting aircraft response represents a coupled lateral and longitudinal motion thus giving a possibility for the investigation of possible variation of lateral parameters with the angle-of-attack.

Attempts for obtaining parameter estimates with high accuracy led many researchers to the development of an optimal input, see Refs 24, 39, 54, 65. Input signals were optimized with respect to the information or covariance matrix of parameters in the output error estimation technique. At the same time, the aircraft was treated as a linear multivariable system with known parameters. In order to arrive at a practical form of an input, an energy constraint was placed on the input signal. Later the determination of an optimal signal was extended to an aircraft represented as a non-linear system.[54] In the same reference

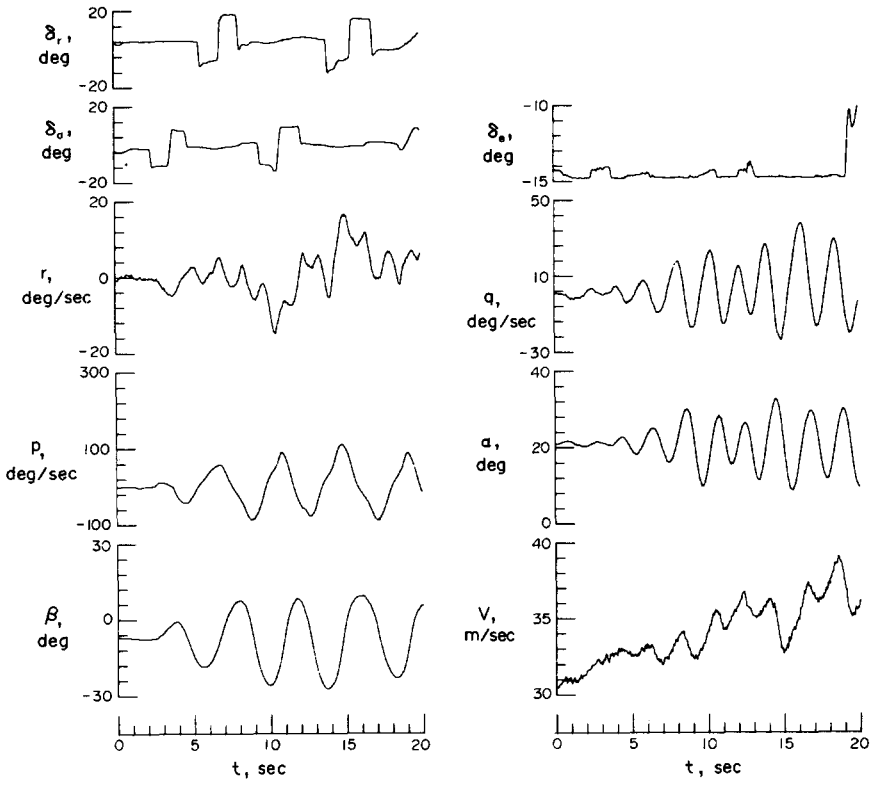

FIG. 15. Measured time histories of input and output variable in coupled longitudinal and lateral maneuver.

theoretical and actual performances of various optimal and non-optimal inputs were compared. Surprisingly, the heuristically designed doublets and multistep inputs performed quite well, thus indicating that a carefully selected realizable input may compete with an input determined by an optimalization procedure.

3.2. Data Compatibility Check

The recorded data are obtained either in the analog or digital form. Digital recording systems sample the continuous time signal at discrete time intervals. An analog signal must be digitized at some point in the processing in order to analyze the data on a digital computer. The digitized data are converted into physical magnitudes using laboratory calibrations of the instrumentation system. The next step in data processing includes data inspection for obvious gross errors and imperfections, such as incorrect sign of measured variables, missing points, extensive noise, etc. When necessary, corrective measures are taken. Inspected data are then corrected for known bias errors which might be due to transducer location (e.g. a c.g. offset and flow corrections) and its dynamic characteristics.[50]

In practice it is very often found that the response data even after careful handling can still contain bias and scale factor errors. In order to verify data accuracy a compatibility check can be applied to the measured aircraft response. This check includes aircraft state estimation, estimation of unknown biases in terms of constant offsets and scale factors, and a comparison of reconstructed responses with those measured. The state and parameter estimation, therefore, constitute a reconstruction problem and for that reason it is sometimes called the flight path reconstruction.

One possible form of the mathematical model used for the data compatibility check is described by three sets of kinematic equations with the state variables consisting of three linear velocities V_x, V_y, and V_z; three Euler angles ϕ, θ, and ψ; and three linear positions x_b, y_b, and z_b. The input variables in these equations are the linear accelerations a_x, a_y, and a_z

and angular velocities p, q, and r. The form of the kinematic (state) equations considered can be found in various references (see, e.g. Ref. 34).

The following variables are assumed to be measured:

(1) The inputs to the system a_x, a_y, a_z, p, q, and r.
(2) The airspeed V, two incidence angles β and α, three Euler angles ϕ, θ, and ψ and altitude $h=-z_b$.

These variables represent the output of the system. The measured variables z are corrupted by systematic and random errors. It is assumed that each of them can be expressed as

$$z=(1+\lambda_y)y+b_y+v_y \tag{3.3}$$

where y is the true value of the output, λ_y is the unknown scale factor error, b_y is the constant bias error, and v_y is the measurement noise. It is further assumed that the scale factor error is equal to zero for all the input variables. This assumption will simplify an estimation procedure for remaining scale factor and bias errors.

The system of state equations is simplified by deleting the equations for x_b and y_b. Then, replacing the input variables in the remaining state equations by their measured values results in the following set of state equations:

$$\begin{bmatrix} \dot{V}_x \\ \dot{V}_y \\ \dot{V}_z \\ \dot{h} \end{bmatrix} = \begin{bmatrix} 0 & r_{R,E}-b_r & -(q_{R,E}-b_q) & 0 \\ -(r_{R,E}-b_r) & 0 & p_{R,E}-b_p & 0 \\ q_{R,E}-b_q & -(p_{R,E}-b_p) & 0 & 0 \\ \sin\theta & -\cos\theta\sin\phi & -\cos\theta\cos\phi & 0 \end{bmatrix} \begin{bmatrix} V_x \\ V_y \\ V_z \\ h \end{bmatrix}$$

$$+\begin{bmatrix} -g\sin\theta & a_{xR,E}-b_{ax}+v_x \\ g\cos\theta\cos\phi & a_{yR,E}-b_{ay}+v_y \\ g\cos\theta\cos\phi & a_{zR,E}-b_{az}+v_z \\ 0 & 0 \end{bmatrix} + \begin{bmatrix} 0 & V_z & -V_y & 0 \\ -V_z & 0 & V_x & 0 \\ V_y & -V_x & 0 & 0 \\ 0 & 0 & 0 & 0 \end{bmatrix} \begin{bmatrix} v_p \\ v_q \\ v_r \\ 0 \end{bmatrix} \tag{3.4a}$$

$$\begin{bmatrix} \dot{\phi} \\ \dot{\theta} \\ \dot{\psi} \end{bmatrix} = \begin{bmatrix} 1 & \sin\phi\tan\theta & \cos\phi\tan\theta \\ 0 & \cos\phi & -\sin\phi \\ 0 & \dfrac{\sin\phi}{\cos\theta} & \dfrac{\cos\phi}{\cos\theta} \end{bmatrix} \begin{bmatrix} p_{R,E}-b_p+v_p \\ q_{R,E}-b_q+v_q \\ r_{R,E}-b_r+v_r \end{bmatrix}. \tag{3.4b}$$

The output equations take the form

$$\begin{aligned} V_R &= (1+\lambda_v)\sqrt{V_x^2+V_y^2+V_z^2}+b_v \\ \beta_R &= (1+\lambda_\beta)\sin^{-1}\frac{V_y}{V_x}+b_\beta \\ \alpha_R &= (1+\lambda_\alpha)\tan^{-1}\frac{V_z}{V_x}+b_\alpha \\ h_R &= (1+\lambda_h)h \\ \phi_R &= (1+\lambda_\phi)\phi+b_\phi \\ \theta_R &= (1+\lambda_\theta)\theta+b_\theta \\ \psi_R &= (1+\lambda_\psi)\psi. \end{aligned} \tag{3.5}$$

In the output equations for h_R and ψ_R the constant bias terms are omitted because the reference values for ψ and h can be selected arbitrarily. Further, in Eqs (3.4) and (3.5) the index R indicates the variable uncorrected for bias errors and index E measured variable.

The general form of the state equations for a given system can be written as

$$\dot{x}(t)=\xi[x(t),\ u(t),\ \theta_1]+g[x(t)]\ w(t),\ x(0)=x_0 \tag{3.6}$$

and the discrete form of the measured equations as

$$z(i)=h[x(i),\ u(i),\ \theta_1]+v(i),\ i=1,\ 2,\ \ldots,\ N \tag{3.7}$$

where x, u, and z are the state, input and measurement vector respectively, θ_1 is the vector of unknown biases and scale factor errors, x_0 is the vector of unknown initial conditions, w and v are the process and measurement noise vectors respectively, and N is the number of data points. The compatibility check can be now formulated as an identification problem which involves the estimation of state and output variables, unknown parameters θ_1 and x_0, and covariance matrices of w and v, from measured data.

The postulated model equations represent a non-linear stochastic system with state-dependent process noise and with non-linear output equations with an additive measurement noise. The state estimation in this case would be an extremely difficult problem. The separate estimation of unknown parameters would be equally complicated because of the resulting form of the sensitivity equations. For these reasons, possible simplifications of the problem have been considered and various methods for the solution of the problem taken. These methods can be divided into two groups.

(1) Methods for estimating separately unknown parameters and states.[43, 54, 69] For parameter estimation the maximum likelihood or non-linear least squares technique are used. For state estimation the system is assumed to be deterministic. That is, the state variables are simply obtained by the integration of model equations.
(2) Methods for estimating states and parameters simultaneously using an extended Kalman filter,[33, 34, 54] or non-linear smoother.[6] A review of various approaches to the problem of airplane state estimation is presented in Ref. 6.

Example. The results of a compatibility check using the ML estimation technique are demonstrated in one example taken from Ref. 43. The estimation technique itself will be explained later in Section 6. One set of measured flight data representing a longitudinal motion of a general aviation airplane was analyzed. The sampling interval for all data was $\Delta t = 0.05$ s. The measured output variables V_R, α_R, and θ_R are presented in Fig. 16. The resulting estimates which include the parameter mean values, their standard errors (Cramer–Rao lower bound) and standard errors of the measurement noise in the output variables are summarized in Table 4. In Case 1 the vector of unknown parameters was postulated as

$$\theta^T=[b_{ax},\ b_{az},\ b_q,\ b_V,\ b_\alpha,\ \lambda_V,\ \lambda_\alpha,\ u_0,\ w_0,\ \theta_0].$$

As can be seen from the results, three pairs of estimated parameters are highly correlated, and the parameters b_{ax} and θ_0, have large standard errors. As the next step, therefore, the parameters b_{ax}, w_0 and λ_V were fixed on their estimated values. The estimation of the remaining parameters was then repeated in Case 2. The new results indicate no change in the mean values but lower standard errors of estimates. The predicted time histories of the output variables are compared with those measured in Fig. 16. The agreement is very good in all variables plotted.

3.3. Model Structure Determination and Parameter Estimation

Model structure determination and parameter estimation form the principle parts of the identification procedure. It was pointed out in the definition of airplane identification that three items are needed for the implementation of identification methodology, namely a mathematical model of the aircraft under test, measured input/output data and an estimation technique. The problem of model formulation will be covered in the next section. The selection of an estimation technique is influenced by the complexity of a postulated

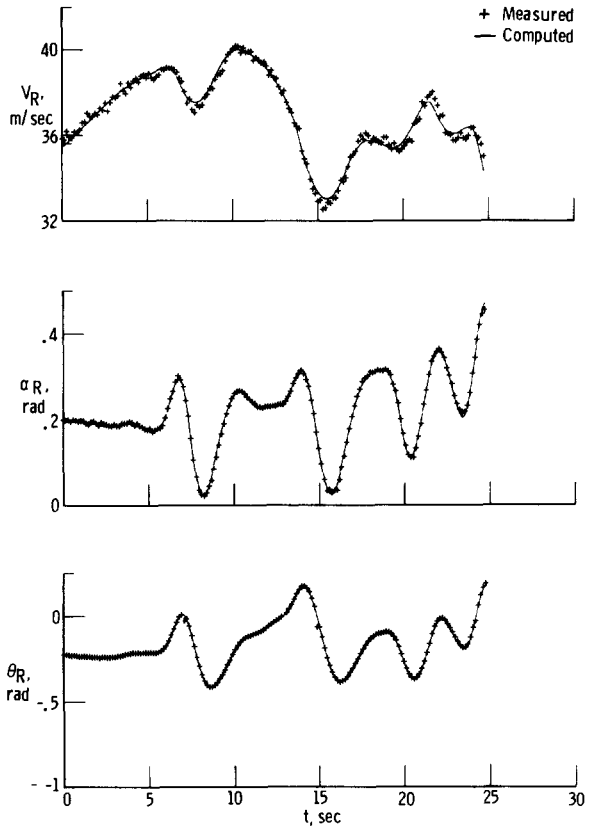

FIG. 16. Comparison of measured time histories in longitudinal maneuver with those computed.

TABLE 4. ESTIMATES OF PARAMETERS FROM LONGITUDINAL FLIGHT DATA OF TWO DIFFERENT RUNS

	Run 1			
	Case 1		Case 2	
Parameter	$\hat{\theta}$	$s(\hat{\theta})$	$\hat{\theta}$	$s(\hat{\theta})$
b_{ax} (g units)	0.004*	0.0065	0.004‡	
b_{az} (g units)	−0.1240	0.00040	−0.1240	0.00021
b_q (deg/s)	1.792	0.0019	1.792	0.0018
b_v (m/s)	−1.2*	0.30	−1.24*	0.098
b_α (deg)	2.6*	0.19	2.631	0.0036
b_θ (deg)	−12.7†		−12.72†	
λ_v	0.018*	0.0077	0.018‡	
λ_α	−0.073	0.0027	−0.073	0.0026
u_0 (m/s)	35.5	0.10	35.5*	0.10
w_0 (m/s)	6.0*	0.13	6.0‡	
θ_0 (deg)	−2.0*	0.37	−0.19	0.025
$s(V)$ (m/s)	0.260		0.260	
$s(\alpha)$ (deg)	0.280		0.280	
$s(\theta)$ (deg)	0.748		0.748	

* Parameters with high correlation.
† Computed from θ_0 and $\theta_{R,E}(0)$.
‡ Fixed parameter.

model, a prior knowledge about the system and by the form of measured data. It is expected that the estimation technique selected will provide two main results, that is the parameter estimates and their accuracies, usually in terms of parameter standard errors or variances.

During the development of airplane identification various techniques have been developed and tested. At present two techniques are mainly used, the equation error and maximum likelihood method. The equation error is based on a linear regression using an

ordinary least squares technique. The unknown aerodynamic parameters are estimated by minimizing the sum of squared differences between measured and predicted aerodynamic forces or moments. This condition can be formulated in terms of the cost function as

$$J = \sum_{i=1}^{N} [y(i) - \hat{y}(i, \theta)]^2 \rightarrow \min,$$

where $y(i)$ and $\hat{y}(i)$ are measured and predicted aerodynamic coefficients, respectively, sampled at time intervals t_i. The prediction $\hat{y}(i, \theta)$ depends on the unknown aerodynamic parameters θ in a linear fashion. When the measured data are obtained from large amplitude, high angle-of-attack maneuvers the problem of formulating aerodynamic model equations may arise. It is expected, in general, that the aerodynamic model will include non-linear terms but it is not known which of these terms should be included. If too many terms are contained in the model an 'identifiability' problem may be faced. This means that it will be impossible either to estimate some of the parameters at all or, in less severe cases, to estimate them with acceptable accuracy. In order to deal with this problem several techniques for model structure determination from measured data have been proposed. One of them, the stepwise regression, found its application to aeronautical problems. It is a model building technique developed from linear regression. From postulated terms in the aerodynamic model only statistically significant terms are selected and the corresponding parameters estimated. The cost function has the form

$$J = \sum_{i=1}^{N} \left[y(i) - \theta_0 - \sum_{k=1}^{l} \theta_k x_k(i) \right]^2,$$

where l is the number of parameters included in the model at each step of the computing algorithm and x_k is the state and input variable or their combinations. Both the linear or stepwise regression are very simple techniques and are easily applicable. They deal with each aerodynamic model equation separately. Their main disadvantage is that the estimates are biased due to measurement errors in output and input variables.

The maximum likelihood (ML) method finds a set of parameters by maximizing the probability density of an outcome of an experiment given a feasible set of parameters. The principle of the ML method is shown in Fig. 17 for a scalar case with one unknown parameter. Let us suppose that θ can take three values θ_1, θ_2 and θ_3. If z is the observed value of Z then θ_2 is the maximum likelihood estimate of θ. The main advantage of the ML technique is that it can be used with a linear or a non-linear model of the aircraft in the presence of process and measurement noise. If there is no process noise and no measurement noise in the output variables a simplified version of the ML method, sometimes called the output error method, is obtained. Applying this method to measured data and a given model, the unknown parameters are obtained by minimizing the sum of squares of weighted differences between the measured and predicted output variables, that is

$$J = \sum_j W_j \sum_{i=1}^{N} [z(i) - \hat{y}_j(i, \hat{\theta})]^2 \rightarrow \min,$$

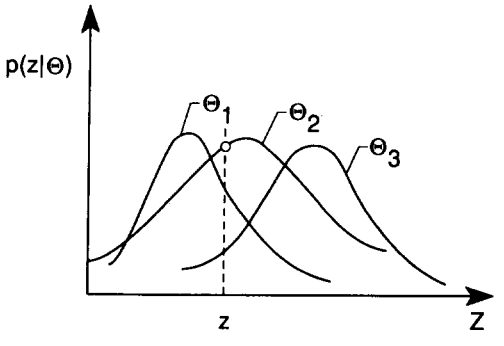

FIG. 17. Principle of maximum likelihood method.

where W_j are the weights. In this expression the predicted output is non-linear in parameters, therefore, the ML method cannot provide direct estimates of unknown parameters. An iterative technique must be used in this case.

Recently a third group of techniques, known as biased estimation techniques, has showed an application in cases where near linear dependency exists among the measured data. This dependency has been observed in experiments on a highly augmented aircraft where the control system deflects various control surfaces in concert and, at the same time, restricts the excitation of some of the aircraft response variables. All the estimation techniques mentioned will be fully described and demonstrated in several examples in the following sections.

3.4. Model Verification

Model verification is the last step in the identification process and should be applied regardless of the complexity of the estimation method. The resulting model must demonstrate that its parameters have physical values and acceptable accuracy, and that it has good prediction capabilities. For that reason the parameter estimates are compared with any information available about the aircraft aerodynamics which can come from theoretical predictions, wind-tunnel measurements or from previous flight measurements using different maneuvers and/or different estimation techniques. During these comparisons limits of theoretical calculations, wind-tunnel measurements and flight results must be taken into consideration.

Prediction capabilities of the model are checked on a set or sets of data not used in the identification process. The measured input is used in computing aircraft responses which are then compared with those measured. The differences between both sets should be random in nature. Some examples of model verification will be presented in the following sections.

4. MATHEMATICAL MODEL OF AN AIRCRAFT

For the estimation of aerodynamic parameters from flight data the mathematical model of an aircraft under test must be given or postulated. As mentioned in the preceding section, in many applications the model can be represented by the rigid body equations of motion referred to a system of axes fixed in the body and with the origin at the body center of gravity, see Fig. 1. These equations are completed by a set of kinematic equations so that the complete state equations can be written as

$$
\begin{aligned}
\dot{V}_x &= -qV_z + rV_y - g\sin\theta + \frac{\rho V^2 S}{2m} C_X + \frac{T}{m} \\
\dot{V}_y &= -rV_x + pV_z + g\cos\theta\sin\phi + \frac{\rho V^2 S}{2m} C_Y \\
\dot{V}_z &= -pV_y + qV_x + g\cos\theta\cos\phi + \frac{\rho V^2 S}{2m} C_Z \\
\dot{p} &= \frac{I_y - I_z}{I_x} qr + \frac{I_{xz}}{I_x}(pq + \dot{r}) + \frac{\rho V^2 Sb}{2I_x} C_l \\
\dot{q} &= \frac{I_z - I_x}{I_y} pr + \frac{I_{xz}}{I_y}(r^2 - p^2) + \frac{\rho V^2 S\bar{c}}{2I_y} C_m \\
\dot{r} &= \frac{I_x - I_y}{I_z} pq + \frac{I_{xz}}{I_z}(\dot{p} - qr) + \frac{\rho V^2 Sb}{2I_z} C_n \\
\dot{\phi} &= p + (q\sin\phi + r\cos\phi)\tan\theta \\
\dot{\theta} &= q\cos\phi - r\sin\phi.
\end{aligned}
\tag{4.1}
$$

The aerodynamic coefficients C_X, C_Y, . . . , C_n are either known or unknown functions of state variables V_x, V_y, V_z, p, q, and r, and input variables δ_a, δ_e, and δ_r. In addition to the angular velocities and Euler angles, the air data and linear accelerations are usually obtained from flight measurements as well. The last two sets of output variables are specified by the output equations as

$$
\begin{aligned}
V &= \sqrt{V_x^2 + V_y^2 + V_z^2} \\
\beta &= \sin^{-1} \frac{V_y}{V} \\
\alpha &= \tan^{-1} \frac{V_z}{V_x} \\
a_x &= \dot{V}_x + qV_z - rV_y + g \sin\theta \\
a_y &= \dot{V}_y + rV_x - pV_z - g \cos\theta \sin\phi \\
a_z &= \dot{V}_z + pV_y - qV_x - g \cos\theta \cos\phi.
\end{aligned} \tag{4.2}
$$

The state and output equations can be written in a concise form as

$$\dot{x} = f(x, u, \theta), \; x(0) = x_0 \tag{4.3}$$

$$y = h(x, \theta), \tag{4.4}$$

where again θ represents the aerodynamic parameters and x_0 is the vector of initial conditions.

In many practical applications the linear model of an aircraft is completely sufficient. The linear equations are well developed and can be formulated in the following way:

(a) the longitudinal equations including only the short-period mode and expressing perturbations with respect to a horizontal steady flight as

$$
\begin{aligned}
\dot{\alpha} &= q + \frac{\rho V_0 S}{2m}\left(C_{Z_\alpha}\alpha + C_{Z_q}\frac{q\bar{c}}{2V_0} + C_{Z_{\delta_e}}\delta_e\right) \\
\dot{q} &= \frac{\rho V_0^2 S\bar{c}}{2I_y}\left(C_{m_\alpha}\alpha + C_{m_q}\frac{q\bar{c}}{2V_0} + C_{m_{\delta_e}}\delta_e\right) \\
\dot{\theta} &= q \\
a_z &= V_0(\dot{\alpha} - q).
\end{aligned} \tag{4.5}
$$

In the pitching-moment equation the $\dot{\alpha}$ term is not explicitly included. For $Cm = Cm'(\alpha, \dot{\alpha}, q, \delta_e)$ it is contained in the derivatives

$$
\begin{aligned}
Cm_\alpha &= Cm'_\alpha + \frac{\rho S\bar{c}}{4m} Cm'_{\dot{\alpha}} C_{Z_\alpha} \\
Cm_q &= Cm'_q + Cm_{\dot{\alpha}}\left(1 + \frac{\rho S\bar{c}}{4m} C_{Z_q}\right) \\
Cm_{\delta_e} &= Cm'_{\delta_e} + \frac{\rho S\bar{c}}{4m} Cm'_{\dot{\alpha}} C_{Z_{\delta_e}}.
\end{aligned} \tag{4.6}
$$

This simplification is obtained by substituting for $\dot{\alpha}$ from the vertical-force equation. This is also a necessary step for avoiding the identifiability problem of $Cm'_{\dot{\alpha}}$.[21, 45]

(b) The lateral equations for the perturbations with respect to a steady flight as

$$
\begin{aligned}
\dot{\beta} + r - \frac{g}{V_0}\cos\theta_0 &= \frac{\rho V_0 S}{2m}\left(C_{Y_\beta}\beta + C_{Y_p}\frac{pb}{2V_0} + C_{Y_r}\frac{rb}{2V} + C_{Y_{\delta_r}}\delta_r\right) \\
\dot{p} - \frac{I_{xz}}{I_x}\dot{r} &= \frac{\rho V_0^2 Sb}{2I_x}\left(C_{l_\beta}\beta + C_{l_p}\frac{pb}{2V_0} + C_{l_r}\frac{rb}{2V_0} + C_{l_{\delta_a}}\delta_a + C_{l_{\delta_r}}\delta_r\right)
\end{aligned}
$$

$$\dot{r}-\frac{I_{xz}}{I_z}\dot{p}=\frac{\rho V_0^2 Sb}{2I_y}\left(C_{n_\beta}\beta+C_{n_p}\frac{pb}{2V_0}+C_{n_r}\frac{rb}{2V_0}+C_{n_{\delta_a}}\delta_a+C_{n_{\delta_r}}\delta_r\right) \tag{4.7}$$

$$\dot{\phi}=p+r\tan\theta_0$$

$$a_y=V_0(\dot{\beta}+r)-(g\cos\dot{\theta}_0)\Phi.$$

The concise form of the linearized equations has the form

$$\dot{x}=Ax+Bu \tag{4.8}$$

$$y=Cx+Du \tag{4.9}$$

where the matrices A, B, C, and D include the aerodynamic parameters in terms of stability and control derivatives C_{Z_α}, C_{Z_q}, . . . , $C_{n_{\delta_r}}$.

Modeling of aerodynamic forces and moments where the linearization cannot be substantiated raises the fundamental question of how complete the model should be. Although a more complete model can be justified for the correct description of aircraft aerodynamics it is not clear in the case of parameter estimation what should be the best relationship between model complexity and measured information. If too many unknown parameters are sought for a limited amount of data, then a reduced accuracy of estimated parameters can be expected or attempts to estimate all parameters might fail.[54]

Where the model structure is to be determined from flight data, the aerodynamic model is postulated. Two forms of postulated model are given. They are developed under the following principal assumptions.

(1) The instantaneous aerodynamic forces and moments depend only on the instantaneous values of response and input variables. That is, no unsteady aerodynamic effects are considered.
(2) There is no speed effect on the aerodynamic coefficients.
(3) The dependence of longitudinal and lateral coefficients on response and input variables can be expressed as

$$C_a=C_a(\beta,\alpha,q,\delta_e) \qquad (a=X, Z \text{ or } m)$$

and

$$C_a=C_a(\beta,\alpha,p,r,\delta_a,\delta_r) \qquad (a=Y, l \text{ or } n).$$

(4) The resulting aerodynamic coefficients are obtained as sums of contributions due to (α, β), and p, q, r, δ_a, δ_e, and δ_r. The second group of these contributions is, in general, α-dependent.

Considering the preceding assumptions, the aerodynamic model equations can be written as

$$C_a=C_a(\alpha,\beta)_{q=\delta_e=0}+C_{a_q}(\alpha)\,q\bar{c}/2V+C_{a_{\delta_e}}(\alpha)\delta_e, \quad (a=X, Z \text{ or } m) \tag{4.10}$$

and

$$C_a=C_a(\alpha,\beta)_{p=r=\delta_a=\delta_r=0}+C_{a_p}(\alpha)\,pb/2V+C_{a_r}\,rb/2V+C_{a_{\delta_a}}(\alpha)\delta_a+C_{a_{\delta_r}}(\alpha)\delta_r,$$
$$(a=Y, l \text{ or } n). \tag{4.11}$$

The expressions for the aerodynamic coefficients are similar to those used in wind-tunnel testing practice. The first terms on the right-hand side of Eqs (4.10) and (4.11) represent 'static' parts with controls fixed at zero deflections. The remaining terms represent contributions of dynamic stability derivatives and control derivatives and their dependence on α. In Eqs (4.10) and (4.11), no $\dot{\alpha}$ and $\dot{\beta}$ terms are explicitly introduced because of their near linear dependence on the remaining variables. The effects of $\dot{\alpha}$ and $\dot{\beta}$ are included primarily in contributions due to angular velocities, see Eq. (4.6).

In longitudinal maneuvers with small lateral coupling, Eq. (4.10) can be further simplified by replacing the two-dimensional terms in (α, β), by two terms in α. These equations then

take the form

$$C_a = C_a(\alpha)_{\beta=q=\delta_e=0} + C_{a_{\beta^2}}(\alpha)\beta^2 + C_{a_q}(\alpha)\, q\bar{c}/2V + C_{a_{\delta_e}}(\alpha)\delta_e \quad (a = X, Z \text{ or } m). \tag{4.12}$$

Equations (4.10) and (4.11) or (4.11) and (4.12) represent a fairly general formulation of aerodynamic coefficients. In each particular case, however, the postulated aerodynamic model equations should reflect any available *a priori* knowledge, based on wind-tunnel and/or theoretical aerodynamic data.

Each term in Eqs (4.10) to (4.12) can be approximated either by polynomials, or by splines in the (α, β) variables or in the α variable. In the first case the aerodynamic model equations have the form

$$C_a = \theta_0 + \theta_1 X_1 + \cdots + \theta_{n-1} x_{n-1}, \tag{4.13}$$

where the x_1 to x_{n-1} are the response and input variables or their combinations. They are formed by linear and higher order terms in the Taylor series expansion of C_a. θ_0 is the value of any particular coefficient corresponding to the initial conditions.

In large amplitude and high angle-of-attack maneuvers the behavior of aerodynamic functions in one region of angle-of-attack may be quite different from and totally unrelated to their behavior in another region. In these cases, the polynomial approximation for some aerodynamic non-linearities would be inadequate. Polynomials are determined everywhere by their values in any interval, no matter how small. They can, therefore, follow a curve in one interval but depart from a curve or even oscillate widely elsewhere. Even if a higher-order polynomial approximates the aerodynamic function sufficiently, the increase in the number of terms can lead to large covariances of their estimates. To avoid the disadvantages of the polynomial representation, spline functions[63] can be used. Splines avoid some difficulties of polynomials because they are defined on pre-selected intervals and because the low-order terms may approximate various non-linearities quite well.

Spline functions are defined as piecewise polynomials of degree m. When continuity restrictions are considered, the function values and derivatives agree at the points where the piecewise polynomials join. These points are called 'knots' and are defined by the value of their projection onto the plane (or axis) of independent variables. A polynomial spline of degree m with continuous derivatives up to degree $m-1$ approximating a function $f(x)$ for $x \in [x_0, x_{\max}]$, can be expressed as

$$s_m(x) = \sum_{h=0}^{m} C_h x^h + \sum_{i=1}^{k} D_i (x - x_i)_+^m \tag{4.14}$$

where

$$(x - x_i)_+^m = \begin{cases} (x - x_i)^m; & (x \geqslant x_i) \\ 0; & (x < x_i). \end{cases}$$

The values $x_1, x_2, \ldots, x_k$ are knots which obey the condition, $x_0 < x_1 < x_2 < \cdots < x_k < x_{\max}$, and C_h and D_i are constants. The special case of Eq. (4.14) for $m = 0$ (a spline of degree zero) represents an approximation by piecewise constants.

The problem of multidimensional splines is addressed in Ref. 63. A space of these splines is constructed by taking the tensor product of one-dimensional spaces of polynomial splines. Because of the tensor nature of the resulting space, many of the simple algebraic properties of ordinary polynomial splines in one dimension are carried over. A spline in two variables x_1 and x_2 can be introduced for the approximation of a function $f(x_1, x_2)$ for $x_1 \in [x_{10}, x_{1\max}]$ and $x_2 \in [x_{20}, x_{2\max}]$. Then, as in the one-dimensional case, the two ranges $[x_{10}, x_{1\max}]$ and $[x_{20}, x_{2\max}]$ are subdivided by sets of knots x_{1i} and x_{2i} where

$$x_{10} < x_{11} < \cdots < x_{1k} < x_{1\max}$$

$$x_{20} < x_{21} < \cdots < x_{2l} < x_{2\max}.$$

The points (x_{1i}, x_{2i}) partition the above rectangle into rectangular panels. A polynomial spline of degree m for x_1 and of degree n for x_2 with continuous partial derivatives up to

$(m-1)+(n-1)$ degree on the rectangle defined by the intervals $[x_{10}, x_{1\max}]$ and $[x_{20}, x_{2\max}]$ can be formulated as

$$S_{mn}(x_1, x_2)=\sum_{h=0}^{m}\sum_{s=0}^{n} C_{hs}x_1^h x_2^s+\sum_{i=1}^{k} P_i(x_2)(x_1-x_{1i})_+^m+\sum_{j=1}^{l} Q_j(x_1)(x_2-x_{2j})_+^n$$
$$+\sum_{i=1}^{k}\sum_{j=1}^{l} D_{ij}(x_1-x_{1i})_+^m(x_2-x_{2j})_+^n, \tag{4.15}$$

where $P_i(x_2)$ and $Q_j(x_1)$ are polynomials of degree n and m, respectively, and C_{hs} and D_{ij} are constants.

As examples of using splines in the approximation of aerodynamic functions, the vertical-force coefficient C_Z and yawing-moment coefficient C_n are considered. In the first case, the form of $C_Z(\alpha, q, \delta_e)$ based on splines can be, according to Eq. (4.12), written as

$$C_Z(\alpha, q, \delta_e)=C_Z(\alpha)_{q=\delta_e=0}+C_{Z_q}(\alpha)q\bar{c}/2V+C_{Z_{\delta_e}}(\alpha)\delta_e \tag{4.16}$$

where

$$C_Z(\alpha)=C_Z(0)+C_{Z_\alpha}\alpha+\sum_{i=1}^{k} D_{\alpha_i}(\alpha-\alpha_i)_+$$
$$C_{Z_q}(\alpha)=C_{Z_q}+C_{Z_{q\alpha}}\alpha+C_{Z_{q\alpha^2}}\alpha^2+\sum_{i=1}^{k} D_{qi}(\alpha-\alpha_i)_+^2 \tag{4.17}$$
$$C_{Z_{\delta_e}}(\alpha)=C_{Z_{\delta_e}}+\sum_{i=1}^{k} D_{\delta_{e,i}}(\alpha-\alpha_i)_+^0.$$

Equation (4.17) indicates that $C_Z(\alpha)$ is approximated by piecewise linear polynomials (the first-degree spline), $C_{Z_q}(\alpha)$ by piecewise quadratic polynomials (the second-degree spline) and $C_{Z_{\delta_e}}(\alpha)$ by piecewise constants (the zero-degree spline).

In the second case,

$$C_n(\alpha, \beta, p, r, \delta_a, \delta_r)=C_n(\alpha, \beta)_{p=r=\delta_a=\delta_r=0}+C_{n_p}(\alpha)pb/2V$$
$$+C_{n_r}(\alpha)rb/2V+C_{n_{\delta_a}}(\alpha)\delta_a+C_{n_{\delta_r}}(\alpha)\delta_r. \tag{4.18}$$

Using Eq. (4.15) for $x_1=\alpha$ and $x_2=\beta$, and selecting $m=0$ and $n=1$, the function $C_n(\alpha, \beta)$ can be approximated as

$$C_n(\alpha, \beta)=C_0+C_1\beta+\sum_{i=1}^{k}(A_{0i}+A_{1i}\beta)(\alpha-\alpha_i)_+^0+\sum_{j=1}^{l} B_{0j}\beta\left(1-\frac{\beta_j}{|\beta|}\right)_+$$
$$+\sum_{i=1}^{k}\sum_{j=1}^{l} D_{ij}\beta\left(1-\frac{\beta_j}{|\beta|}\right)_+(\alpha-\alpha_i)_+^0 \tag{4.19}$$

where

$$\beta\left(1-\frac{\beta_j}{|\beta|}\right)_+=\begin{cases}0 & (|\beta|<\beta_j)\\ \beta-\beta_j & (\beta\geqslant\beta_j)\\ \beta+\beta_j & (\beta\leqslant-\beta_j).\end{cases}$$

There is always a positive value for β_j. In this approximation of $C_n(\alpha, \beta)$, it is assumed that $C_n(\beta)$ is an odd function. The remaining functions in Eq. (4.18) are then represented by splines in α. As in the case of polynomial approximation, a general form of aerodynamic model equations is given by Eq. (4.13) with x_1 to x_{n-1} representing terms in spline approximation of C_a.

5. LINEAR REGRESSION USED IN PARAMETER ESTIMATION AND MODEL STRUCTURE DETERMINATION

The linear regression technique is employed to estimate a functional relationship of a dependent variable to one or more independent variables. It is assumed that the dependent

variable can be closely approximated as a linear combination of the independent variables. As shown in the previous section, the general form of aerodynamic model equations can be written as

$$y(t)=\theta_0+\theta_1 x_1+\ \ldots\ +\theta_{n-1}x_{n-1}. \tag{5.1}$$

In this equation $y(t)$ represents the dependent variable, x_1 to x_{n-1} are the independent variables or regressors.

5.1. Least Squares Estimates

Let us assume that the structure of Eq. (5.1) is known and a sequence of N observations on both y and x has been made at times $t_1, t_2, \ldots, t_N$. If the measured data are denoted by $y(i)$ and $x_1(i), x_2(i), \ldots, x_{n-1}(i)$ where $i=1, 2, \ldots, N$, then these data can be related by the following set of N linear equations:

$$y(i)=\theta_0+\theta_1 x_1(i)+\ \cdots\ +\theta_{n-1}x_{n-1}(i)+\varepsilon(i). \tag{5.2}$$

Because Eq. (5.1) is only an approximation of the actual aerodynamic relations, the right-hand side of Eq. (5.2) includes an additional term $\varepsilon(i)$, often referred to as the equation error. For $N>n$, the unknown parameters can be estimated from the measurement by the method of least squares as

$$\hat{\theta}=(X^TX)^{-1}X^TY, \tag{5.3}$$

where $\hat{\theta}$ is the $n\times 1$ vector of parameter estimates, Y is the $N\times 1$ vector of measured values of $y(i)$, and X is the $N\times n$ matrix of measured independent variables.

The properties of the least squares (LS) estimates depend upon the postulated assumptions concerning the measured dependent variables and equation errors. These assumptions are

(1) ε is a stationary vector with zero mean value,
(2) ε is uncorrelated with X,
(3) X is a deterministic quantity (i.e. the state and input variables are measured without errors),
(4) $\varepsilon(i)$ is identically distributed and uncorrelated with zero mean and variance σ^2.

Under assumptions 1 and 2, the LS estimates are unbiased. When assumptions 3 and 4 are considered, it can be shown that the LS estimates are also consistent and efficient.[27] The covariance matrix of parameter errors has the form

$$s^2=\frac{1}{N-n}\sum_{i=1}^{N}\hat{\varepsilon}^2(i) \tag{5.4}$$

where

$$\hat{\varepsilon}(i)=y(i)-\hat{y}(i) \tag{5.5}$$

and

$$\hat{y}(i)=\hat{\theta}_0+\hat{\theta}_1 x_1(i)+\ \cdots\ +\hat{\theta}_{n-1}x_{n-1}(i). \tag{5.6}$$

When assumptions 1 and 4 are extended by the assumption of a normal distribution for $\varepsilon(i)$, confidence intervals for the estimates can be found and some hypothesis tests can be employed.[15] The first one represents the test of overall regression with the null and alternative hypothesis formulated as

$$H_0:\ \theta_1=\theta_2=\ \ldots\ \theta_{n-1}=0$$

$$H_1:\ \text{not all } \theta_j=0.$$

The null hypothesis is rejected if $F>F(\nu_1, \nu_2, \alpha_p)$ where

$$F=\frac{\hat{\theta}^TX^TY-N\bar{y}^2}{(n-1)s^2}, \tag{5.7}$$

is a random variable having an F-distribution with the number of degrees of freedom $v_1 = n-1$ and $v_2 = N-n$ and where $F(v_1, v_2, \alpha_p)$ are the tabulated values of the F-distribution for the significance level $1-\alpha_p$.

The second test is of the significance of individual terms in the regression (a partial F-test). The hypotheses are

$$H_0\colon\ \theta_j = 0$$

$$H_1\colon\ \theta_j \neq 0$$

and the testing criterion is

$$F_p = \frac{\hat{\theta}_1^2}{s^2(\hat{\theta}_j)}. \tag{5.8}$$

The null hypothesis is rejected if $F_p > F(v_1, v_2, \alpha_p)$ where $v_1 = 1$ and $v_2 = N-n$. In Eq. (5.7),

$$\bar{y} = \frac{1}{N}\sum_{i=1}^{N} y(i)$$

and, in Eq. (5.8) $s^2(\hat{\theta}_j)$ is the variance estimate of θ_j.

The random variable F specified by Eq. (5.7) is related to the squared multiple correlation coefficient

$$R^2 = \frac{\sum_i [\hat{y}(i) - \bar{y}]^2}{\sum_i [y(i) - \bar{y}]^2} = \frac{\hat{\theta}^T X^T Y - N\bar{y}^2}{Y^T Y - N\bar{y}^2}, \tag{5.9}$$

by the equation

$$F = \frac{N-n}{n-1}\frac{R^2}{1-R^2}. \tag{5.10}$$

In an actual experiment, assumptions 1 and 4 and the normality of $\varepsilon(i)$ are not generally met. Because of the measurement errors in the independent variables, the LS estimates are asymptotically biased, inconsistent, and inefficient.[15, 27] However, experience with flight data indicates that the LS estimates still could be accurate enough and even could be comparable to those from the maximum likelihood method, which is expected to give consistent and asymptotically unbiased results. It is also believed that the F-tests can be formed with real flight data because of the robustness of the F-statistic with respect to the normality assumption. On the other hand, Eq. (5.4) for the covariance matrix usually gives optimistic values for the parameter variances.

5.2. Stepwise Regression

For the unknown structure of aerodynamic coefficients, Eq. (5.1) represents a postulated model where the significant terms in this equation will have to be found from measured data. Several techniques for the selection of the regression model have been developed.[15] One of them, the stepwise regression, has been preferably used by statisticians and researchers in many applications.

The stepwise regression is a procedure which inserts independent variables into the regression model, one at a time, until the regression equation is satisfactory. The order of insertion is determined by using the partial correlation coefficient as a measure of the importance of variables not yet in the regression equation. The procedure starts with the postulation of a regression model given by Eq. (5.2). The first independent variable from the postulated model is chosen as the one which is most closely correlated with y. The correlation coefficient is given by the expression

$$r_{jy} = \frac{S_{jy}}{(S_{jj}S_{yy})^{1/2}}, \tag{5.11}$$

where

$$S_{jy}=\sum_{N}[x_j(i)-\bar{x}_j][y(i)-\bar{y}] \tag{5.12a}$$

$$S_{jj}=\sum_{N}[x_j(i)-\bar{x}_j]^2 \tag{5.12b}$$

$$S_{yy}=\sum_{N}[y(i)-\bar{y}]^2 \tag{5.12c}$$

$$\bar{x}_j=\frac{1}{N}\sum_{N}x_j(i). \tag{5.12d}$$

If x_j is selected as x_1, then the model

$$y=\theta_0+\theta_1 x_1+\varepsilon \tag{5.13}$$

is used to fit the data. A new independent variable z_2 is constructed by finding the residuals of x_2 after regressing it on x_1, that is, the residuals from fitting the model

$$x_2=a_0+a_1x_1+\varepsilon. \tag{5.14}$$

The variable z_2 is, therefore, given as

$$z_2=x_2-\hat{a}_0-\hat{a}_1x_1. \tag{5.15}$$

Similarly the variables $z_3, z_4, \ldots, z_{n-1}$ are formed by regressing the variable x_3 on x_1, x_4 on x_1, and so forth. A new dependent variable y^* is represented by residuals of y regressed on x_1 using the model given by Eq. (5.13); that is,

$$y^*=y-\hat{\theta}_0-\hat{\theta}_1x_1. \tag{5.16}$$

In the next step, a new set of correlations which involve the variables $y^*, z_2, z_3, \ldots, z_{n-1}$ is formulated. These partial correlations can be written as $r_{jy.1}$ meaning the correlations of z_j and y^* are related to the model containing the variable x_1. The expression for the partial correlation coefficients $r_{jy.1}$ is given by Eqs (5.11) and (5.12) after replacing y and x_j by y^* and z_j. The next variable added to the regression model is the variable x_j whose partial correlation coefficient was the greatest. If the second independent variable selected in this way is x_2, then the third stage of the selection procedure involves partial correlations of the form $r_{jy.12}$; that is, the correlations between the residuals of x_j regressed on x_1 and x_2 and residuals of y regressed on x_1 and x_2.

At every step of the regression, the variables incorporated into the model in previous stages and a new variable entering the model are reexamined. The partial F_p criterion given by Eq. (5.8) is evaluated for each variable and compared with the pre-selected percentage point of the appropriate F-distribution. This provides a judgement on the contribution made by each variable. Any variable which provides a non-significant contribution (small value of F_p) is removed from the model. A variable which may have been the best single variable to enter at an early stage may, at a later stage, be superfluous because of the relationship between it and other variables now in the regression. The process of selecting and checking variables continues until no more variables will be admitted to the equation and no more are rejected.

Experience with stepwise regression showed that the model based only on the statistical significance of individual parameters on the regression equation can still include too many parameters. It is, therefore, recommended that more quantities and their variations be examined as possible criteria for selection of an adequate model. An adequate model is a model which sufficiently fits the data, facilitates the successful estimation of unknown parameters, and has good prediction capabilities. Several quantities which could be examined include the following.

(a) The computed values of F_p for each parameter in the model. Because F_p is the inverse of the relative parameter variance, it should have the maximum values for an adequate model.

(b) The computed value of F, which is given as the ratio of regression mean square to residual mean square. The model with the maximum F-value has already been recommended as the 'best' one for a given set of data.[25]

(c) The value of the squared multiple correlation coefficient R^2 which can be interpreted as measuring the proportion of the variation explained by the terms other than θ_0 in the model. However, the improvement in R^2 due to adding new terms to the model must have some real significance and should not reflect only the effect of the increased number of parameters. The value of R^2 varies from 0 to 1 (perfect fit). Its variation is often expressed in per cent.

(d) The value of the residual sum of squares (RSS) defined for the lth model as

$$\mathrm{RSS}_l = \sum_{i-1}^{N} [y(i) - \hat{y}(i)_l]^2$$

This value is the measure of the 'goodness of fit' and, for its improvement, the same note applies as that for R^2.

(e) The value of residual variance $s^2(\varepsilon)$ estimated from

$$s^2(\varepsilon) = \frac{\mathrm{RSS}}{N-n},$$

which should be compared with an unbiased estimate of the variance $\sigma^2(\varepsilon)$, if available.

(f) The residuals $\hat{\varepsilon}(i)$. For an adequate model, their time history should be close to a random sequence which is uncorrelated and gaussian.

(g) The mean square prediction error $E\{y-\hat{y}\}^2$ which can be implemented by the prediction sum of squares (PRESS) criterion as

$$\mathrm{PRESS} = \sum_{i=1}^{N} \{y(i) - \hat{y}[i|x(1), \ldots, x(i-1), x(i+1), \ldots, x(N)]_l\}^2,$$

where $\hat{y}(i|\ldots)_l$ is the estimate of $Ey(i)$ using the lth subset and excluding the ith observation. It means that PRESS uses $(N-1)$ data points for the estimation and one data point for the prediction. A more convenient scheme for computing PRESS is proposed as[4]

$$\mathrm{PRESS} = \sum_{i=1}^{N} \frac{[y(i) - \hat{y}(i)]^2}{1 - \left(\dfrac{\mathrm{Var}\{\hat{y}(i)\}}{\sigma^2}\right)}$$

where $\hat{y}(i)$ is now based on all data points.

One learns from experience that not all of the five criteria listed above are 'optimally' satisfied for any single model. However, the stepwise regression and its associated information criteria do significantly reduce the number of possible models from which the user must choose. Moreover, as the model structure is determined, so are the parameter estimates. Finally, ambiguity in the model selection can also be resolved by requiring that the estimated parameters make sense physically and that the selection model has good prediction capability. More detailed description of stepwise regression and its application to the estimation of aerodynamic parameters is given in Refs 39 and 40. The complete computing scheme can be found in Ref. 15 and the computer program in Ref. 8.

5.3. Data Partitioning

In the field of aircraft identification, estimation methods are usually applied to small maneuvers that are executed by an aircraft about trim flight conditions. For these maneuvers a linear aerodynamic model can be assumed. In order to obtain more detailed information about aircraft aerodynamic maneuvers involving large variations in angle-of-attack, sideslip and control position are analyzed.

Large maneuvers can be categorized as either commanded or unanticipated. For commanded large maneuvers, it was shown in Refs 39 and 40 that a proper application of system identification methodology can reveal an aerodynamic model that would otherwise require many small manèuvers. Of possibly more interest are those large maneuvers that are unanticipated. Here the aircraft has lost either stability, damping or control effectiveness in a way neither previously known to the pilot nor reflected in the aerodynamic model. To prevent further incidents, the post-flight analysis of these large maneuvers should give some good indication of the cause of the unanticipated motion.

Implicit to the analysis of the large maneuvers and their non-linearities in several reports was the procedure of partitioning, i.e. the dividing of a maneuver that covers a large range of some variable into several portions, each of which spans a smaller range of that variable. The technique was introduced in an application to real flight data in Ref. 7. The general applicability of the partitioning technique has now become apparent by its successful application to the diverse aircraft types investigated over the past several years.[40-42, 60]

To understand the basis for partitioning let

$$y(t)=f(x_1(t), x_2(t), \ldots, x_n(t)).$$

Now suppose that for any time, t, we want to eliminate the dependence of $y(t)$ in one of the variables $x_i(t)$, say $x_p(t)$. Then, by partitioning we mean redefining $y(t)$ on proper subsets of $x_1, x_2, \ldots, x_n$ as:

$$f_1(x_1(t), x_2(t), \ldots, x_{p-1}(t), x_{p+1}(t) \ldots, x_n(t)) \text{ for } x_{p0}<x_p<x_{p1}$$

$$y(\bar{x}_p, t)=f_2(x_1(t), x_2(t), \ldots, x_{p-1}(t), x_{p+1}(t) \ldots, x_n(t)) \text{ for } x_{p1}<x_p<x_{p2}$$

$$f_m(x_1(t), x_2(t), \ldots, x_{p-1}(t), x_{p+1}(t) \ldots, x_n(t)) \text{ for } x_{pm-1}<x_p<x_{pm}$$

where $\bar{x}_p=\dfrac{x_{p_{i+1}}+x_{p_i}}{2}$, $\quad i=1, 2, \ldots, m.$

That is, each $n+1$ tuple in (x_1, y) is reduced to several n-tuple's—each associated with a particular value on a small range of x_p. The supposition is that as the range defined by x_p becomes smaller, the variation in f due to x_p can be neglected. For example, an aircraft might perform a mostly lateral maneuver but with the angle-of-attack, α, varying by 20°. One could expect that due to separation effects on the lifting surfaces in this α region that the lateral aerodynamic force and moment coefficients C_y, C_l, and C_n might well depend on α in a non-linear way, i.e. $C_n=C_n(\alpha, \beta, p, r, \delta_a, \delta_r)$. Then, to partition one would simply analyze the data in separate groupings as follows:

$$C_n(\bar{\alpha}=21°)=C_n(\beta, p, r, \delta_a, \delta_r)_{20°<\alpha<22°}$$

$$C_n(\bar{\alpha}=23°)=C_n(\beta, p, r, \delta_a, \delta_r)_{22°<\alpha<24°}$$

$$C_n(\bar{\alpha}=29°)=C_n(\beta, p, r, \delta_a, \delta_r)_{28°<\alpha<30°},$$

that is: all data corresponding to $20°<\alpha<22°$ are put into one group for analysis, data corresponding to parts of the maneuver in which $22°<\alpha<24°$ are put into a second group, and so forth until all data have been accounted for.

If any grouping still appears to be dependent on α, it can be subdivided further (assuming a sufficient number of data points exists). In this example one can now analyze $C_n=f(\beta, p, r, \delta_a, \delta_r)$ at characteristic values of α given by the mean value of α for each grouping.

In selecting the data for a subset, the only consideration here is the value of α. Therefore, it will quite possibly be the case that the data in a given subset are not all continuous in time. Several sections of the maneuver will probably be combined. For example (Fig. 18) in partitioning a large maneuver which lasted 20 s, segment 2 contains 4 non-continuous time sections of data (all data corresponding to $4°<\alpha<8°$) viz. the segment from 0 to 4 s, a segment around 6 s, a segment around 7 s, and a segment around 12.5 s. Moreover, data from several large maneuvers may be combined and the resulting combined set partitioned.

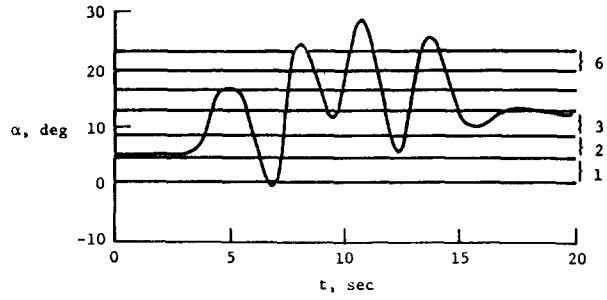

FIG. 18. Data partitioning for a large-amplitude longitudinal maneuver.

After the subsets are established, the model structure determination and parameter estimation can proceed. The model structure determination is still necessary, since large variations also may have occurred in variables other than the one on which the partitioning is based. The model structure determination and parameter estimation then proceeds by applying a stepwise regression algorithm to each subset of partitioned data.

5.4. EXAMPLES

The use of linear regression method is demonstrated in four examples. In all of these examples the data were obtained from the measurement of a general aviation aircraft. The basic characteristics of the airplane and instrumentation system are presented in Ref. 37. Later, this airplane had undergone certain wing leading-edge modifications which allowed the airplane to be trimmed at angles-of-attack up to approximately 24°. The measured data were available in the form of input and output time histories sampled at 0.05 s intervals. The input variables included the directly measured control-surface deflections. The variables α and β were measured by wind vanes, and the airspeed was measured by an anemometer. These measurements were corrected for the local airflow and offset with respect to the airplane center of gravity. The remaining output variables included angular rates and linear accelerations. These variables, together with the airspeed, were used to compute the aerodynamic coefficients,[39] for which the angular accelerations were obtained by numerical differentiation of spline fits of measured angular rates.

Example 5.1. This example is related to a lateral motion of the aircraft.[37] Its purpose is to evaluate the accuracy of the LS estimates, to compare the LS estimates with those obtained by the ML method and to verify prediction qualities of the final model. For the estimate of parameters, 28 maneuvers initiated from steady level flights at different airspeeds were available. The measured data were obtained from two flights. A model for the aerodynamic coefficients included conventional stability and control derivatives. For example the yawing moment coefficient was expressed as

$$C_n = C_{n_0} + C_{n_\beta}\beta + C_{n_p}\frac{pb}{2V} + C_{n_r}\frac{rb}{2V} + C_{n_{\delta_a}}\delta_a + C_{n_{\delta_r}}\delta_r .$$

The results from eight repeated measurements at the same airspeed are given in Table 5. They include the ensemble mean values and standard errors, the average standard errors of a single measurement computed from Eqs (5.4) and (5.5), and the ratio of these two standard errors presented. The standard errors estimated from the ensemble do not agree with the standard errors of a single measurement. The ratio of these two estimates varies between 1 and 6. High values and variability in these ratios could be caused by bias errors in the estimates resulting from various modeling errors.

The estimated parameters from all 28 runs are plotted against the lift coefficient, C_L in Fig. 19 and Fig. 20. In these figures only stability derivatives of C_l and C_n coefficients are included. The ML estimates in both figures are represented by fitted curves to individual

TABLE 5. PARAMETERS AND THEIR STANDARD ERRORS ESTIMATED FROM REPEATED MEASUREMENTS BY LINEAR REGRESSION

Parameter	Mean value $\bar{\Theta}$ (*)	Standard errors $s(\hat{\Theta})$ (†)	Standard errors $s(\hat{\Theta})$ (‡)	Ratio (†)/(‡)
C_{Y_β}	−0.647	0.012	0.0061	2.0
C_{Y_p}	−0.04	0.093	0.016	5.8
$C_{Y_{\delta_r}}$	0.097	0.011	0.0065	1.7
C_{l_β}	−0.0810	0.0025	0.0025	1.0
C_{l_p}	−0.532	0.018	0.018	1.0
C_{l_r}	0.16	0.040	0.016	2.5
$C_{l_{\delta_a}}$	−0.227	0.010	0.0065	1.5
$C_{l_{\delta_r}}$	0.015	0.0051	0.0036	1.4
C_{n_β}	0.0745	0.0043	0.00090	4.8
C_{n_p}	−0.042	0.029	0.0064	4.5
C_{n_r}	−0.130	0.017	0.0059	2.9
$C_{n_{\delta_a}}$	0.019	0.0087	0.0022	4.0
$C_{n_{\delta_r}}$	−0.072	0.0031	0.0013	2.4

* Ensemble mean value.
† Ensemble standard error.
‡ Average standard error of estimates.

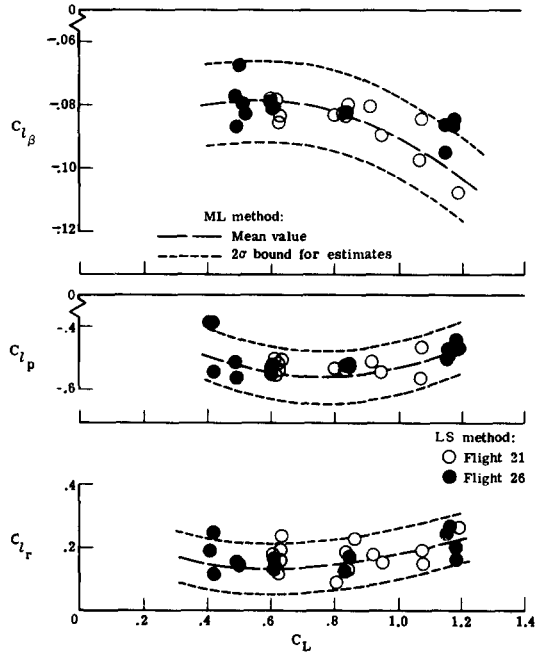

FIG. 19. Comparison of rolling-moment stability derivatives estimated from flight data using linear regression and maximum likelihood method.

points using either linear or quadratic polynomials. The 2σ-boundaries represent the maximum and minimum standard error of the fitted curve $\hat{\theta} = \hat{\theta}(C_L)$ within the given range of C_L. Practically all the LS estimates are within these boundaries thus indicating good agreement between LS and ML estimates. The scatter in various estimated parameters demonstrate that the accuracy of yawing-moment derivatives is less than that for the rolling-moment parameters. This conclusion can be also drawn from results in Table 5. The computed time histories of lateral variables using the LS estimates are compared with the measured time histories in Fig. 21. The agreement between all measured and predicted output variables is very good.

Example 5.2. In this example the stepwise regression technique for model structure determination was applied to the measured data of a lateral response at $\alpha \approx 20°$. The time

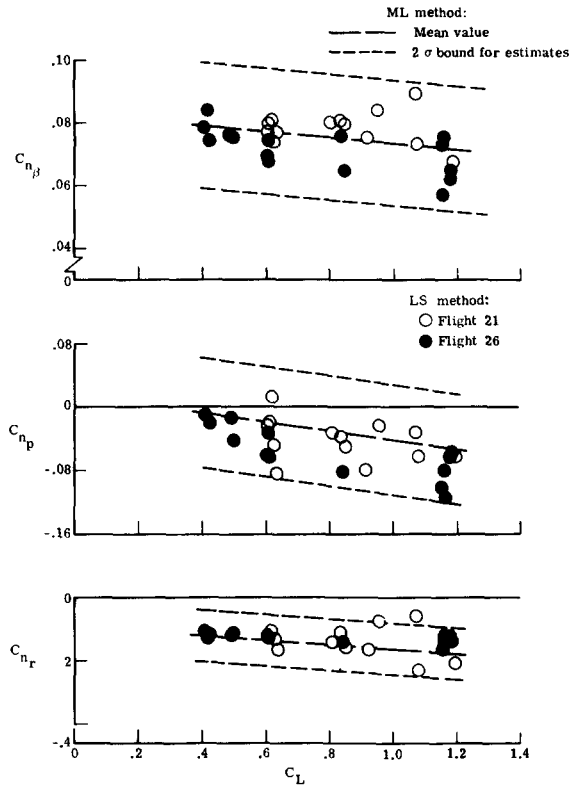

FIG. 20. Comparison of yawing-moment stability derivatives estimated from flight data using linear regression and maximum likelihood method.

histories of the input and some output variables are plotted in Fig. 15. The response variables indicate that the airplane exhibits a limit-cycle type of lateral motion which is also strongly coupled with the short-period longitudinal mode. The postulated model for lateral aerodynamic coefficients included 24 candidate variables.

$$\beta, p, r, \delta_a, \delta_r, \beta\alpha, p\alpha, r\alpha, \delta_a\alpha, \delta_r\alpha,$$
$$\beta\alpha^2, p\alpha^2, r\alpha^2, \delta_a\alpha^2, \delta_r\alpha^2, \beta^2, \beta^3, \beta^4, \beta^5,$$
$$\beta^3\alpha, \beta^3\alpha^2, \alpha, \alpha^2, \text{ and } \alpha^3.$$

The corresponding parameters represented the stability and control derivatives, variation of these derivatives with angle-of-attack and non-linear variation of the coefficients with angle-of-attack and sideslip.

In this example the computing scheme for the selection of an adequate model was modified in such a way that the five linear terms in the model were examined first. They entered the regression according to their partial correlation coefficients and were kept in the model regardless of the value of F. This means that during this part of the procedure no hypothesis testing was applied. When all linear terms were included, the procedure continued as for the ordinary stepwise regression. The non-linear terms postulated were searched and the null hypothesis concerning their significance, and the significance of all terms already in the model (linear and non-linear), tested. The stepwise regression technique with the constraint mentioned is referred to as the modified stepwise regression (MSR).[39]

In Fig. 22, the F, PRESS and R^2 values for the coefficients examined are plotted against the number of entries into the MSR.

An adequate model for the side-force coefficient was selected at the eighth entry where PRESS has its minimum and F the second maximum. For the coefficient C_l, the F-criterion indicates an adequate model at the sixth entry, the PRESS at the ninth. The difference in R^2

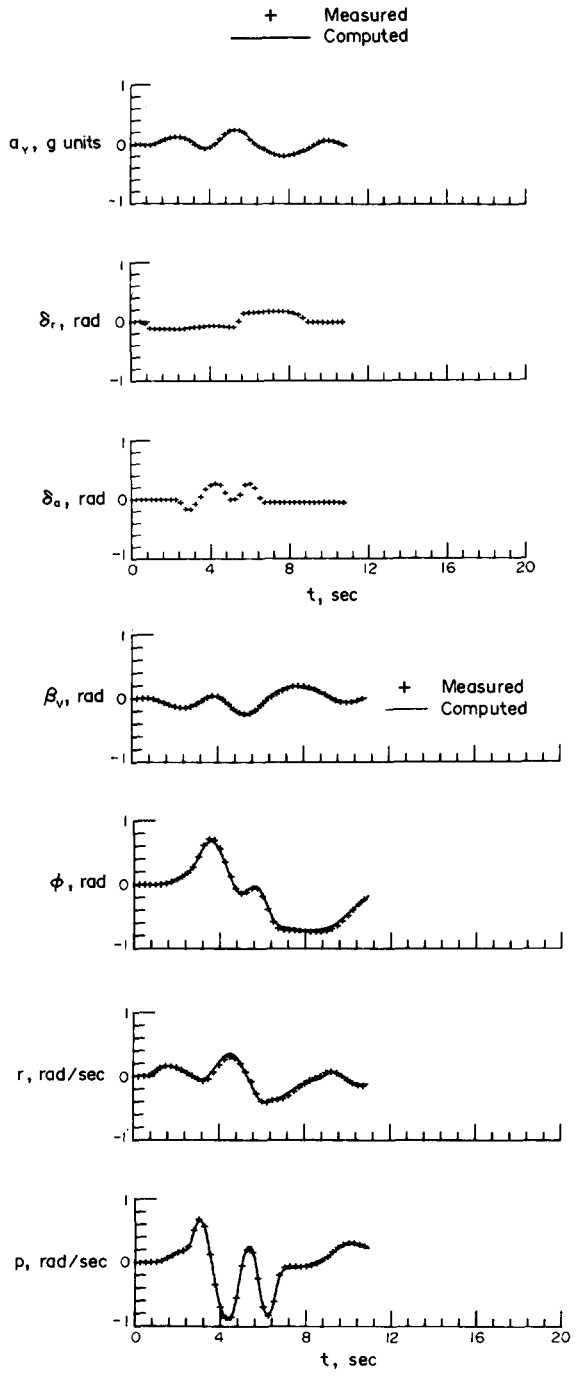

FIG. 21. Measured lateral flight data time histories and those computed by using least squares parameter estimates.

at these two entries is only 2%. Therefore, in consideration of the principle of parsimony, the model with the smaller number of parameters was selected. For the coefficient C_n, the changes in the F, PRESS, and R^2 values after the fifth entry are apparent. These changes indicate that the linear model (first five entries) is completely inadequate and that some non-linear terms must be included. An adequate model was selected at the seventh entry where the PRESS values have their minimum and F-values their maximum. Comparisons between measured and computed time histories of C_n for the linear model and for an adequate model

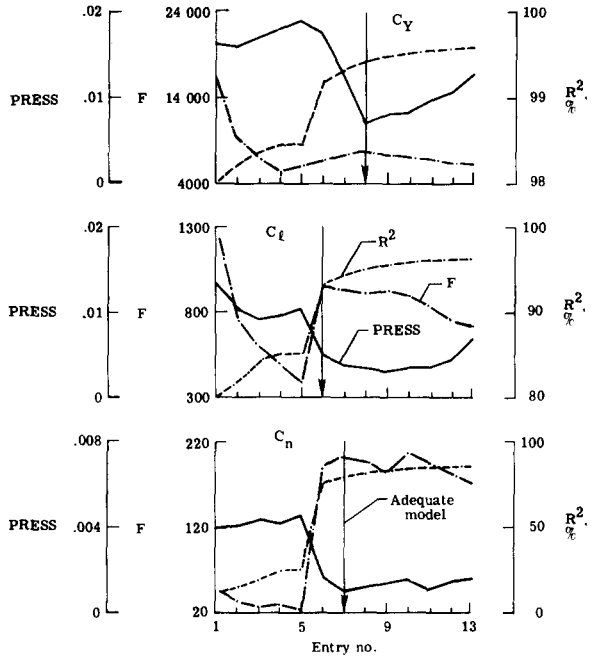

FIG. 22. Values of F and PRESS criteria and squared multiple correlation coefficient at different entries of stepwise regression algorithm.

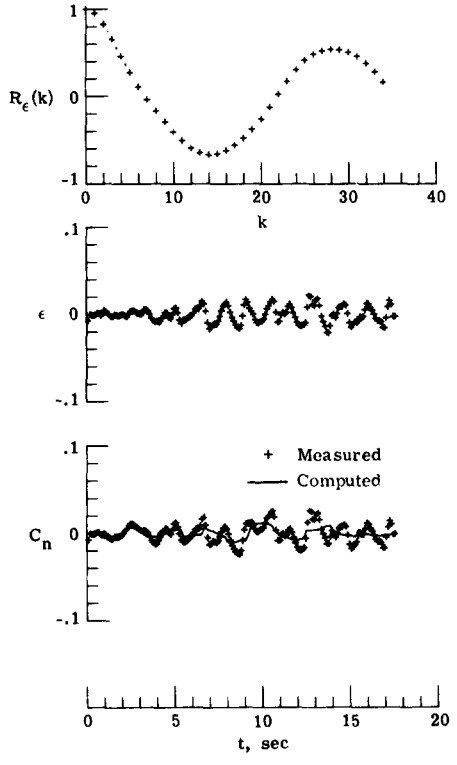

FIG. 23. Time histories of measured and computed yawing-moment coefficient, residuals, and autocorrelation function of residuals; linear model.

are presented in Figs 23 and 24, respectively. Also included are the residual time histories and the autocorrelation functions of residuals. For the linear model, the fit to the data is poor. By adding two non-linear terms $p\alpha$ and $r\alpha$, the fit was improved substantially and the autocorrelation function of residuals was close to that for the uncorrelated random variable.

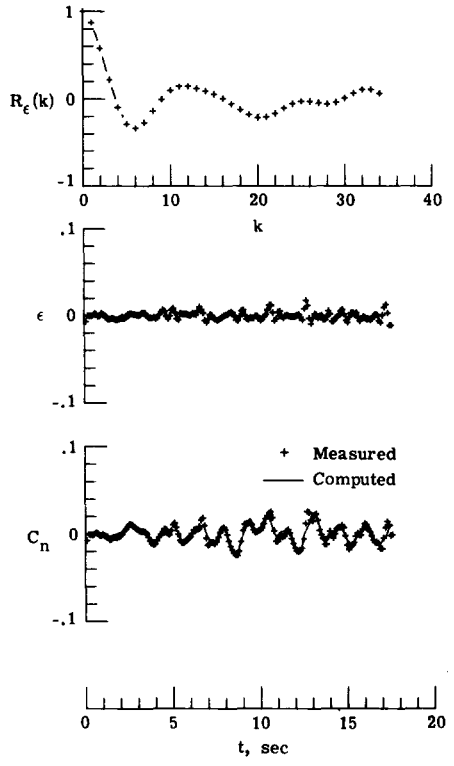

FIG. 24. Time histories of measured and computed yawing-moment coefficient, residuals, and autocorrelation function of residuals; adequate model.

The variables included in the adequate models for the three coefficients are summarized below, in the order that they entered the model, for

$$C_y\text{: } \beta, \delta_r, r, \delta_a, p, p\alpha, r\alpha^2, \alpha^2$$

$$C_l\text{: } \beta, p, \delta_a, r, p\alpha$$

$$C_n\text{: } \delta_a, p, \beta, \delta_r, r, p\alpha, r\alpha.$$

In Fig. 25, the measured output time histories are compared with those predicted using the model for C_y, C_l, and C_n determined by the MSR. The agreement in these time histories is good except for the yawing velocity, which could be caused by insufficient excitation of this variable.

The next step in the airplane identification included estimation of the parameters by using the maximum likelihood method[40] with the model structure determined by the MSR. In this estimation process, the non-linear parameters were kept fixed on the least squares estimates. Any attempt to estimate the whole set of aerodynamic parameters failed because of a divergence in the ML algorithm. The resulting ML and MSR estimates are presented in Table 6. Some differences in the estimated parameters from both methods exist, mainly in the damping derivative C_{l_p} and the cross derivative C_{n_p}. All these differences might be caused by undetected modeling errors and by the correlation between linear and non-linear parameters. Simulated studies of the flight regime analyzed also showed that the data were very sensitive to even small changes in certain parameters.

Example 5.3. A large-amplitude longitudinal maneuver was analyzed using the polynomial spline representation of aerodynamic force and moment coefficients. The time histories of the input and response variables in this maneuver are presented in Fig. 26. From these time histories the aerodynamic functions C_X, C_Z, and C_m were computed, and they are plotted in Fig. 27 against α rather than time. In Fig. 28 the variation of rate of pitch q and

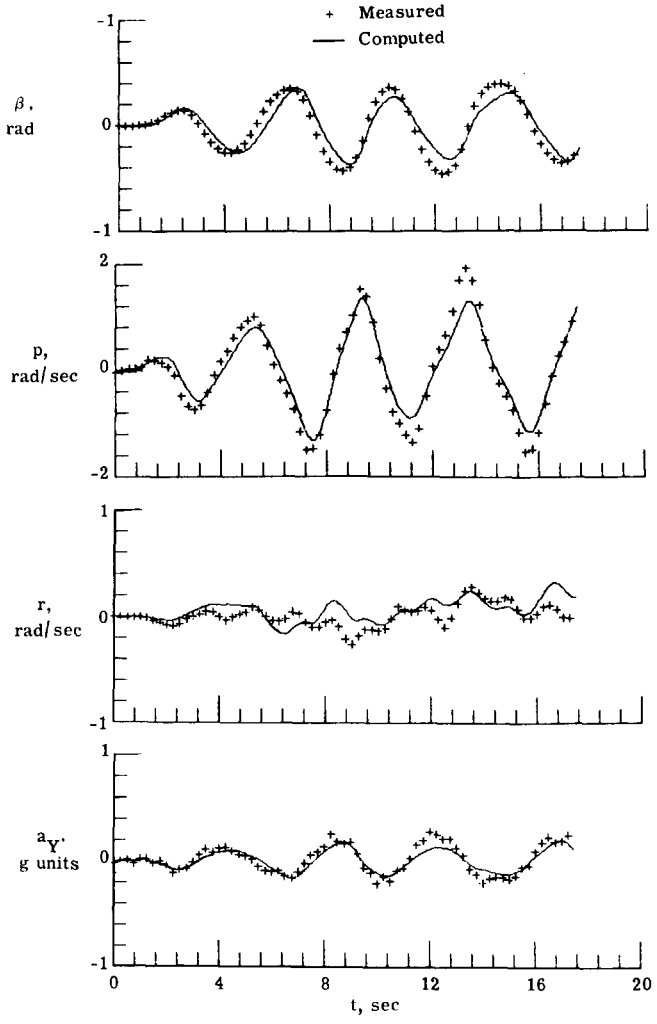

FIG. 25. Time histories of measured lateral flight data and those computed using parameters obtained by modified stepwise regression.

elevator deflection δ_e with α is also shown. Both figures indicate the range of dependent and independent variables available for use in the regression equations and the distribution of measured points within the α-range. This information can be utilized for the selection of knots and degree of splines in the postulated model structure.

For the spline approximation of all three aerodynamic coefficients, the form of Eq. (4.16) was used, with the same degree of splines for $C_X(\alpha)$, $C_Z(\alpha)$, and $C_m(\alpha)$ as indicated by Eq. (4.17). Seventeen knots for each spline were postulated as $\alpha_1 = 6°, \alpha_2 = 7°, \ldots, \alpha_{17} = 22°$. The final estimates of polynomial spline terms representing the two aerodynamic coefficients are plotted against α in Fig. 29. The aerodynamic function estimates are compared with the estimates from small-amplitude maneuvers and show very good agreement with those results. The fit of the polynomial and spline models to the data and the usefulness of the terms in those models can be revealed by the comparison of standard error of aerodynamic coefficient $\hat{\sigma}$ and the squared multiple correlation coefficient R^2. (See Ref. 33 for a more detailed explanation.) The values of both coefficients are summarized in Table 7. For small-amplitude maneuvers, the low values of $\hat{\sigma}$ and high values of R^2 correspond to low angle-of-attack regimes; conversely, $\hat{\sigma}$ is larger and R^2 smaller for values of α between 20° and 24°.

In Fig. 30, the spline terms of $C_Z(\alpha)$ and $C_m(\alpha)$ functions are compared with the measurement of these relationships in the quasi-steady flight. This measurement resulted in a double-value function $C_Z(\alpha)$ and $C_m(\alpha)$ for values of α between 10° and 22°, depending on

TABLE 6. PARAMETERS AND THEIR STANDARD ERRORS ESTIMATED FROM MEASUREMENTS USING TWO ESTIMATION METHODS

	MSR		ML	
Parameter	Estimate $\hat{\theta}$	Standard error $s(\hat{\theta})$	Estimate $\hat{\theta}$	Standard error* $s(\hat{\theta})$
$C_{Y,0}$	0.0064		0.011	0.0024
C_{Y_β}	−0.567	0.0024	−0.57	0.013
C_{Y_p}	−0.102	0.0048	−0.01	0.020
C_{Y_r}	0.88	0.041	1.0	0.16
$C_{Y_{\delta_a}}$	−0.074	0.0066	−0.14	0.027
$C_{Y_{\delta_r}}$	0.051	0.0040	0.025	0.019
$C_{Y_{p\alpha}}$	1.33	0.037	†1.33	
$C_{Y_{r\alpha^2}}$	−51.0	2.3	†−51.0	
$C_{Y_{\alpha^2}}$	0.47	0.052	†0.47	
$C_{l,0}$	−0.00013		0.0005	0.00024
C_{l_β}	−0.116	0.0021	−0.1215	0.00096
C_{l_p}	−0.152	0.0042	−0.106	0.0020
C_{l_r}	0.21	0.036	0.39	0.016
$C_{l_{\delta_a}}$	−0.091	0.0058	−0.076	0.0017
$C_{l_{p^2}}$	1.03	0.033	†1.03	
$C_{n,0}$	−0.00086		−0.00042	0.000061
C_{n_β}	0.0316	0.00097	0.0300	0.00068
C_{n_p}	−0.0616	0.0019	−0.0392	0.00093
C_{n_r}	−0.071	0.017	−0.094	0.0050
$C_{n_{\delta_a}}$	0.013	0.0027	0.0225	0.00082
$C_{n_{\delta_r}}$	−0.033	0.0016	−0.027	0.0012
$C_{n_{p\alpha}}$	0.77	0.015	†0.77	
$C_{n_{r\alpha}}$	−1.3	0.14	†−1.3	

* Cramer–Rao lower bound.
† Fixed values.

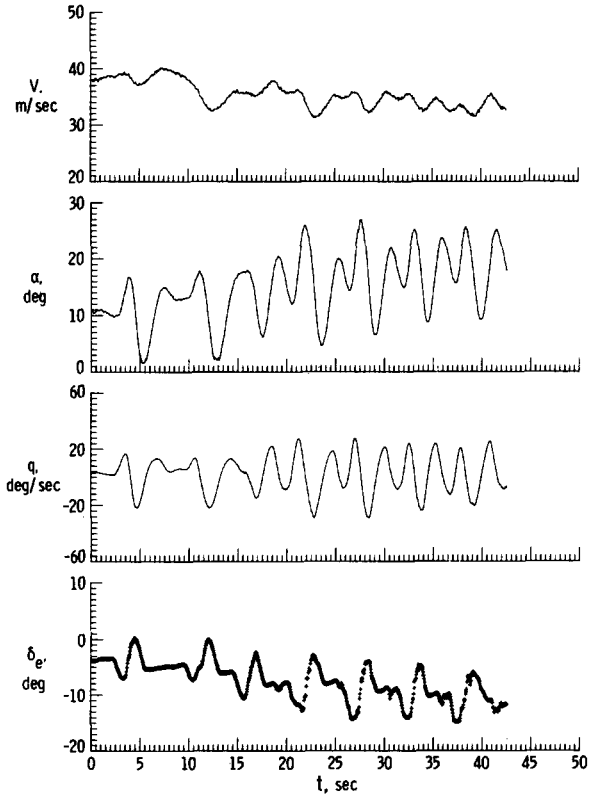

FIG. 26. Time histories of measured longitudinal variables in large-amplitude maneuver.

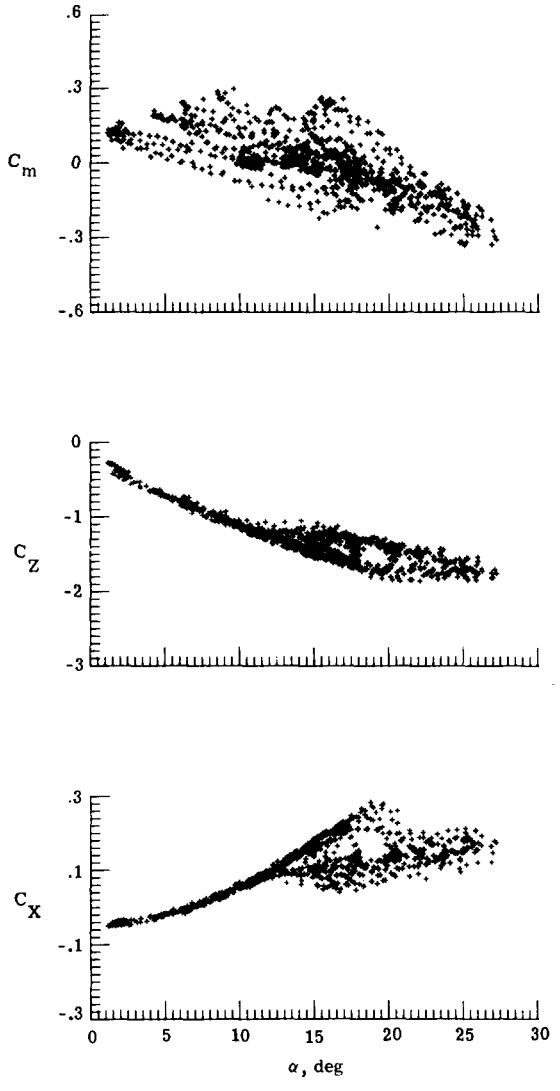

FIG. 27. Time histories of longitudinal aerodynamic coefficients in large-amplitude maneuver plotted against angle-of-attack.

increasing or decreasing values of α. This phenomenon can be caused by the aerodynamic hysteresis and by the hysteresis in the control system. Because of the relatively small differences in both branches of $C_Z(\alpha)$ and $C_m(\alpha)$ curves with respect to the accuracy of these estimates, the hysteresis was not modeled in Eq. (4.16).

Even if the agreement between the results from small- and large-amplitude maneuvers is very good, the resulting model is further verified by simulating the airplane longitudinal response. This is done by using the extended model approximated by splines and by using the elevator deflection time history from a selected independent maneuver. The time histories of input and response variables are presented in Fig. 31, and the response variables V, α, and q, are compared with those predicted by the model. The comparison reveals good prediction capabilities for the model.

Example 5.4. This example deals with analysis of commanded large-amplitude maneuvers. The emphasis is on: (1) a comparison of the results from partitioning to those achieved with 30 small-amplitude maneuvers and (2) the ability to discover non-linearities in β after partitioning with respect to α.

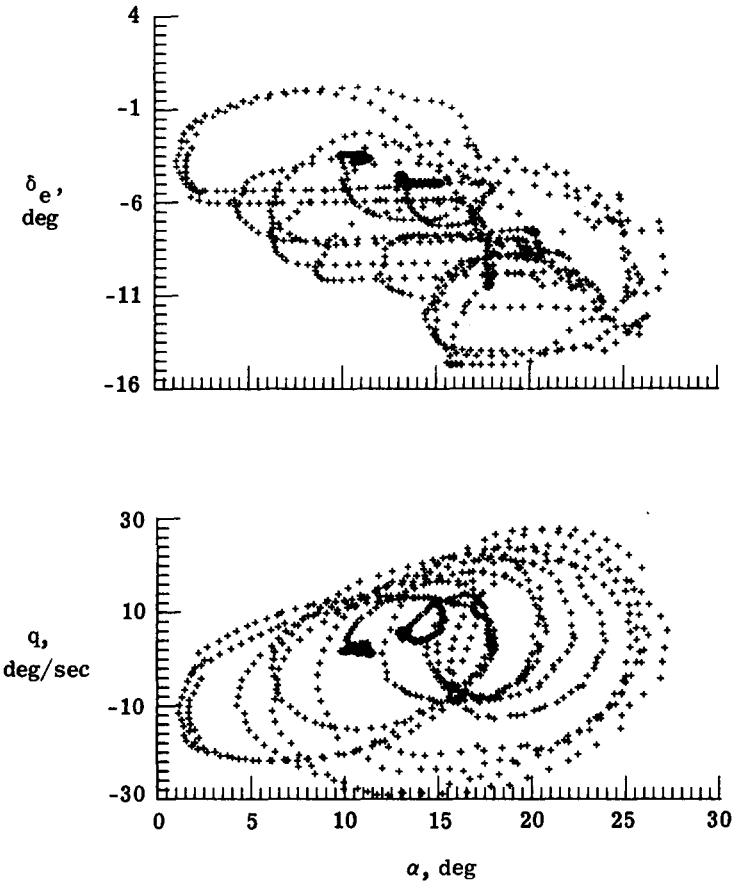

FIG. 28. Variation of two longitudinal variables with angle-of-attack in large-amplitude maneuver.

The measured data comprised two sets of maneuvers. For the first set, 30 small-amplitude lateral maneuvers were excited by control-surface deflections at trimmed conditions within the range of α between 4° and 24°. From these maneuvers local models of aerodynamic coefficients were estimated. The second set of data consisted of large-amplitude combined longitudinal and lateral maneuvers with the α variation between 0° and 30°. The combined maneuvers were accomplished by persistent excitation of lateral responses by rudder and aileron doublets superimposed on a steadily increasing angle-of-attack due to slow but steady increase in elevator deflection. The time histories of one of these maneuvers are given in Fig. 32. The measurements from 12 combined maneuvers were joined together into one set of data. The resulting ensemble of about 13,000 data points was then partitioned into 22 subsets according to the values of α. The modeling of the lateral parameters was conducted mostly on 1° subspaces of the 0° to 30° α-space. As an example, the model for C_n was postulated as

$$C_n(\bar{\alpha}, \beta, p, r, \delta_a, \delta_r) = C_{n_\beta}\beta + \sum_{i=1}^{5} C_{n_{\beta_i}}\beta\left(1-\frac{\beta i}{|\beta|}\right)_+ + C_{n_p}pb/2V + C_{n_r}rb/2V + C_{n_{\delta a}}\delta a + C_{n_{\delta r}}\delta r,$$

where

$$\left(1-\frac{\beta i}{|\beta|}\right)_+ = \begin{cases} 0 & (|\beta| < \beta_i) \\ \beta-\beta_i & (\beta \geqslant \beta_i) \\ \beta+\beta_i & (\beta \leqslant -\beta_i). \end{cases}$$

The knots of spline in β were selected at 4°, 8°, 12°, 16°, and 20°. The estimates of the stability derivatives of C_l and C_n coefficient from partitioned data are presented in Fig. 33. In general,

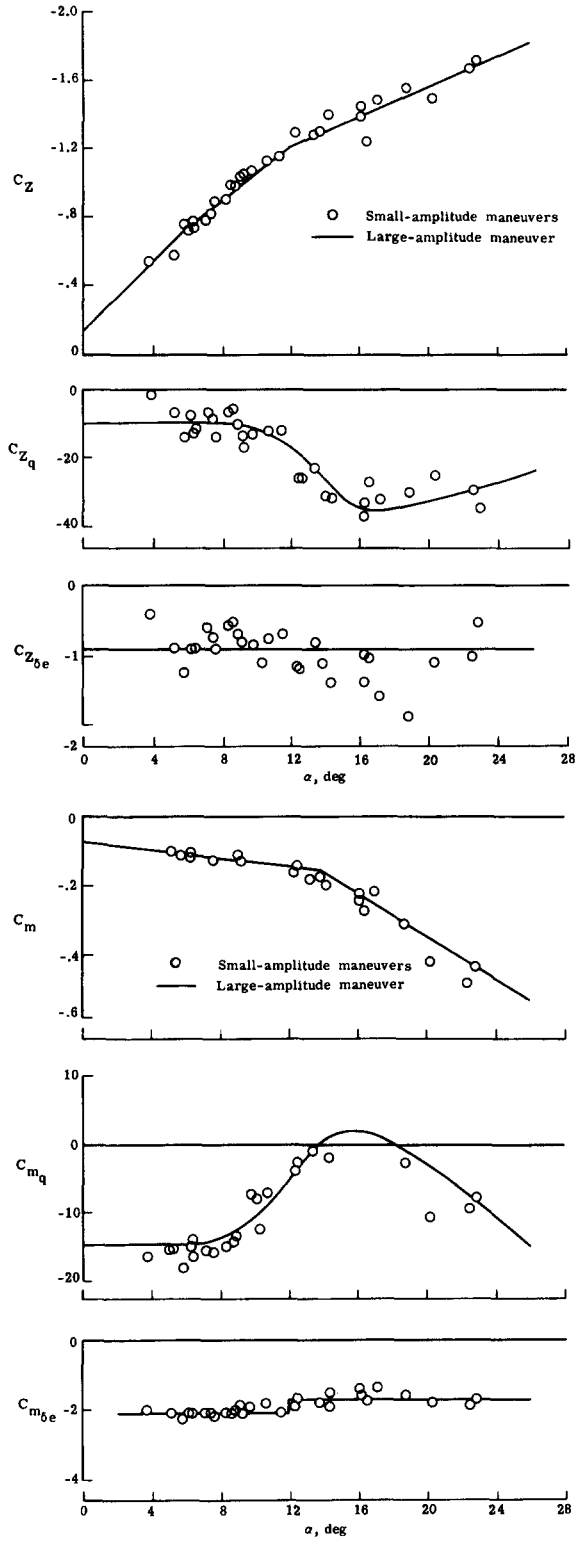

FIG. 29. Comparison of longitudinal parameters estimated from different maneuvers.

these estimates are consistent with the results from small-amplitude maneuvers. Some differences in derivatives of C_n arise for $\alpha > 13°$ and continue to $\alpha = 28°$. The reason for such a discrepancy might be explained by Fig. 34, in which the non-linearity of C_n with β for $\alpha > 15°$ is clearly shown. These estimates could not be achieved from the small-amplitude maneuvers

TABLE 7. COMPARISON OF STANDARD ERRORS AND SQUARED MULTIPLE CORRELATION COEFFICIENTS FROM DIFFERENT MANEUVERS FOR LONGITUDINAL DATA

Aerodynamic coefficient	Small-amplitude maneuvers				Large-amplitude maneuvers	
	$\hat{\sigma}$		R^2			
	Min.	Max.	Min.	Max.	$\hat{\sigma}$	R^2
C_X	0.0011	0.020	71.5	99.9	0.014	96.5
C_Z	0.0064	0.042	88.3	99.9	0.039	98.6
C_m	0.0052	0.028	89.1	99.5	0.033	93.5

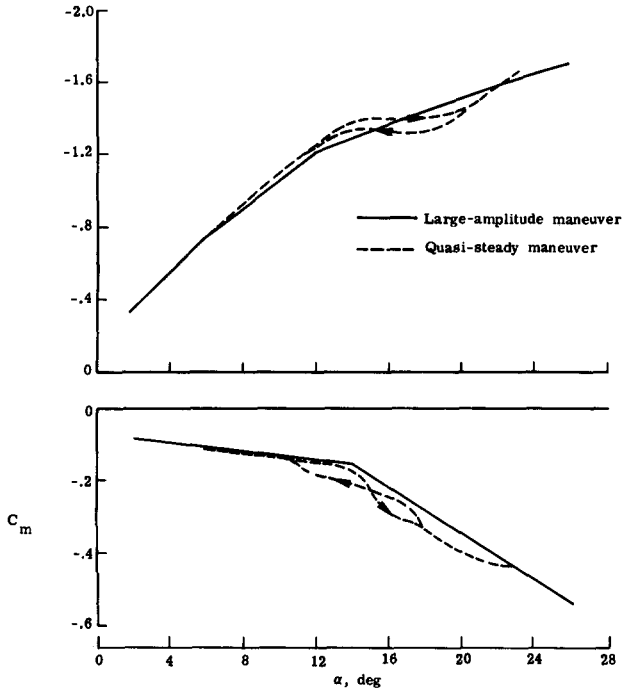

FIG. 30. Comparison of vertical-force and pitching-moment coefficient in steady conditions from different maneuvers.

and indicate the power of partitioning in achieving an aerodynamic model that is valid over a large range of angle-of-attack and sideslip.

For the verification of the estimated lateral parameters, the aerodynamic model from partitioned data was used. The equations of motion for $\alpha = 22.5°$ were integrated with the initial conditions and control time histories from a flight trimmed at $\alpha = 20°$. The control input for this independent maneuver consisted of a doublet in aileron followed by a doublet in rudder. The predicted time histories are plotted against the actual flight data in Fig. 35. The comparison of these time histories shows an acceptable agreement between them.

6. MAXIMUM LIKELIHOOD METHOD FOR PARAMETER ESTIMATION

The principle of maximum likelihood used in parameter estimation was introduced by R. A. Fisher in 1912 and further developed by him in a series of papers.[17] The use of this technique for the analysis of flight data was suggested in Ref. 15 and later expanded in Refs 28 and 65. Now there exists a great number of papers and reports with the application of ML estimation to various types of aircraft and flight conditions. A substantial part of these

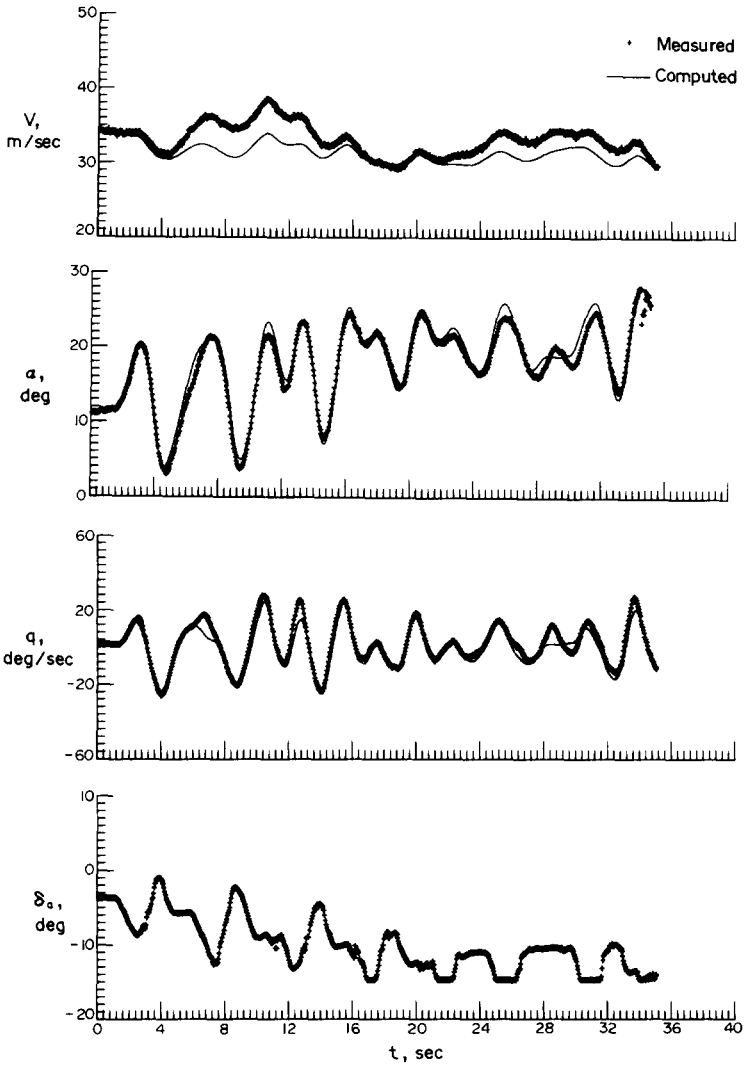

FIG. 31. Time histories of measured longitudinal flight data and those computed using parameters obtained by stepwise regression with spline approximation.

applications and new developments were initiated at NASA Ames/Dryden Flight Test Research Facility where the ML technique is being used extensively. Detailed treatment of the ML technique complete with examples and extensive lists of references can be found in Refs 49 and 50. Various computing algorithms and programs are presented in Refs 32, 46, 48, 55 and 62.

The development of the ML method assumes that the outcome Z of an experiment depends on unknown parameters θ. The ML estimates of the unknown parameters are those values of θ for which the observed value z would be 'most likely' to occur. 'Most likely' is defined to mean maximization of the so-called likelihood function. The likelihood function is the conditional probability density function of the observation z given θ. The problem of ML estimation can be therefore stated as

$$\hat{\theta} = \max\, p[z|\theta], \tag{6.1}$$

where $\hat{\theta}$ is the maximum likelihood estimation of θ and $p[z|\theta]$ is the conditional probability of z given θ.

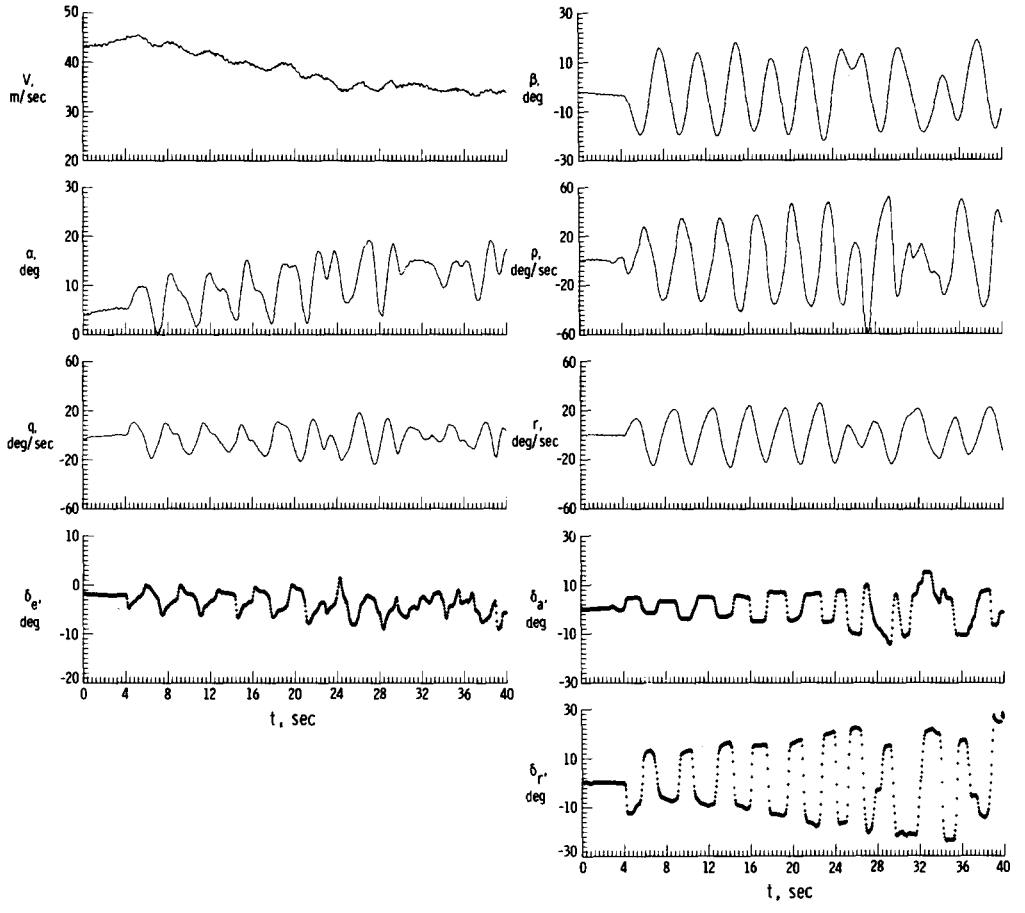

FIG. 32. Time histories of measured input and response variables in a large-amplitude maneuver.

6.1. SYSTEM WITH PROCESS NOISE

For the illustration of the ML estimation the scalar first-order system with process noise is considered. The model is formed as

$$\dot{x}(t) = \theta_1 x(t) + u(t) + w(t) \tag{6.2}$$

$$z(i) = x(i) + v(i) \tag{6.3}$$

$$i = 1, 2, \ldots, N,$$

where

$$E\{x(0)\} = x_0 \text{ and } E\{[x(0) - x_0]^2\} = p_0.$$

In Eqs (6.2) and (6.3) $w(t)$ and $v(i)$ are uncorrelated gaussian white noise sources with zero mean, that is

$$E\{w(t)\} = 0,\ E\{w(t)w(\tau)\} = q\,\delta(t-\tau)$$

$$E\{v(i)\} = 0,\ E\{v(i)v(j)\} = r\delta_{ij},$$

where $\delta(t-\tau)$ is the Dirac delta function, δ_{ij} is the Kronecker delta notation.

The vector of unknown parameters contains the coefficient θ_1, and the variances q and r, whereas x_0 and p_0 are assumed to be known. It means that

$$\theta = [\theta_1, q, r]^T.$$

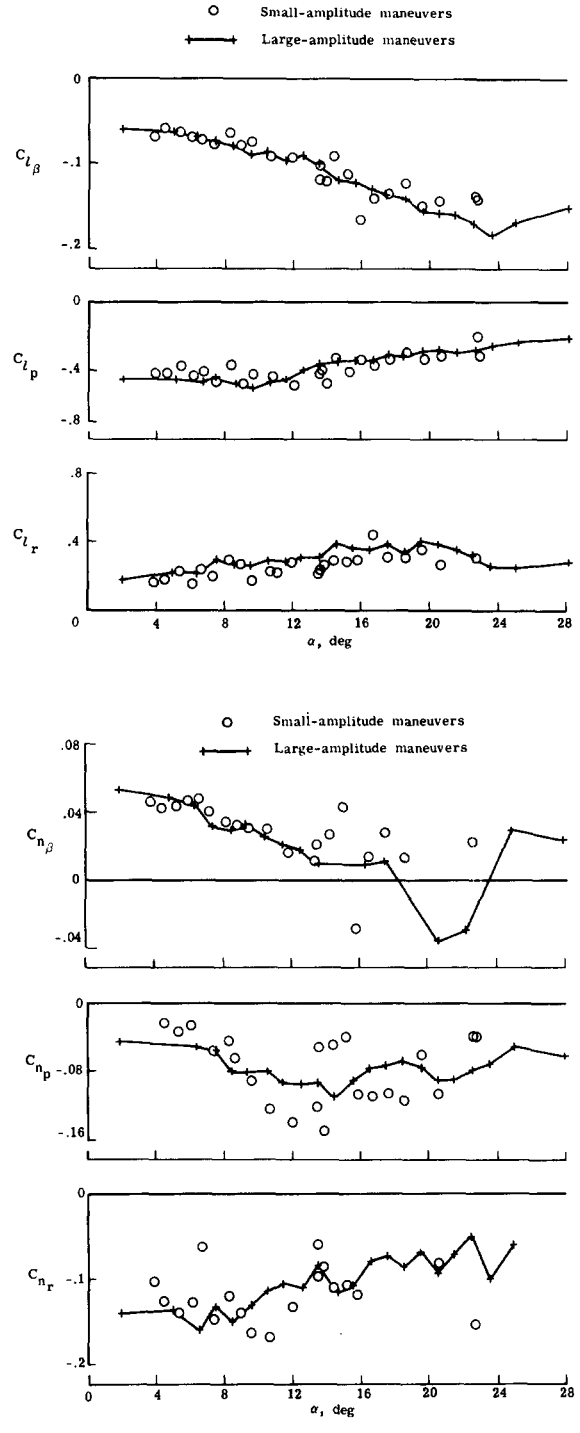

FIG. 33. Comparison of lateral stability derivatives estimated from small- and large-amplitude maneuvers with partitioned data.

The likelihood function is now

$$L(\theta) = p[z(1), z(2), \ldots, z(N)|\theta]. \tag{6.4}$$

To obtain this function, the vector Z_N consisting of all measured outputs is introduced

$$Z_N = [z(1), z(2), \ldots, z(N)]^T. \tag{6.5}$$

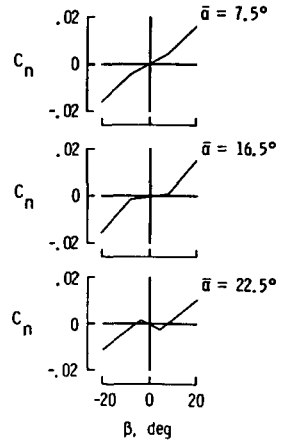

FIG. 34. Steady values of yawing-moment coefficient estimated from large-amplitude maneuvers with partitioned data.

If the probability distribution of Z_N has a density $p[Z_N|\theta]$, it then follows from the definition of conditional probabilities that

$$p[Z_N|\theta] = p[z(N)|Z_{N-1}, \theta]\, p[Z_{N-1}|\theta]. \tag{6.6}$$

Repeated use of this formula gives the following expression for the likelihood function

$$\begin{aligned} L(\theta) &= p[Z_N|\theta] = p[z(N)|Z_{N-1}, \theta]\, p[z(N-1)|Z_{N-2}, \theta] \cdots p[z(2)|z(1), \theta] p[z(1)] \\ &= \prod_{i=1}^{N} p[z(i)|Z_{i-1}, \theta]. \end{aligned} \tag{6.7}$$

To find the probability distribution of $z(i)$ given Z_{i-1} and θ, the mean value and variance are determined first. By definition

$$E\{z(i)|Z_{i-1}, \theta\} \triangleq \hat{y}(i|i-1),$$

which means that the expected value is the best possible estimate of measurement at a point given the measurements up to and including the previous point. From the definition of the variance it follows that

$$E\{[z(i) - \hat{y}(i|i-1)]^2\} = E\{v^2(i)\} \triangleq b(i)$$

where v are the innovations

$$v(i) = z(i) - \hat{y}(i|i-1). \tag{6.8}$$

It has been shown that for the high sampling rate the innovations $v(i)$ tend toward having a gaussian density. The distribution of $v(i)$ is, therefore, gaussian, also $z(i)$ given Z_{i-1} and θ is gaussian, i.e.

$$p[z(i)|Z_{i-1}, \theta] = \frac{1}{\sqrt{2\pi b(i)}} \exp\left\{-\frac{1}{2}\frac{v^2(i)}{b(i)}\right\}. \tag{6.9}$$

In the parameter estimation problem it is usually more convenient to work with the negative of the logarithm of the likelihood function. It is possible to do so because the logarithm is a monotonic function. From Eq. (6.9) the logarithm of the probability distribution is

$$\log p[z(i)|Z_{i-1}, \theta] = -\frac{1}{2}\frac{v^2(i)}{b(i)} - \frac{1}{2}\ln b(i) + \text{constant}. \tag{6.10}$$

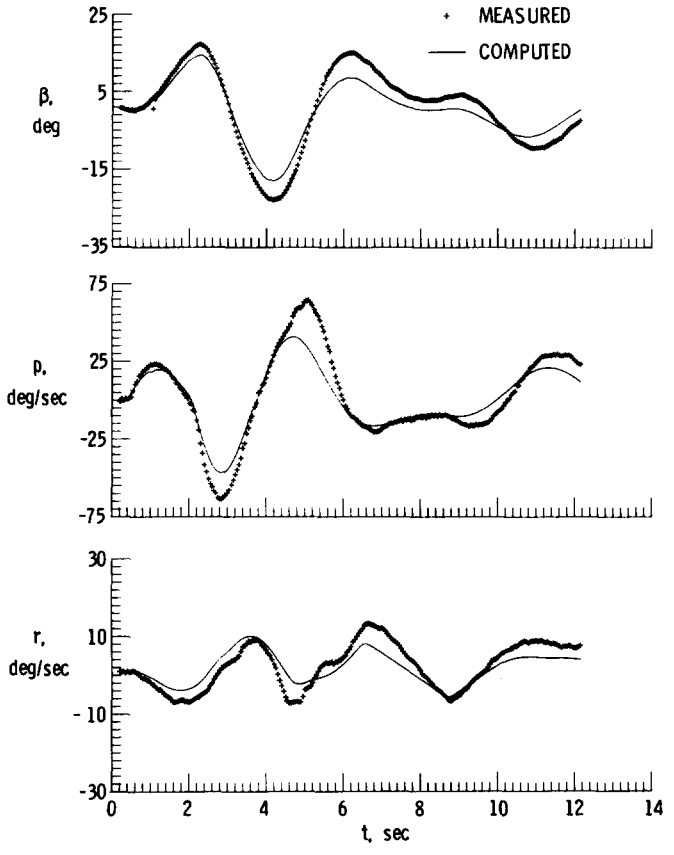

FIG. 35. Time histories of measured lateral flight data and those computed using parameters obtained by stepwise regression from partitioned data.

Then, using Eqs (6.7) and (6.10), the negative log–likelihood function can be written as

$$J(\theta)=\frac{1}{2}\sum_{i=1}^{N}\left\{\frac{v^2(i)}{b(i)}+\ln b(i)\right\}. \tag{6.11}$$

The log–likelihood function depends on the innovations and their covariance. To optimize this function, a way must be found for determining these quantities. Both innovations and their covariance are output of a Kalman filter. This filter is an algorithm which can be divided into two parts. In the first part, called the prediction equations, the state equations and state estimate covariance equations are propagated in time from one measurement point to the next. In the second part, called the measurement update equations, the measurements and associated measurement noise covariances are used to improve state covariance estimates.

The Kalman filter equations are developed, for example in Ref. 12. For the system described by Eqs (6.2) and (6.3) they are as follows:

The prediction equations:

$$\frac{\mathrm{d}}{\mathrm{d}t}\hat{x}(t|t_{i-1})=\theta_1\hat{x}(t|t_{i-1})+u(t),\ \hat{x}(t_0|t_0)=x_0 \tag{6.12}$$

$$\frac{\mathrm{d}}{\mathrm{d}t}p(t|t_{i-1})=2\theta_1 p(t|t_{i-1})+q,\ p(t_0|t_0)=p_0 \tag{6.13}$$

$$t_{i-1}\leqslant t\leqslant t_i.$$

The measurement update equations:

$$\hat{x}(i|i) = \hat{x}(i|i-1) + k(i)v(i) \tag{6.14}$$

$$p(i|i) = [1 - k(i)]p(i|i-1) \tag{6.15}$$

where

$$v(i) = y(i)\hat{x}(i|i-1) \tag{6.16}$$

$$k(i) = p(i|i-1)b^{-1}(i) \tag{6.17}$$

$$b(i) = p(i|i-1) + r. \tag{6.18}$$

The computing scheme of a Kalman filter for one stage is presented in Fig. 36.

The minimization of $J(\theta)$ with respect to θ subjected to the Kalman filter constraint leads to the non-linear parameter estimation. The solution to this problem can be found by using an iterative optimalization procedure. If the modified Newton–Raphson method (explained in the next section) is used the parameter estimates are obtained as

$$\hat{\theta} = \theta_0 - \bar{M}_0^1 \frac{\partial J}{\partial \theta}\bigg|_{\theta_0}, \tag{6.19}$$

where θ_0 is an initial estimate of θ, and M_0 and $\partial J/\partial\theta$ are computed for $\theta = \theta_0$. The gradient vector of the negative log-likelihood function is

$$\frac{\partial J(\theta)}{\partial \theta_k} = \sum_{i=1}^{N} \left\{ \frac{v}{b}\frac{\partial v}{\partial \theta_k} - \frac{1}{2}\frac{v^2}{b^2}\frac{\partial b}{\partial \theta_k} + \frac{1}{2b}\frac{\partial b}{\partial \theta_k} \right\}, \tag{6.20}$$

where θ_k is the kth component of the θ vector. The matrix M is now the so-called Fisher information matrix defined as

$$M = -E\left\{ \frac{\partial^2 J(\theta)}{\partial\theta\partial\theta^T} \right\}, \tag{6.21}$$

with the elements computed from the expression

$$M_{kl} = \sum_{i=1}^{N} \left\{ \frac{1}{b}\frac{\partial v}{\partial \theta_l}\frac{\partial v}{\partial \theta_k} - \frac{v}{b^2}\left[\frac{\partial b}{\partial \theta_l}\frac{\partial v}{\partial \theta_k} + \frac{\partial v}{\partial \theta_l}\frac{\partial b}{\partial \theta_k} \right] + \left(\frac{v^2}{b^3} - \frac{1}{2b^2} \right)\frac{\partial b}{\partial \theta_l}\frac{\partial b}{\partial \theta_k} \right\}. \tag{6.22}$$

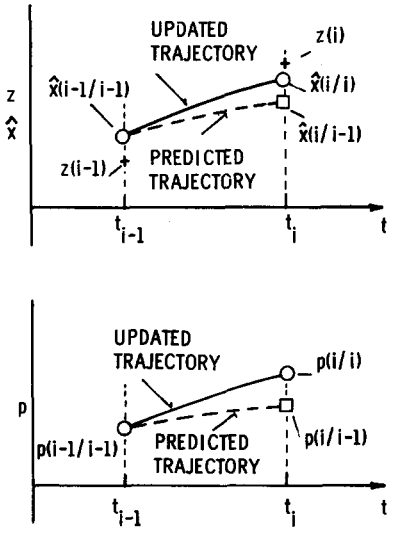

FIG. 36. Computing scheme for Kalman filter.

The partial derivatives in Eqs (6.20) and (6.22) represent sensitivities in v and b. Because of Eqs (6.16) and (6.18) they can be written as

$$\frac{\partial v}{\partial \theta_k} = -\frac{\partial \hat{x}(i|i-1)}{\partial \theta_k}$$

$$\frac{\partial b}{\partial \theta_k} = \frac{\partial p(i|i-1)}{\partial \theta_k} + \frac{\partial r}{\partial \theta_k}.$$

The sensitivity equations follow from Kalman filter Eqs (6.12) to (6.15) as

$$\frac{\mathrm{d}}{\mathrm{d}t}\frac{\partial \hat{x}(t|t_{i-1})}{\partial \theta_k} = \theta_1 \frac{\partial \hat{x}(t|t_{i-1})}{\partial \theta_k} + \frac{\partial \theta_1}{\partial \theta_k}\hat{x}(t|t_{i-1}), \quad \frac{\partial \hat{x}(t_0|t_0)}{\partial \theta_k} = 0$$

$$\frac{\mathrm{d}}{\mathrm{d}t}\frac{\partial p(t|t_{i-1})}{\partial \theta_k} = 2\theta_1 \frac{\partial p(t|t_{i-1})}{\partial \theta_k} + 2\frac{\partial \theta_1}{\partial \theta_k} p(t|t_{i-1}) + \frac{\partial q}{\partial \theta_k}, \quad \frac{\partial p(t_0|t_0)}{\partial \theta_k} = 0$$

$$\frac{\partial \hat{x}(i|i)}{\partial \theta_k} = \frac{\partial \hat{x}(i|i-1)}{\partial \theta_k} + \frac{\partial k(i)}{\partial \theta_k} v(i) + k(i)\frac{\partial v(i)}{\partial \theta_k}$$

$$\frac{\partial p(i|i)}{\partial \theta_k} = [1-k(i)]\frac{\partial p(i|i-1)}{\partial \theta_k} - \frac{\partial k(i)}{\partial \theta_k} p(i|i-1),$$

where

$$\frac{\partial k(i)}{\partial \theta_k} = \frac{\partial p(i|i-1)}{\partial \theta_k} b^{-1}(i) - \frac{1}{b^2(i)}\frac{\partial b(i)}{\partial \theta_k} p(i|i-1).$$

After obtaining the estimates from (6.19) these values are used as new initial values θ_0 and the whole process is repeated until some convergence criteria are met. A simplified block-scheme of the ML method is given in Fig. 37.

The final ML estimates of unknown parameters have the following main properties:[5, 49]

(1) they are consistent, i.e.

$$\lim_{t\to\infty} P\{|\theta(t)-\theta| \leqslant \varepsilon\} = 1$$

with ε arbitrarily small

where $P\{\ \}$ indicates the probability and θ the true value of parameters,

(2) they are asymptotically unbiased, i.e.

$$\lim_{t\to\infty} E\{\hat{\theta}(t)\} = \theta$$

(3) they are asymptotically efficient with

$$E\{(\hat{\theta}-\theta)(\hat{\theta}-\theta)^T\} \geqslant -E\left\{\frac{\partial^2 J(\theta)}{\partial\theta\partial\theta^T}\right\}^{-1}. \tag{6.23}$$

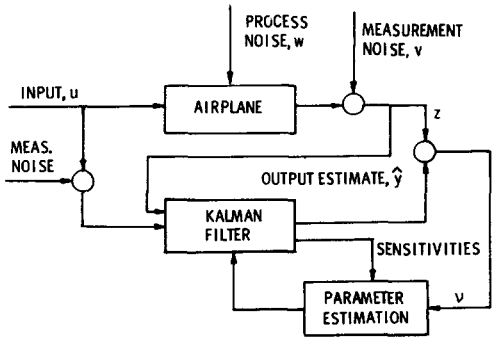

FIG. 37. Computing scheme for parameter estimation using maximum likelihood method.

Because of Eqs (6.21) and (6.23), the inverse of the information matrix provides the lower bounds on the variance and the covariance of the errors in the estimated parameters. This lower bound is known as the Cramer–Rao lower bound and is to be viewed as the maximum achievable accuracy in the parameter estimates.

(4) They are asymptotically normal, that is, they approximate the gaussian distribution with the mean θ and covariance M^{-1}.

The ML estimation method in the form presented can be rather time consuming even for a simple scalar system. Substantial simplification can be achieved by assuming that the process noise is absent. If the process noise is zero and the initial state is known, the covariance of the error in the predicted state is also zero. For the system under investigation it follows from (6.17) that the Kalman gain is zero and the innovations are the output errors

$$v(i)=z(i)-\hat{x}(i). \tag{6.22}$$

The innovation variance is $b(i)=r$ and the negative log–likelihood function is simplified as

$$J(\theta)=\frac{1}{2r}\sum_{i=1}^{N} v^2(i)+\frac{N}{2}\ln r. \tag{6.23}$$

When (6.23) is optimized for the unknown parameter r it gives

$$\hat{r}=\frac{1}{N}\sum_{i=1}^{N} v^2(i). \tag{6.24}$$

Substituting $\hat{r}$ into (6.23) the log–likelihood function can be written as

$$J(\theta)=\frac{1}{2\hat{r}}\sum_{i=1}^{N} v^2(i)+\text{constant}. \tag{6.25}$$

Expression (6.25) is the same as the cost function for the output error method with the measurement noise variance used as a weight.

For the case when no measurement noise in the state variable exists, the log–likelihood function is formulated as

$$J(\theta)=\frac{1}{2\sigma^2}\sum_{i=1}^{N}[\dot{z}(i)-\theta_1 x(i)-u(i)]^2, \tag{6.26}$$

which is the sum of squares of the equation error at sampling times. Thus, the ML estimates are identical to the LS estimates where

$$\sigma^2=E\{[\dot{z}(i)-\dot{x}(i)]^2\}$$

is assumed to be known.

6.2. Output Error Method

The ML method outlined in the preceding section can be extended for a linear or non-linear system representing an aircraft.[31, 65] In these cases the negative log–likelihood

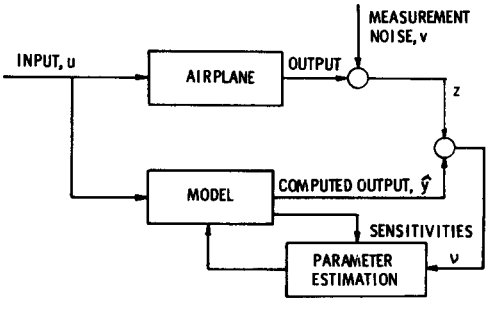

FIG. 38. Computing scheme for parameter estimation using output error method.

function is formulated as

$$J(\theta)=\frac{1}{2}\sum_{i=1}^{N} v^T(i)B^{-1}(i,\theta)v(i)+\frac{N}{2}\ln|B(i,\theta)| \tag{6.27}$$

where

$$B(i,\theta)\triangleq E\{v(i)v^T(i)\}.$$

For a practical use in aircraft parameter estimation no process noise is considered. This means the assumption of perfect state variable model with no external disturbances. Then the simplified ML estimation algorithm can be developed for a model

$$\dot{x}=f(x,u,\theta),\ x(0)=x_0$$

$$y=h(x,u,\theta),$$

which is completed by the measurement equation in discrete form

$$z(i)=y(i)+v(i),\ i=1,2,\ldots,N.$$

The measurement noise is assumed to be gaussian with

$$E\{v(i)\}=0,\ E\{v(i)v^T(j)\}=R\delta_{ij}.$$

For the case with no process noise the negative log–likelihood function is simplified as

$$J(\theta)=\frac{1}{2}\sum_{i=1}^{N} v^T(i)R^{-1}v(i)+\frac{N}{2}\ln|R| \tag{6.28}$$

where

$$v(i)=z(i)-y(i,\hat{\theta}). \tag{6.29}$$

In the expression for $J(\theta)$ it is assumed that the unknowns are the aircraft aerodynamic parameters and elements of the R matrix. The initial conditions could also be included among the unknowns but it is preferred to estimate x_0 as part of the data compatibility check.

The unknown R is estimated by minimization of the likelihood function with respect to R. This produces

$$\hat{R}=\frac{1}{N}\sum_{i=1}^{N} v(i)v^T(i), \tag{6.30}$$

where the residuals are completed from (6.29) for $\hat{\theta}=\theta_0$. After substituting the estimated $\hat{R}$ into Eq. (6.28) the cost function for the output error is obtained as

$$J(\theta)=\sum_{i=1}^{N} v^T(i)\hat{R}^{-1}v(i). \tag{6.31}$$

The modified Newton–Raphson method accomplishes the minimization of (6.31) by expanding the computed output vector about θ_0, the initial unknown parameter vector. A Taylor series expansion of y retaining only linear terms is

$$y(\hat{\theta})=y(\theta_0)+\left.\frac{\partial y}{\partial\theta}\right|_{\theta_0}\Delta\theta, \tag{6.32}$$

where $\Delta\theta=\hat{\theta}-\theta_0$. Substituting (6.32) into (6.31) results in a quadratic approximation of J with $\Delta\theta$ as unknowns. Differentiating J with respect to θ and equating the derivative to zero results in

$$\frac{\partial J(\theta)}{\partial\theta}=\sum_{i=1}^{N} H^T(i)\hat{R}^{-1}v(i)+\sum_{i=1}^{N} H^T(i)\hat{R}^{-1}H(i)\Delta\theta=0 \tag{6.33}$$

where

$$H(i)=\frac{\partial y_k(i)}{\partial \theta_l},$$

and y_k and θ_l are both kth and lth elements of y and θ respectively. Solving (6.33) for $\Delta\theta$ gives

$$\Delta\hat{\theta}=\left[\sum_{i=1}^{N} H^T(i)\hat{R}^{-1}H(i)\right]^{-1}\sum_{i=1}^{N} H^T(i)\hat{R}^{-1}v(i), \tag{6.34}$$

which is often written as

$$\Delta\hat{\theta}=-M_0^{-1}\left.\frac{\partial J}{\partial\theta}\right|_{\theta_0}. \tag{6.19}$$

The approximation to the Fisher information matrix is obtained from

$$M=\sum_{i=1}^{N} H^T(i)\hat{R}^{-1}H(i).$$

The elements of the sensitivity matrix H can be computed by solving sensitivity equations

$$\frac{\mathrm{d}}{\mathrm{d}t}\frac{\partial x}{\partial\theta_l}=\frac{\partial f}{\partial x}\frac{\partial x}{\partial\theta_l}+\frac{\partial f}{\partial\theta_l}$$

$$\frac{\partial y}{\partial\theta_l}=\frac{\partial h}{\partial x}\frac{\partial x}{\partial\theta_l}+\frac{\partial h}{\partial\theta_l}.$$

The other possibility is to compute the sensitivities by a numerical method. The simplest one is using a finite difference approximation to $y(\theta)$. A more accurate and efficient method based on surface approximation of $y(\theta)$ is developed in Ref. 55.

For the rth iteration the estimates $\hat{\theta}_{r+1}$ are obtained from

$$\hat{\theta}_{r+1}=\hat{\theta}_r+\Delta\hat{\theta}_{r+1}.$$

In Ref. 55 the convergence criteria were selected as

$$\frac{J_r-J_{r-1}}{J_r}=0.001 \text{ and } \frac{\Delta\theta_r}{\theta_r}=0.001.$$

The accuracy of the parameters is given by the inverse of the information matrix, M^{-1}. As was pointed out in the preceding section, the diagonal elements of M^{-1} form the Cramer–Rao lower bound on parameter variance. The off-diagonal terms are the covariances $\sigma_k\sigma_l\rho_{kl}$ where the correlation coefficient ρ_{kl} is a measure of the statistical dependence between parameters θ_k and θ_l. Although the Cramer–Rao bound is commonly used to qualify the accuracy of the ML parameter estimates, it is also well known that in aircraft applications these bounds do not accurately reflect the true parameter variance. The difference between the lower bound and the actual parameter variance can be due to incorrect assumptions about the measurement and process noise or due to modeling errors in the state and output equations. Also the non-linearity of the estimation problem appears to contribute significantly. A problem of the accuracy of estimated parameters is discussed in Ref. 47. An approach for determining confidence intervals by the analysis of confidence region contours is presented in Refs 55 and 56.

6.3. Examples

Parameter estimates obtained by the ML method have already been introduced in Examples 5.1 and 5.2. In this section two more examples are given. As in the previous cases the measured data were taken from the measurement of a general aviation aircraft.[37, 40]

Example 6.1. The ML estimates presented here are obtained from the identical data set used in Example 5.1. The results from eight repeated lateral maneuvers are summarized in

Table 8. Similar to Table 5 they include the ensemble mean values and standard errors, average Cramer–Rao lower bounds on standard errors of a single measurement and finally the ratios of the ensemble standard error to the Cramer–Rao bound. Thus, the last column of Table 8 indicates the differences between the lower bounds and the estimates of standard errors based on repeated measurements. These differences are pronounced mainly for parameters in the yawing-moment equation which is in agreement with the results in Table 5.

For the further demonstration of the accuracy of estimated parameters, their values from 28 runs were plotted against the lift coefficient, C_L. The values of six stability derivatives are included in Figs 39 and 40 together with the fitted lines. The consistency of results is worse

TABLE 8. PARAMETER AND THEIR STANDARD ERRORS ESTIMATED FROM REPEATED MEASUREMENTS BY MAXIMUM LIKELIHOOD METHOD

Parameter	Mean value $\bar{\Theta}$ (*)	Standard errors $s(\hat{\Theta})$ (†)	Standard errors $s(\hat{\Theta})$ lower bound (‡)	Ratio (†)/(‡)
C_{Y_β}	−0.649	0.0097	0.0064	1.5
C_{Y_p}	−0.09	0.12	0.016	7.5
$C_{Y_{\delta_r}}$	0.094	0.014	0.0068	2.1
C_{l_β}	−0.0816	0.0042	0.00079	5.3
C_{l_p}	−0.559	0.053	0.0055	9.6
C_{l_r}	0.13	0.027	0.0053	5.1
$C_{l_{\delta a}}$	−0.241	0.022	0.0018	12.2
$C_{l_{\delta r}}$	0.007	0.0068	0.0012	5.7
C_{n_β}	0.0772	0.0055	0.00031	17.7
C_{n_p}	−0.024	0.031	0.0028	11.1
C_{n_r}	−0.145	0.030	0.0022	13.6
$C_{n_{\delta a}}$	0.024	0.0096	0.0010	9.6
$C_{n_{\delta r}}$	−0.074	0.0073	0.00060	12.2

* Ensemble mean value.
† Ensemble standard error.
‡ Average standard error of estimates.

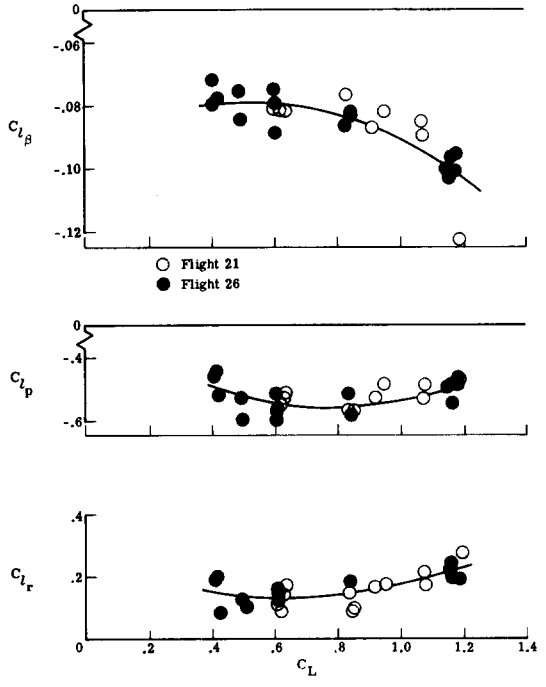

FIG. 39. Estimated rolling-moment stability derivatives from flight data using maximum likelihood method.

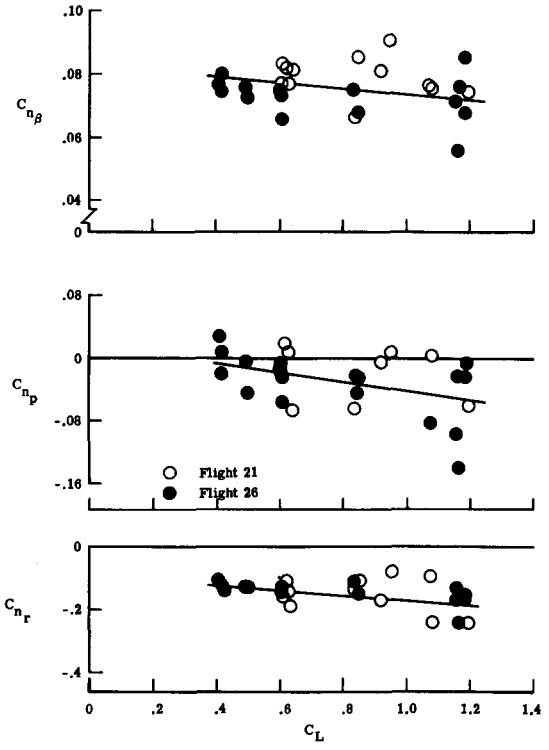

FIG. 40. Estimated yawing-moment stability derivatives from flight data using maximum likelihood method.

for the yawing-moment stability derivatives than that for the rolling-moment derivatives, a phenomenon already confirmed by results in Tables 5 and 8, and Fig. 20.

Measured flight data time histories and those computed by using the ML parameter estimates are compared in Fig. 41 for one selected run. The corresponding residuals are shown in Fig. 42 together with the standard errors of measured output variables. For some variables the residuals exhibit substantial departure from random behavior thus indicating a presence of modeling errors and/or uncorrected bias errors in measured data. A comparison of LS and ML estimates in this example and Example 5.1 indicates no significant differences between the two sets of results.

Example 6.2. In this example a comparison is made between the LS and ML estimates of several parameters over a wide range of the angle-of-attack. In Fig. 43, the three important longitudinal stability parameters estimated from 30 small-amplitude maneuvers are plotted against the angle-of-attack corresponding to the trimmed conditions. All these maneuvers were analyzed by the modified stepwise regression (MSR). Although the definition of 'best model' is subjective and an exhaustive search of all candidate models is prohibitive in both cost and time, experience has shown that the MSR gives an adequate model. For the verification of results obtained, the maximum likelihood estimation technique was applied to nine test runs. In this analysis, the model structure was the same as determined by MSR. The ML estimates are represented in Fig. 43 by closed circles. Also plotted in Fig. 43 are the parameters estimated from steady flight using expressions from Section 2.

The values of three lateral parameters obtained from 30 small-amplitude lateral maneuvers are given in Fig. 44. In this case the yawing-moment derivatives were selected. These parameters exhibit large scatter mainly in the stall and post-stall region. This scatter is caused by small excitation of yawing motion of the tested airplane. The estimates of the remaining lateral parameters are shown subsequently to be more consistent. As in the previous case, some runs were also analyzed by the ML method, and the results are presented in Fig. 44. The results in Figs 43 and 44 again demonstrate that a good agreement

between parameters obtained by linear regression and the maximum likelihood estimation method can be achieved if sufficient care is taken in the design of an experiment, data processing and selection of an adequate model.

7. DATA COLLINEARITY AND BIASED ESTIMATION

The introduction of highly maneuverable, highly augmented and often inherently unstable aircraft has been presenting new challenges to aircraft identification and parameter

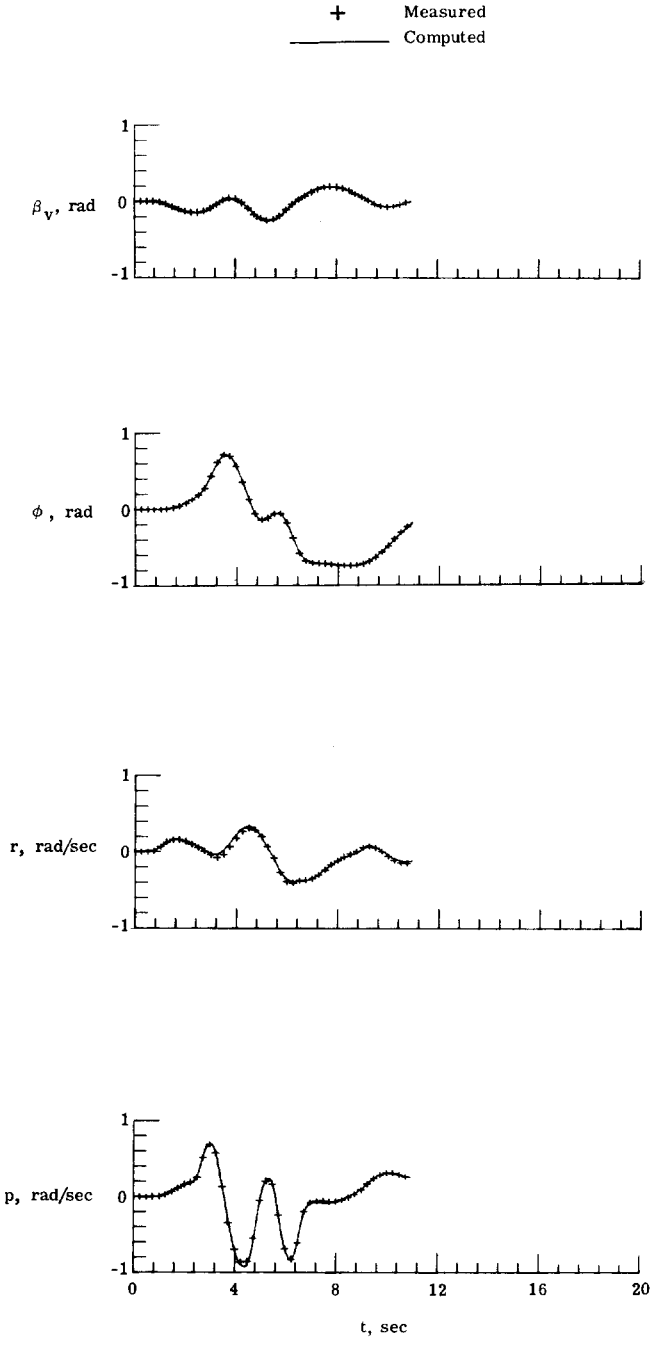

FIG. 41.

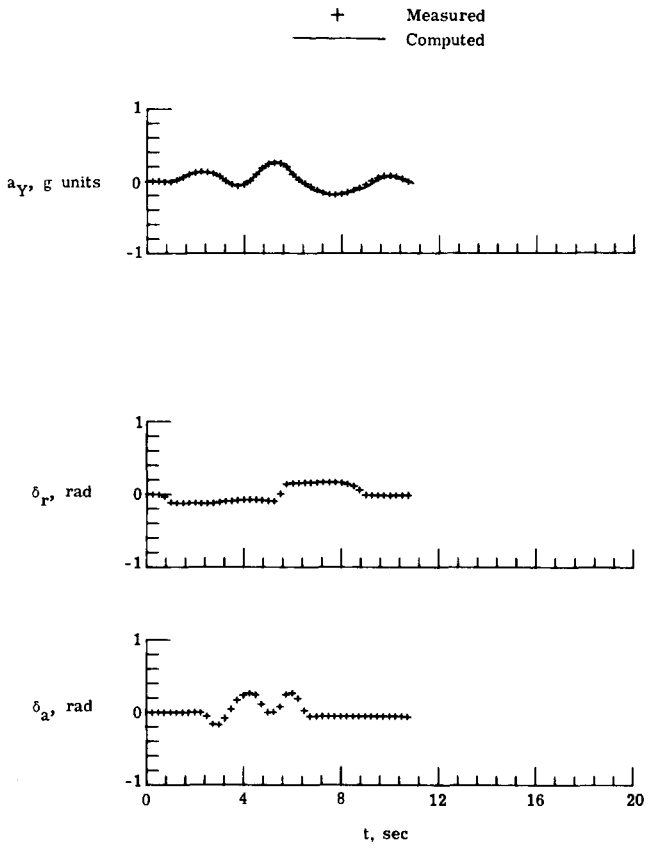

FIG. 41. Measured lateral flight data histories and those computed using parameters obtained by equation error method.

estimation. These new aircraft may have more control surfaces which are moved through a flight control system. Such a system can introduce a close relationship between deflections of various surfaces and at the same time can preclude maneuvers suitable for system identification. These characteristics can be reflected in the inability to estimate the effectiveness of individual control surfaces and to obtain accurate estimates of the remaining parameters. One of the reasons for these problems are related to the near linear relationship among several variables entering the model for various estimation techniques.

Near linear dependency among variables in the linear regression, often called collinearity, has been studied by many statisticians.[10, 53] In this paper the collinearity in a model for linear regression, detection of collinearity and its remedy will be briefly discussed.

As was shown before, the linear regression model (5.2) can be formulated as

$$Y = X\theta + \varepsilon, \tag{7.1}$$

where X is the matrix of regressors and ones.

For further discussion and analysis it will be more convenient to deal with regressor variables which are centered and scaled to unit length.[15] There, the matrix X^TX is the $(n \times n)$ matrix of correlations, $R = X^TX$, because the off-diagonal elements of R are quite often referred to as correlation coefficients, although the regressors are not necessarily random variables. Denoting $X_j, j = 1, 2, \ldots, n$, as the columns of the X matrix with centered and scaled regressors, the matrix X can be expressed as

$$X = [X_1, X_2, \ldots, X_n]. \tag{7.2}$$

If $X_j^TX_k = 0, j \neq k$, the regressors are orthogonal and the R matrix is a diagonal matrix. The vectors $X_1, X_2, \ldots, X_{n--}$ are called linearly dependent if there is a set of constants, a_j, not

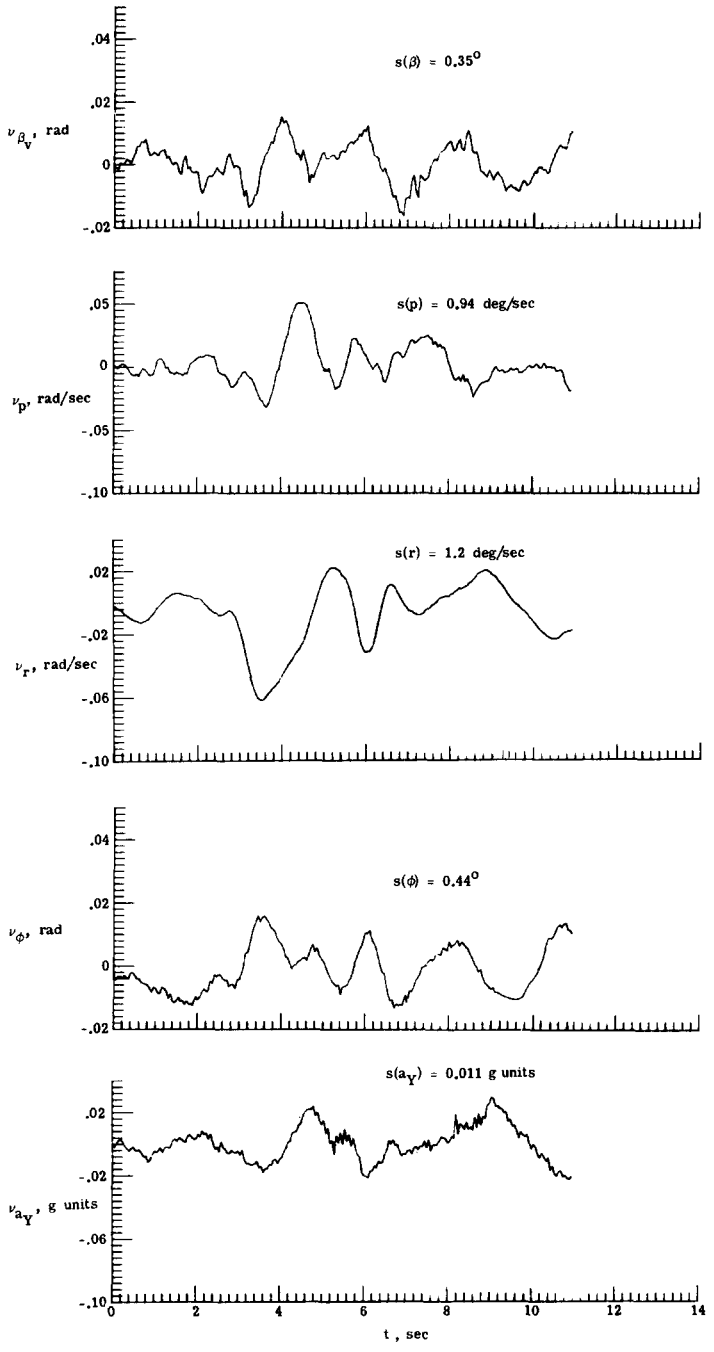

FIG. 42. Time histories and standard errors of residuals.

all zero, such that

$$\sum_{j=1}^{n} a_j X_j = 0. \tag{7.3}$$

Then, the rank of $X^T X$ is less than n and $(X^T X)^{-1}$ does not exist.

In many practical applications of linear regression Eq. (7.3) is only approximately true. This indicates near linear dependency in X and the problem of collinearity exists. In such cases $X^T X$ is ill-conditioned. Because that collinearity can cause computational problems and reduce the accuracy of estimates. Thus in the context of linear regression, collinearity is a data problem, not a statistical phenomenon.

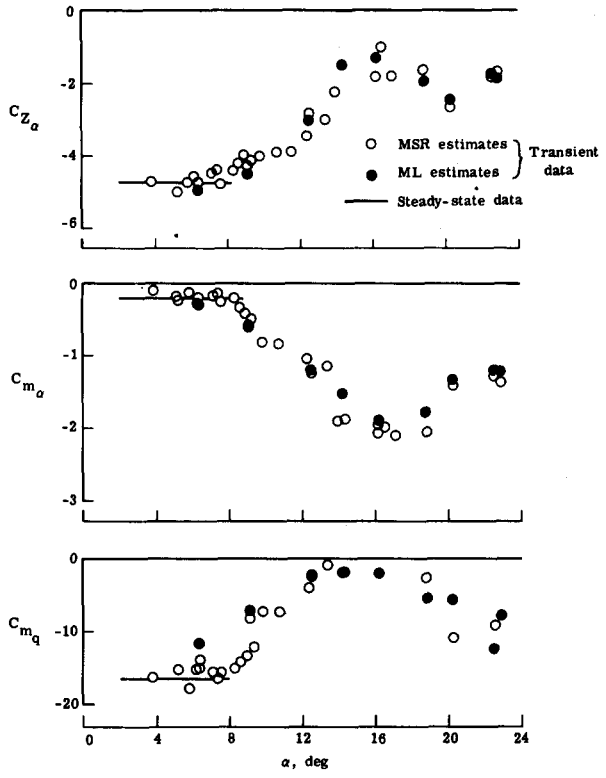

FIG. 43. Estimated longitudinal parameters from steady flights and transient maneuvers.

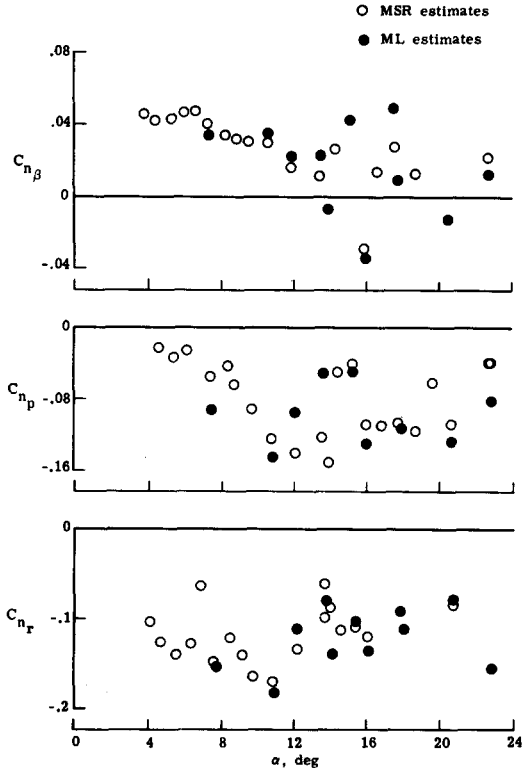

FIG. 44. Estimated lateral parameters from transient maneuvers.

There are at least three different sources of collinearity, namely

(a) design of an experiment,
(b) constraints in the data,
(c) model specification.

If the experiment is designed in such a way that the resulting data is specified mostly on a subspace of the region defined approximately by (7.3), then collinearity might occur. This type of problem can arise during the test of a dynamic system where one or more variables representing regressors in (7.1) were not sufficiently excited. The constraints in the data could be caused by an inherent property of the system under test. For example, aircraft stability augmentation systems can deflect various control surfaces in concert thus causing near linear dependence among their deflections. Finally, to avoid collinearity, a specified model should not be over parameterized. For example, it should not include non-linear terms, such as x_1^2, or x_1, x_2, if x_1, is small.

The presence of collinearity usually results in various unwanted properties of the least squares estimates of unknown parameters. Two of them, illustrated in Ref. 53, include too large absolute values for parameter estimates and their large variances and covariances. Many procedures have been employed for detecting collinearity.[53] The three often used are:

(1) examination of the correlation matrix and its inverse,
(2) eigensystem analysis and singular value decomposition,
(3) parameter variance decomposition.

Examination of the correlation matrix and its inverses is the simplest and most straightforward procedure. A high correlation coefficient between two regressors can point to a possible collinearity problem. The absence of high correlation, however, cannot be viewed as evidence of no problem. The correlation matrix is unable to reveal the presence of several coexisting near dependencies among the regressors.[53] Because of shortcomings mentioned in regard to the use of R as a diagnostic measure of collinearity, the usefulness of its inverse is also limited.

For the eigensystem analysis the correlation matrix is decomposed as

$$X^T X = T^T \Lambda T, \tag{7.4}$$

where Λ is a $(n \times n)$ diagonal matrix whose diagonal elements are the eigenvalues λ_j, $j = 1, 2, \ldots, n$, of $X^T X$, and T is an orthogonal matrix whose columns are the eigenvectors of $X^T X$. The eigenvalues close to zero indicate near linear dependency in the data. The elements of the corresponding eigenvectors could reveal the nature of this dependency. Collinearity is, therefore, indicated by the presence of a "small' eigenvalue. Unfortunately there is no specification of what "small" is. In order to avoid this problem some authors are using the condition number of $X^T X$ defined as

$$\kappa_j = \frac{\lambda_{\max}}{\lambda_j}, \quad j = 1, 2, \ldots, n. \tag{7.5}$$

Then, they consider the condition number exceeding 1000 as an indication of severe collinearity.[10]

An approach using singular-value decomposition for diagnosing collinearity is proposed in Ref. 10. It is based on the decomposition of matrix X as

$$X = UDT^T \tag{7.6}$$

where U is a $(N \times n)$ matrix and $U^T U = T^T T = I$. The matrix D is a $(n \times n)$ diagonal matrix with non-negative diagonal elements μ_j, $j = 1, 2, \ldots, n$, which are called the singular values of X. The singular-value decomposition (SVD) is closely related to the concept of eigenvalues and eigenvectors, since from (7.4) and (7.6)

$$X^T = TD^2 T^T = T \Lambda T^T. \tag{7.7}$$

The diagonal elements of D^2 are therefore the eigenvalues of X^TX and the columns of U are the eigenvectors of X^TX associated with its n non-zero eigenvalues. The degree of ill-conditioning depends on how small the singular value is relative to the maximum singular value. In this connection a condition index of the matrix X is proposed as

$$\eta_j = \frac{\mu_{\max}}{\mu_j}, \quad j = 1, 2, \ldots, n. \tag{7.8}$$

It is further suggested considering η_j from 30 to 100 as evidence of moderately to strongly collinear data.

The SVD of the matrix X provides similar information to that given by the eigensystem of X^TX. The use of SVD is, however, preferred by many authors, mainly because of greater numerical stability of its computing in comparison to that of the eigensystem of X^TX. This may be especially true when X^TX is ill-conditioned. On the other hand, computing problems of SVD may arise when the number of data points is too large.

The parameter variance decomposition approach for detecting collinearity was proposed in Ref. 10. It follows from the covariance matrix of parameter estimates $\hat{\theta}$ which is obtained as

$$\mathrm{Cov}\{\hat{\theta}\} = \sigma^2 X^T X = \sigma^2 T^T \Lambda T. \tag{7.9}$$

The variance of each parameter is equal to

$$\sigma^2(\hat{\theta}_j) = \sigma^2 \sum_{k=1}^{n} \frac{t_{jk}^2}{\lambda_j} = \sigma^2 \sum_{k=1}^{n} \frac{t_{jk}^2}{\mu_j^2}, \tag{7.10}$$

where t_{jk} are the elements of eigenvector t_j associated with λ_j. Equation (7.10) decomposes the variance of each parameter into a sum of components, each corresponding to one and only one of the n singular values μ_j. In (7.10) the singular values appear in the denominator, so one or more small singular values can substantially increase the variance of θ_j. This means that an unusually high proportion of the variance of two or more coefficients for the same small singular value can provide evidence that the corresponding near dependency is causing problems. Introducing

$$\phi_{jk} = \frac{v_{jk}^2}{\mu_j^2} \text{ and } \phi_j = \sum_{k=1}^{n} \phi_{jk},$$

the j, k variance proportion as the proportion of the variance of the jth regression coefficient associated with the kth components of its decomposition in Eq. (7.10) is given as

$$\pi_{kj} = \frac{\phi_{jk}}{\phi_j}, \quad j, k = 1, 2, \ldots, n. \tag{7.11}$$

Since two or more regressors are required to create near dependency then two or more variances will be adversely affected by high variance proportions associated with a single singular value. Variance proportions greater than 0.5 are recommended as a guideline for possible collinearity problems.[10]

There are several ways of dealing with the problem of collinearity. They include a collection of additional data, redesign of an experiment, model respecification and use of different estimation techniques from the ordinary least squares procedure. This report will address only the last possibility mentioned.

As discussed previously, the application of ordinary least squares technique to the set of data with collinearity problems can result in large estimated values for parameters and large values for their covariances. The least squares technique provides an unbiased estimator which, according to the Gauss–Markoff theorem, has minimum variance in the class of unbiased linear estimators. There is no guarantee, however, that this variance will be small. Figure 45 illustrates a situation of two distributions of a parameter estimate. One estimate, $\hat{\theta}$, is unbiased (a possible result of least squares technique), the other, $\tilde{\theta}$, is biased (obtained by a biased estimation technique). In the first case the variance of $\hat{\theta}$ is large, indicating a large confidence interval on θ and unstable point estimate $\hat{\theta}$. In the second case the estimate $\tilde{\theta}$ is

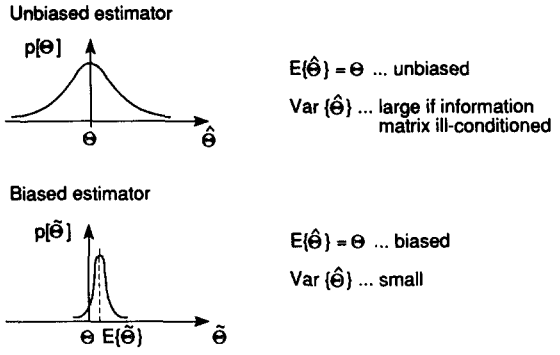

FIG. 45. Distributions of unbiased and biased estimators of θ.

subjected to bias error, $E(\tilde{\theta})-\theta$, but much smaller variance. The resulting mean square error of the estimator $\tilde{\theta}$ is

$$\text{MSE}(\tilde{\theta})=E\{\tilde{\theta}-\theta\}^2=\sigma^2(\tilde{\theta})+[E\{\tilde{\theta}\}-\theta]^2. \tag{7.12}$$

It is possible that for small bias error the MSE $(\tilde{\theta})$ could be smaller than the variance of the least squares estimator $\sigma^2(\hat{\theta})$. This possibility has inspired a development of various biased estimation techniques.[53] Two of them, the principal components regression and mixed estimation, will be described and applied to experimental data.

7.1. Principal Components Regression

The development of principal components regression starts by transforming the original regressors x_j to the space of orthogonal regressors z_j. This transformation is accomplished by letting

$$Z=XT \tag{7.13}$$

and

$$\theta=T\gamma. \tag{7.14}$$

The columns of Z, formed by the orthogonal regressors z_j, are referred to as principal components. After, the transformation regression model becomes

$$Y=Z\gamma=\varepsilon. \tag{7.15}$$

The least squares estimates of γ are formed as

$$\hat{\gamma}=(Z^TZ)^{-1}Z^TY=\Lambda^{-1}Z^TY, \tag{7.16}$$

and the covariance matrix of $\hat{\gamma}$ as

$$\text{Cov}\{\hat{\gamma}\}=\sigma^2\Lambda^{-1} \tag{7.17}$$

Because of the orthogonality of regressors, Eq. (7.16) can also be expressed as

$$\hat{\gamma}=\sum_{j=1}^{n}\frac{1}{\lambda_j}t_j^TX^TY. \tag{7.18}$$

and Eq. (7.17) as

$$\text{Cov}\{\hat{\gamma}\}=\sigma^2\sum_{j=1}^{n}\frac{1}{\lambda_j}. \tag{7.19}$$

The principal regression deals with collinearity by using less than the full set of principal components in (7.15). To obtain the principal components estimates, it is assumed that the regressors z_j are arranged in order of decreasing eigenvalues $\lambda_1\geqslant\lambda_2\geqslant\cdots\geqslant\lambda_n>0$. It is further assumed that the last r of these eigenvalues are approximately equal to zero. The principal components corresponding to near zero eigenvalues are removed from the analysis

and the least squares is applied to the remaining components. Using Eqs (7.14), (7.18) and (7.19) the principal component estimator of θ takes the form

$$\tilde{\theta}_{PC}=\sum_{j=1}^{n-r}\frac{1}{\lambda_j}t_j^T X^T Y t_j, \tag{7.20}$$

and the covariance matrix from

$$\mathrm{Cov}\{\tilde{\theta}_{PC}\}=\sum_{j=1}^{n-r}\frac{1}{\lambda_j}t_j t_j^T. \tag{7.21}$$

The principal components regression can improve the accuracy of parameter estimates over the least squares estimates when the data are ill-conditioned.[23]

7.2. Mixed Estimation

The mixed estimation is a procedure which uses prior information to augment the measured data directly instead of through a prior distribution. Mixed estimation includes the usual regression model given by Eq. (7.1) and the additional assumption that a set of prior conditions on θ can be written as

$$a=P\theta+\xi, \tag{7.22}$$

where P is a matrix of known constants and ξ is a vector of random variables with $E\{\xi\}=0$ and $E\{\xi\xi^T\}=S$. After augmenting Y and X in (7.1) the new regression model takes the form

$$\begin{bmatrix} Y \\ a \end{bmatrix}=\begin{bmatrix} X \\ P \end{bmatrix}\theta+\begin{bmatrix} \varepsilon \\ \xi \end{bmatrix} \tag{7.23}$$

By applying least squares to (7.23) the unbiased mixed estimator is[68]

$$\hat{\theta}_{ME}=\left[\frac{1}{\sigma^2}X^T X+P^T S^{-1}P\right]^{-1}\left[\frac{1}{\sigma^2}X^T Y+P^T S^{-1}a\right], \tag{7.24}$$

with the covariance matrix

$$\mathrm{Cov}\{\hat{\theta}_{ME}\}=\left[\frac{1}{\sigma^2}X^T X+P^T S^{-1}P\right]^{-1}. \tag{7.25}$$

In practical application of mixed estimation the relationship given by (7.22) is not exactly known, therefore, the resulting estimator is biased. The S matrix is formed as a diagonal matrix with the elements expressing the uncertainty in prior values.

7.3. Example

The detection of collinearity and the two biased estimation techniques are demonstrated in an example using the longitudinal data of a highly augmented, inherently unstable research aircraft. The longitudinal motion of this aircraft was controlled by three surfaces, canard, flaperon and strake, moved by an automatic control system. The aircraft longitudinal short-period response to a series of commanded pitch doublets is illustrated in Fig. 46. Shown are time histories of stick displacement (the closed-loop input), three longitudinal control surfaces δ_c, δ_f, and δ_s (the open-loop input) and three response variables α, q, and a_z. Inspection of Fig. 46 reveals a very close relationship among all three open-loop inputs, thus indicating strong possibility for data collinearity.

Because of small changes in the input and output variables, the equation for the vertical-force and pitching-moment coefficient were formulated as

$$C_a=C_{a_0}+C_{a_\alpha}\alpha+C_{a_q}\frac{q\bar{c}}{2V}+C_{a_{\delta_c}}\delta_c+C_{a_{\delta_f}}\delta_f+C_{a_{\delta_s}}\delta_s, \tag{7.26}$$

for $a=Z$ or m.

In order to obtain some preliminary feel for the importance of parameters in (7.26), the time histories of individual terms in this equation were computed using the wind-tunnel data for the aerodynamic parameters and measured variables in Fig. 46. The resulting time histories for the vertical force are plotted in Fig. 47. They show that C_Z depends mainly on $C_{Z_\alpha}\alpha$ term, whereas the contribution of the remaining parameters is very small, especially that of $C_{Z_{\delta_e}}$ and C_{Z_q}. It was demonstrated in a similar way that the pitching moment was formed mainly by terms with parameters C_{m_α} and $C_{m_{\delta_c}}$. In addition to collinearity, low sensitivity of several terms in the aerodynamic model equation could also aggravate the estimation procedure and the accuracy of the estimates.

For further detection and assessment of collinearity the singular values of the matrix X and the parameter variance proportions were investigated. The singular values and condition indexes are presented in Table 9. The singular values vary between 0.1 and 12.65, and there is one condition index greater than 50. Table 9 also includes the variance proportions associated with bias terms and the remaining regressors in (7.26). For the

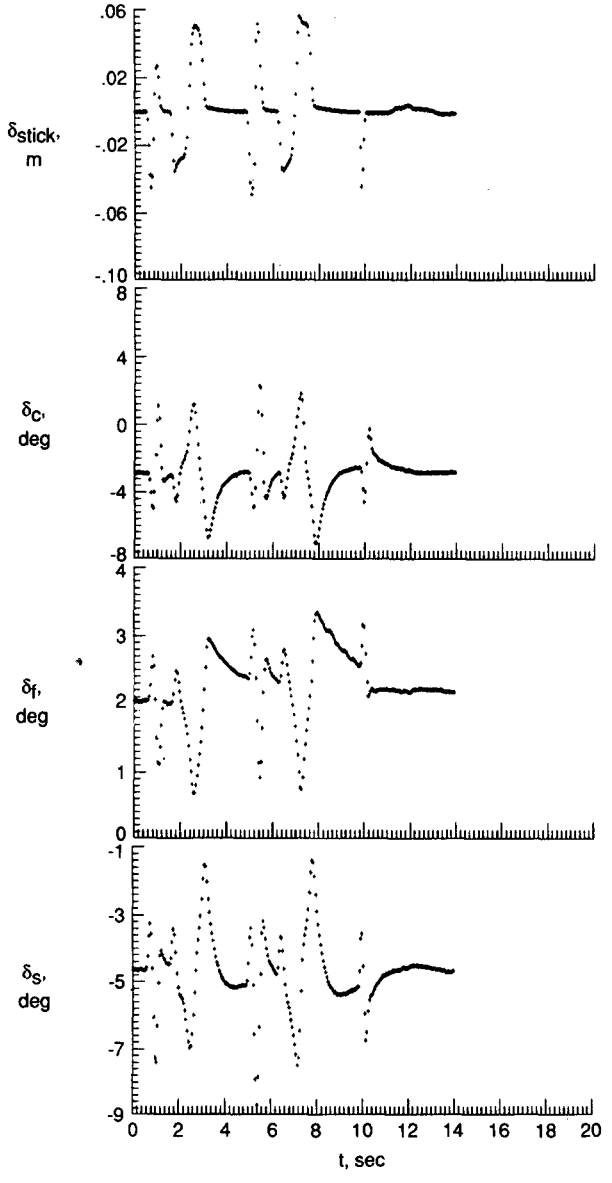

FIG. 46.

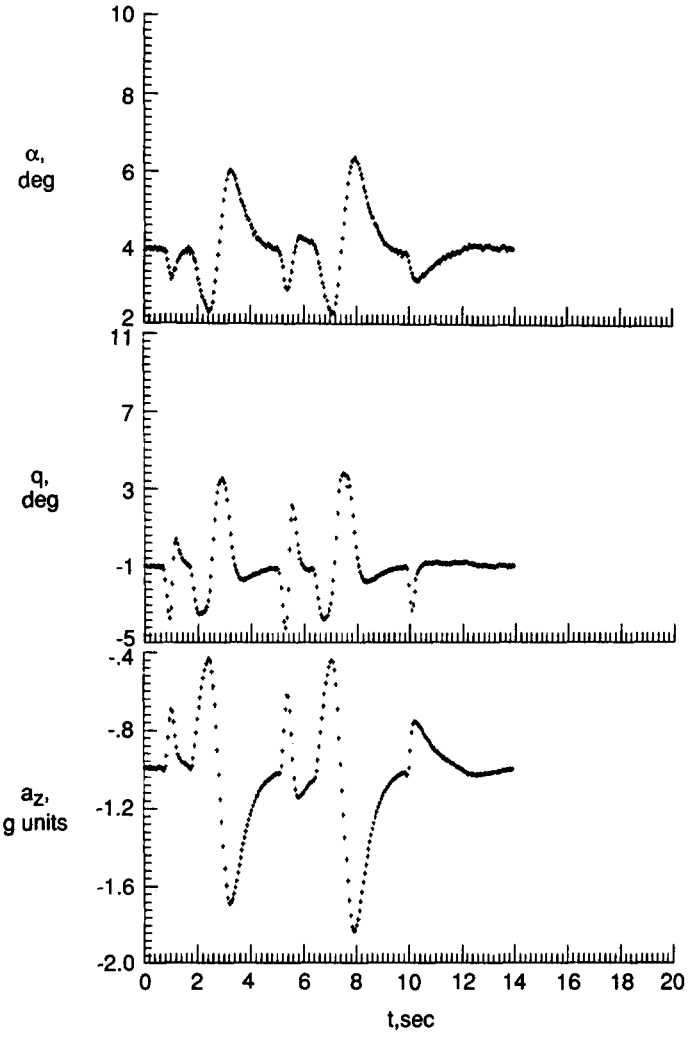

FIG. 46. Measured time histories of input and output time histories in a longitudinal maneuver.

condition index 130 there are, perhaps, three damaging dependencies involving δ_c, δ_s and q. It was therefore decided to set the smallest eigenvalue of X^TX equal to zero, thus reducing the rank of the X^TX matrix by one for the principal components regression. For the mixed estimation the parameters $C_{Z_{\delta_s}}$ and $C_{m_{\delta_s}}$ were set at their wind-tunnel values with the uncertainty estimated from repeated measurements in different testing facilities and for different configurations.

The parameter estimates for vertical-force coefficient from ordinary linear regression, principal components regression and mixed estimation are summarized in Table 10. These estimates are compared with results from wind-tunnel measurements given in the last column of the table. The use of ordinary LS resulted in non-physical values for parameters $C_{Z_{\delta_s}}$ and $C_{Z_{\delta_c}}$ and large negative value for $C_{Z_{\delta_r}}$. The principal components estimates of these parameters are close to the wind-tunnel data and also show smaller standard errors than the LS estimates. Only the estimated value of the less sensitive parameter C_{Z_q} is not correct. The mixed estimation with a prior value $C_{Z_{\delta_s}} = -0.21 \pm 0.02$ improves the parameter values even further. The estimate of C_{Z_α} has the same value for all three techniques which is the result of the very high sensitivity of this parameter. As indicated by the last row in Table 10 the LS fit error, given as the estimated standard error of C_Z, is not significantly degraded by the other two techniques.

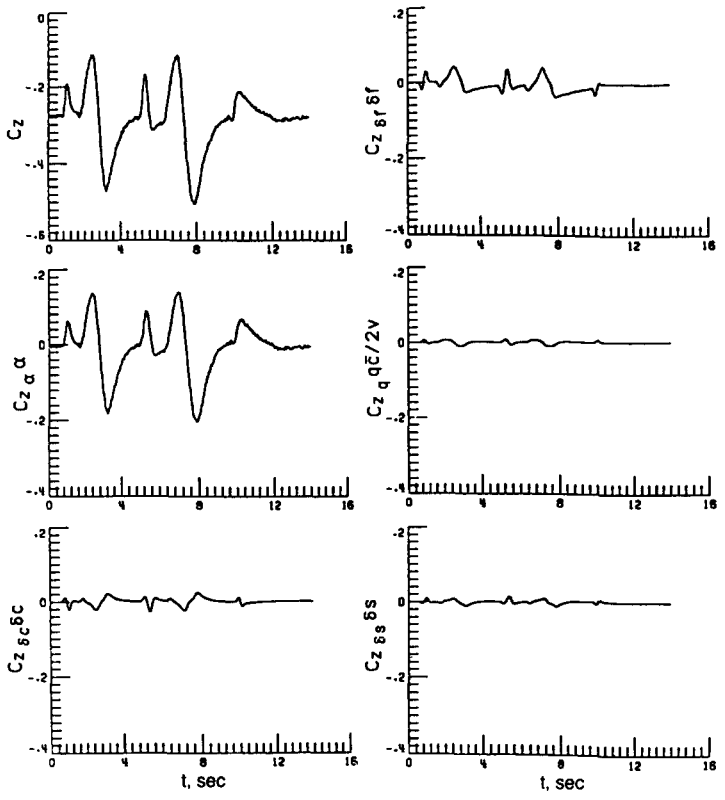

FIG. 47. Time histories of the vertical-force coefficient and its components.

TABLE 9. DETECTION AND ASSESSMENT OF DATA COLLINEARITY

Singular value (μ)	Condition index (η)	Variance proportions					
		1	α	q	δ_s	δ_f	δ_c
12.65	1	1.000	0.000	0.000	0.000	0.000	0.000
1.73	7	0.000	0.023	0.005	0.002	0.006	0.002
1.24	10	0.000	0.006	0.041	0.000	0.092	0.001
0.52	24	0.000	0.036	0.247	0.000	0.509	0.006
0.43	30	0.000	0.929	0.035	0.019	0.046	0.012
0.10	130	0.000	0.006	0.672	0.979	0.347	0.979

8. PARAMETER ESTIMATION IN FREQUENCY DOMAIN

Many of the early approaches to the estimation of aircraft parameters from flight data were based on measurement results presented in frequency rather than time domain.[14, 22, 52] Usually the measured frequency response curves were used because they provided good insight into the physics of the system and reduced data analysis to the use of simple algebra. With the availability of modern digital computers, the frequency domain for aircraft parameter estimation was almost forgotten and the measured data have been mostly analyzed in the time domain. However, the recent attempts to identify an aeroelastic aircraft,[61] aircraft with unsteady aerodynamics,[44, 59] aircraft flying in turbulance,[38] unstable aircraft,[58] and rotorcraft[67] brought attention back to the frequency domain. It was shown in Refs 36 and 38 that it is possible to formulate the existing methods for aircraft parameter estimation equally well in the frequency domain. For this formulation it is necessary to transform the data and the model, and then to form a cost function. The transformation is based on the Fourier integral. The Fourier transform pair associated with

TABLE 10. ESTIMATED AIRCRAFT PARAMETERS FROM FLIGHT DATA USING DIFFERENT REGRESSION TECHNIQUES AND FROM WIND-TUNNEL MEASUREMENTS

Parameter	Estimate of parameter (*) Least squares	Principal components regression	Mixed estimation	Wind-tunnel data
C_{Z_0}	−0.166 (0.0086)	−0.215 (0.0049)	−0.190 (0.0064)	—
C_{Z_α}	−5.23 (0.058)	−5.29 (0.065)	−5.22 (0.058)	−5.50
C_{Z_q}	−26.0 (4.0)	0.024 (0.0035)	−13.0 (2.5)	−14.0
$C_{Z_{\delta e}}$	0.2 (0.10)	−0.30 (0.072)	−0.21 (0.010)	−0.21
$C_{Z_{\delta f}}$	−2.3 (0.16)	−1.4 (0.11)	−1.9 (0.13)	−1.4
$C_{Z_{\delta c}}$	0.02 (0.070)	−0.34 (0.048)	−0.26 (0.020)	−0.19
$s(C_Z)$	0.00328	0.00371	0.00347	—

* Numbers in parantheses are standard errors.

the variable y has the form

$$\tilde{y}(j\omega)=\int_0^\infty y(t)\exp(-j\omega t)\,dt \tag{8.1}$$

$$y(t)=\frac{1}{2\pi}\int_{-\infty}^{\infty}\tilde{y}(j\omega)\exp(j\omega t)\,d\omega \tag{8.2}$$

where $j=\sqrt{-1}$ and ω is the angular frequency. Equation (8.1) can also be written as

$$\tilde{y}(j\omega)=\int_0^\infty y(t)\cos\omega t\,dt-j\int_0^\infty y(t)\sin\omega t\,dt.$$

These two integrals can be evaluated by various numerical methods. For a deterministic signal the Filon integration formula[16] proved to be quite suitable. It approximates the function $y(t)$, rather than the modulated functions $y(t)\cos\omega t$ and $y(t)\sin\omega t$, by a sequence of parabolas. Thus, the accuracy of Filon's formula is insensitive to the values of the parameter ω.

The linear model of an aircraft, specified in Eqs (4.8) and (4.9), is expressed in the frequency domain as

$$\tilde{x}=(j\omega I-A)^{-1}B\tilde{u} \tag{8.3}$$

$$\tilde{y}=C\tilde{x}+D\tilde{u}, \tag{8.4}$$

and the measurement equation as[38]

$$\tilde{z}(n)=\tilde{y}(n)+\tilde{v}(n).$$

The transformed discrete variable $\tilde{z}(n)$ is defined as

$$\tilde{z}(n)\triangleq\tilde{z}(n\Delta\omega),$$

where $\Delta\omega=2\pi/N\Delta t$, $n=N/2,\ldots,0,1,\ldots,N/2-1$, and Δt is the sampling time for $z(t)$. A similar definition holds for $\tilde{y}(n)$ and $\tilde{v}(n)$. The transformed measurement noise $\tilde{v}(n)$ is a random sequence which is assumed to be uncorrelated, orthogonal and gaussian[38] with

$$E\{\tilde{v}(n)\}=0 \quad \text{and} \quad E\{\tilde{v}(n)\tilde{v}^*(n)\}=\frac{S_{vv}}{N}$$

where S_{vv} is the spectral density of $v(t)$ and $\tilde{v}^*(n)$ is the complete conjugate of $\tilde{v}^T(n)$.

The output error cost function is formulated as[38]

$$J = -N \sum_n \tilde{v}^*(n) S_{vv}^{-1} \tilde{v}(n), \tag{8.6}$$

where

$$\tilde{v}(n) = \tilde{y}(n) - T(n, \theta_0)\tilde{u}(n) \tag{8.7}$$

and

$$T(n) = C[jn\Delta\omega - A]^{-1}B + D. \tag{8.8}$$

Optimizing the cost function for parameters in S_{vv} gives

$$\hat{S}_{vv} = \sum_n \tilde{v}(n)\tilde{v}^*(n). \tag{8.9}$$

The estimates of the remaining unknown parameters using the modified Newton–Raphson method are given by Eq. (6.19) as

$$\Delta\hat{\theta} = -M_0^{-1} \left.\frac{\partial J(\theta)}{\partial \theta}\right|_{\theta_0}$$

where

$$M = 2N \operatorname{Re} \sum_\eta H^*(n) \hat{S}_{vv}^{-1} H(n) \tag{8.10}$$

$$\frac{\partial J}{\partial \theta} = -2N \operatorname{Re} \sum_n H^*(n) \hat{S}_{vv}^{-1} \tilde{v}(n), \tag{8.11}$$

and Re denotes the real part of a complex number. The elements of the sensitivity matrix $H(n)$ are equal to $\partial[T(n, \theta_0)\tilde{u}(n)]/\partial\theta_l$.

The frequency domain identification has several features which are distinct from the time domain approach. They are mainly associated with the model representation and estimation algorithm. There is, however, the equivalence in the cost function used in the time and frequency domain as expressed by Parceval's theorem. This theorem postulates the relationship between the squared magnitudes of the Fourier transform pairs. It, therefore, states that the time domain cost function

$$J_{TD} = \sum_i v^T(i) S_{vv}^{-1} v(i)$$

is equal to the frequency domain cost function[38]

$$J_{FD} = \frac{1}{N} \sum_n \tilde{v}^*(n) S_{vv}^{-1} \tilde{v}(n).$$

The equivalence of both approaches is no longer valid if the frequency domain cost function is restricted to a given frequency range. Such a restriction is not necessary, but it is an option which is a strong point in favor of frequency domain analysis with respect to time domain analysis. The selected frequency range of interest was used for example in Ref. 61 where airplane rigid modes were separated from elastic ones. For similar results in the time domain the data must be filtered accordingly.

As it was pointed out above, the early estimation techniques were using measured frequency curves only. In general, however, transformed input–output time histories are preferred in frequency domain parameter estimation. The inaccuracies of frequency response curves computed from transformed inputs and outputs can be quite pronounced for frequencies in which the harmonic content of an input is close to zero.

The transformation of model equations into the frequency domain replaces differentiation and convolution with multiplication. As a result the sensitivity equations in the non-linear estimation algorithm are reduced to uncoupled algebraic expressions. This simplification can be appreciated mainly in cases for which convolution integrals are included in the equations of motion.[59]

The computational differences between the time and frequency domain discussed so far could be viewed as advantages of the frequency domain analysis. There is, however, a substantial disadvantage of the airplane identification in the frequency domain. This

approach is limited, for practical reasons, to only linear equations of motion. The computed time needed for parameter estimation in the frequency domain (transformation of measured data included) is about 50% more than in the time domain.

8.1. Example

The following example compares the longitudinal parameters of a general aviation aircraft estimated in the time and frequency domain.[38] The frequency domain data were obtained from measurement in still and turbulent air. The measured time histories of variables δ_e, α_v, q and a_z are presented in Fig. 48. From these time histories the transformed data and frequency response curves relating all three outputs to the elevator deflection were obtained. The aircraft model was developed from Eqs (4.5) as

$$\begin{bmatrix} j\omega - k_1 C_{Z_\alpha} & -(1 + k_2 C_{Z_q}) \\ -k_3 C_{m_\alpha} & j\omega - k_4 C_{m_q} \end{bmatrix} \begin{bmatrix} \tilde{\alpha} \\ \tilde{q} \end{bmatrix} = \begin{bmatrix} k_1 C_{Z_{\delta e}} \\ k_3 C_{m_{\delta e}} \end{bmatrix} \tilde{\delta}_e \tag{8.12}$$

$$\begin{bmatrix} \tilde{\alpha}_v \\ \tilde{q} \\ \tilde{a}_z \end{bmatrix} = \begin{bmatrix} k_5 & k_6 \\ 0 & 1 \\ \dfrac{V_0}{g} j\omega & -\dfrac{V_0}{g} \end{bmatrix} \begin{bmatrix} \tilde{\alpha} \\ \tilde{q} \end{bmatrix} \tag{8.13}$$

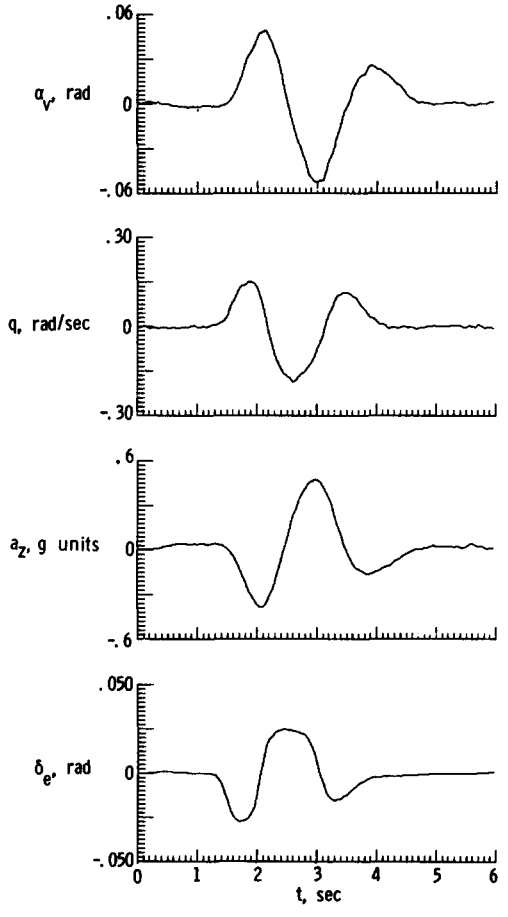

FIG. 48. Time histories of measured output and input time variables. Flight in still air.

with the unknown parameter vector $\theta=[C_{Z_\alpha}, C_{Z_q}, C_{Z_{\delta e}}, C_{m_\alpha}, C_{m_q}, C_{m_{\delta e}}]^T$. In Eq. (8.12)

$$k_1=\frac{V_0 S}{2m}, \qquad k_2=k_1\frac{\bar{c}}{2V_0},$$

$$k_3=\frac{V_0^2 S\bar{c}}{2I_y}, \qquad k_4=k_3\frac{\bar{c}}{2V_0}.$$

In Eq. (8.13) k_5 and k_6 are known constants. The unknown parameters were estimated from transformed input–output data and also from frequency response curves. The corresponding cost functions were

$$J=-N\sum_n[\tilde{y}(n)-T(n,\theta_0)\tilde{u}(n)]^*\hat{S}_{vv}^{-1}[\tilde{y}(n)-T(n,\theta_0)\tilde{u}(n)] \tag{8.6}$$

and

$$J=-N\sum_n[T_E(n)-T(n,\theta_0)]^*\hat{S}_{vv}^{-1}[T_E(n)-T(n)\theta_0], \tag{8.14}$$

respectively. The transfer functions $T(n,\theta_0)$ were computed from Eqs (8.12) and (8.13) for $\omega=\omega_n$ and $\theta=\theta_0$.

The estimated parameters are given in the third and fourth columns of Table 11, and they are compared with the results from the time domain estimation given in the second column of the same table. The three sets of estimates from the same flight agree well. The standard errors of the estimates in the frequency domain are, however, higher than those in the time domain. This could be due to truncation of the transformed data and additional inaccuracies in measured frequency response curves caused by taking the ratios of two complex numbers. The transformed vertical acceleration and that computed, are plotted in Fig. 49. The measured and computed frequency response curves $\tilde{a}_z/\tilde{\delta}_e(j\omega)$ are plotted in Fig. 50. It can be seen from this figure that the measured frequency response curve is inaccurate around the frequency 6.4 rad/s as a result of the low harmonic contents of the input at the same frequency.

The response of the airplane to turbulence was measured in two flights (designated as Run 1 and Run 2 in Table 11) with minimum pilot interference. From the time histories of the measured response variables the spectral density of the vertical gust velocity, S_{w_g},

TABLE 11. ESTIMATED AIRCRAFT PARAMETERS FROM MEASUREMENTS IN TURBULENT AND STILL AIR

	Estimate of parameter (*)				
	still air			turbulent air	
				Frequency domain (§)	
Parameter	Time domain	Frequency domain (†)	Frequency domain (‡)	Run 1	Run 2
C_{Z_α}	−5.67 (0.057)	−5.70 (0.086)	−5.6 (0.19)	−4.2 (0.47)	−4.4 (0.61)
C_{Z_q}	−10.3 (0.92)	−8.0 (3.5)	−4.0 (4.7)	−9.0 (8.0)	−4.0 (10)
$C_{Z_{\delta e}}$	−0.6 (0.16)	−0.6 (0.28)	−0.6 (0.33)	—	—
C'_{m_α}	−0.783 (0.0074)	−0.81 (0.011)	−0.82 (0.027)	−0.9 (0.16)	−0.9 (0.17)
C'_{m_q}	−26.6 (0.40)	−28.6 (0.50)	−26.3 (0.92)	−24.0 (4.3)	−26.0 (4.6)
$C_{m_{\dot{\alpha}}}$	—	—	—	‖ −7.0 (2.6)	‖ −5.0 (2.5)
$C'_{m_{\delta e}}$	−3.21 (0.030)	−3.54 (0.040)	−3.38 (0.060)	—	—

* Numbers in parentheses are Cramer–Rao lower bounds on standard error.
† Transformed input and output time histories.
‡ Frequency response curves.
§ Spectral and cross-spectral densities.
‖ Computed from estimated C_{m_q} and $C^0_{m_q}$.

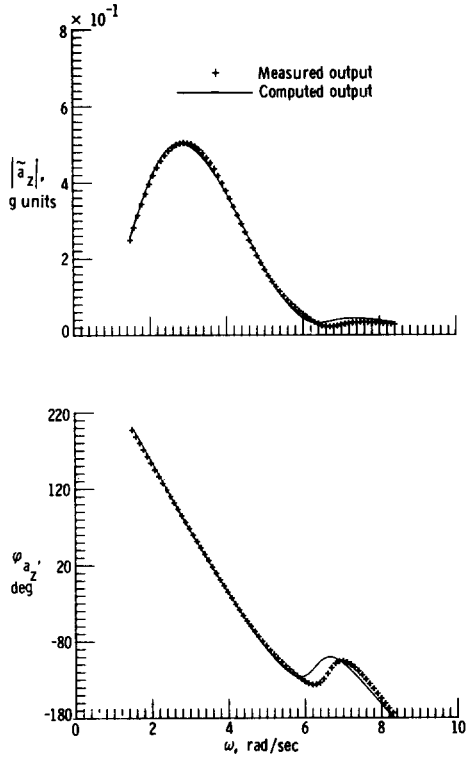

FIG. 49. Measured transformed time history of vertical acceleration and that computed using estimated parameters.

and the cross-spectral densities $S_{w_g q}$ and $S_{w_g a_z}$ were computed. They are related by the mathematical model resulting from Eqs (8.12) and (8.13) as

$$\begin{bmatrix} j\omega - k_1 C_{Z_\alpha} & -(1+k_2 C_{Z_q}) \\ -k_3 C_{m_\alpha} & j\omega - k_4 C_{m_q} \end{bmatrix} \begin{bmatrix} S_{w_g \alpha} \\ S_{w_g q} \end{bmatrix} = \begin{bmatrix} \dfrac{k_1}{V_0} C_{Z_\alpha} \\ \dfrac{k_3}{V_0} C_{m_\alpha} - j\omega \dfrac{k_4}{V_0} C^0_{m_q} \end{bmatrix} S_{w_g w_g} \tag{8.15}$$

$$\begin{bmatrix} S_{w_g q} \\ S_{w_g a_z} \end{bmatrix} = \begin{bmatrix} 0 & 1 \\ \dfrac{V_0}{g} j\omega & -\dfrac{V_0}{g} \end{bmatrix} \begin{bmatrix} S_{w_g \alpha} \\ S_{w_g q} \end{bmatrix} \tag{8.16}$$

where

$$C^0_{m_q} = C'_{m_q} - C_{m_{\dot{\alpha}}}(1 + k_2 C_{Z_q}).$$

The estimates of unknown parameters are given in the last two columns of Table 11. From the estimates C_{m_q} and $C^0_{m_q}$ the value of $C_{m_{\dot{\alpha}}}$ was computed and included among the unknown parameters. The agreement between the results for both runs is very good. The parameters also agree with the estimates from the still air measurement with the exception of the parameter C_{Z_α}. This parameter has smaller value than expected, probably because of some modeling errors in Eqs (8.15) and (8.16). One of the measured cross-spectral densities from Run 1 and the density computed by using the estimated parameters are plotted in Fig. 51. The estimates from turbulent-air measurement demonstrated a possibility for using these data also for airplane stability and control parameter estimation. The example also shows that for a certain model formulation, the derivative of pitching-moment coefficient with respect to the rate of change in angle-of-attack can be estimated explicitly.

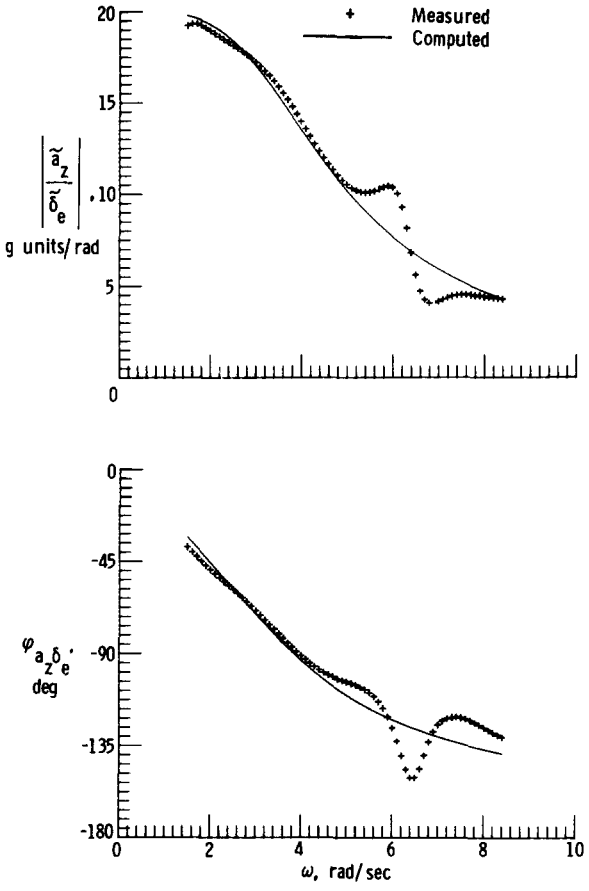

FIG. 50. Measured frequency response curve and that computed using estimated parameters.

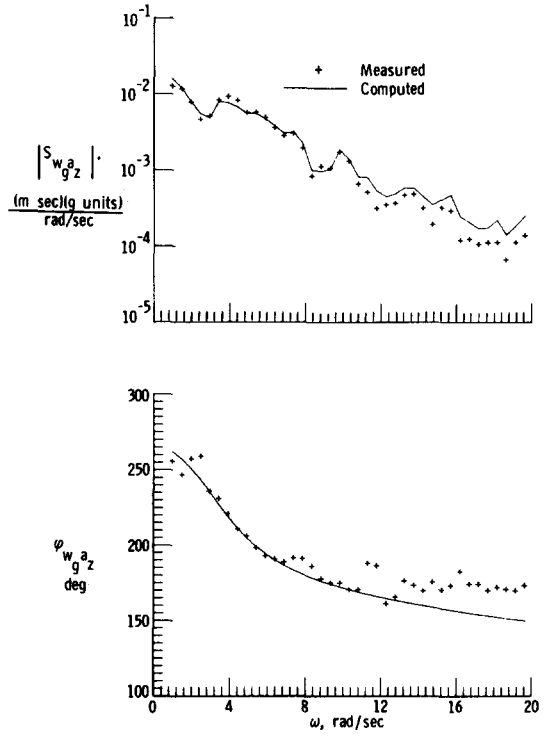

FIG. 51. Measured cross-spectral density and that computed using estimated parameters.

9. CONCLUDING REMARKS

Presently used methods for estimation of aircraft aerodynamic parameters from flight data were outlined. The simplest method is using data from steady or quasi-steady flights from which static longitudinal parameters can be determined. A general approach to the problem, however, is based on system identification methodology applied to data from various transient maneuvers. This methodology includes four basic steps; design of an experiment, measured data compatibility check, model structure determination and parameters estimation, and model verification. The main purpose of the first step is the selection of suitable input signals for the excitation of aircraft maneuvers. The second step compares measured and predicted aircraft responses, and estimates bias errors in the measured data.

The main part of aircraft identification procedure includes techniques for the determination of a structure for aerodynamic model equations and the estimation of corresponding parameters in these equations. At present two techniques are mainly used, the equation error method and the maximum likelihood method. The equation error method is essentially a linear regression using the ordinary least squares. Modified forms of linear regression can be used for model structure determination. One of them, the stepwise regression, found its application to aeronautical problems. These problems are often related to parameter estimation from high angle-of-attack maneuvers where, in general, the aerodynamic model is not known. Other modifications of the ordinary linear regression resulted in a relatively new group of biased estimation techniques. These techniques proved useful in parameter estimation where some of the measured data are nearly linearly related. This situation very often occurs in measured data from augmented aircraft where various control surfaces are deflected by a control system commanded by the pilot. Two of these biased techniques, the principal components regression and mixed estimation, are described together with tools for the detection and assessment of near-linear dependency in the data.

The maximum likelihood method finds a set of parameters for a known model by applying the maximum likelihood principle to measured data. This method is very general with the estimates having favorable statistical properties. The maximum likelihood technique is also being applied in the frequency domain with some advantages in parameter estimation of an aeroelastic aircraft, aircraft with unsteady aerodynamics, aircraft flying in turbulence and inherently unstable aircraft.

Despite the advances in aircraft identification methodology, new challenges are still facing aeronautical researchers and analysts. Most of these are associated with the identification of high performance aircraft of advanced configurations which are able to perform rapid maneuvers extending well into the high angle-of-attack regimes. Modeling of these aircraft might include aeroelastic effects and highly non-linear, perhaps unsteady aerodynamics. To deal with these problems aircraft identification will require better instrumentation for data measurements, carefully designed experiments and new advances in estimation and model verification techniques.

ACKNOWLEDGEMENTS

The author would like to thank Mr James G. Batterson from NASA Langley Research Center for reading the manuscript, and for his advice and discussion during the preparation of the paper.

REFERENCES

1. ANON. (1955) Royal Aeronautical Society Data Sheet, Aircraft, 08.01.01 and 08.01.02.
2. ANON. (1975) Methods for Aircraft State and Parameter Identification. AGARD-CP-172.
3. ANON. (1979) Parameter Identification. AGARD-LS-104.
4. ALLEN, D. M. (1971) The Prediction Sum of Squares as a Criterion for Selecting Predictor Variables. Techn. Rep. No. 23, University of Kentucky, Lexington, USA.
5. ÅSTRÖM, J. J. and EYKHOFF, P. (1979) System identification—a survey, *Automatica* **7 (2)**, 123–162.

6. BACH, R. E. and WINGROVE, R. C. (1985) Application of state estimation in aircraft flight data analysis, *J. Aircr.* **22 (7)**, 547–554.
7. BATTERSON, J. G. (1981) Estimation of airplane stability and control derivatives from large amplitude longitudinal maneuvers. NASA TM-83185.
8. BATTERSON, J. G. (1986) STEP and SETPSPL—Computer programs for aerodynamic model structure determination and parameter estimation. NASA TM-86410.
9. BATTERSON, J. G. and KLEIN, V. (1987) Partitioning of flight data for aerodynamic modeling of aircraft at high angles of attack. AIAA Paper No. 87-2621-CP.
10. BELSLEY, D. B., KUHN, E. and WELSH, R. E. (1980) *Regression diagnostics, Identifying Influential Data and Sources of Collinearity*, John Wiley and Sons, Inc.
11. BREEMAN, J. H. *et al.* (1979) Aspect of flight test instrumentation in parameter identification, AGARD-LS-104, pp. 4–1 to 4–22.
12. BRYSON, R. E., JR. and HO, Y. CH. (1969) *Applied Optimal Control*, Ginn and Company.
13. CANNADAY, R. L. and SUIT, W. T. (1977) Effects of control inputs on the estimation of stability and control parameters of a light airplane. NASA TP-1043.
14. DONEGAN, J. J., ROBINSON, S. W., JR. and GATES, O. B., JR. (1955) Determination of lateral-stability derivatives and transfer-function coefficients from frequency–response data for lateral motion. NACA Rep. 1225.
15. DRAPER, N. R. and SMITH, H. (1966) *Applied Regression Analysis*, John Wiley and Sons, Inc.
16. FILON, L. N. G. (1928/29) On a quadrature formula for trigonometric integrals, *Proc. R. Soc. Edinburgh*, **49**, 38–47.
17. FISHER, R. A. (1950) *Contributions to Mathematical Statistics*, John Wiley and Sons, Inc.
18. GATES, S. B. and LYON, H. M. (1944) A continuation of longitudinal stability and control analysis. Part I—General theory. R&M No. 2027.
19. GATES, S. B. and LYON, H. M. (1944) A continuation of longitudinal stability and control analysis. Part II—Interpretation of flight test. R&M No. 2028.
20. GERLACH, O. H. (1970) The determination of stability derivatives and performance characteristics from dynamic maneuvers. SAE Paper No. 700236.
21. GREENBERG, H. (1949) Determination of stability derivatives from flight data, *J. Aero. Sci.* **16 (1)**, 62.
22. GREENBERG, H. (1951) A survey methods for determining stability parameters of an airplane from dynamic flight measurements. NACA TN-2340.
23. GUNST, R. F. and MASON, R. L. (1977) Biased estimation regression; an evaluation using mean squared error, *J. Am. Stat. Assoc.* **72**, 616–628.
24. GUPTA, N. K. and HALL, W. E., JR. (1975) Input design for identification of aircraft stability and control derivative. NASA CR-2493.
25. HALL, W. E., JR., GUPTA, N. K. and SMITH, R. G. (1974) Identification of aircraft stability and control coefficients for the high angle-of-attack regime. Systems Control. Inc., Techn. Rep. No. 2.
26. HESS, R. A. (1986) Effects of wing modification on an aircraft's aerodynamic parameters as determined from flight data. NASA TM-87591.
27. HSIA, T. C. (1977) *System Identification*, pp. 20–22, D.C. Heath and Co.
28. ILIFF, K. W. and TAYLOR, L. W., JR. (1972) Determination of stability derivatives from flight data using a Newton–Raphson minimization technique. NASA TN D-6579.
29. ILIFF, K. W. (1977) Maximum likelihood estimation of lift and drag from dynamic aircraft maneuvers, *J. Aircr.* **14 (12)**, 1175–1181.
30. ILIFF, K. W. (1978) Identification and stochastic control of an aircraft flying in turbulence, *J. Guid. Control*, **1 (2)**, 101–108.
31. JATEGAONKAR, R. V. and PLAETSCHKE, E. (1987) Maximum likelihood estimation of parameters in linear systems with process and measurement noise. DFVLR Rep. FB 87-20.
32. JATEGAONKAR, R. V. and PLAETSCHKE, E. (1987) A FORTRAN program for maximum likelihood estimation of parameters in linear systems with process and measurement noise—User's manual. DFVLR-IB 111-87/21.
33. JONKERS, H. L. (1976) Application of the Kalman filter to flight path reconstruction from flight data including estimation of instrumental bias error corrections. Ph.D. Dissertation, Delft Univ. of Techn., Delft, The Netherlands.
34. KLEIN, V. and SCHIESS, J. R. (1977) Compatibility check of measured aircraft responses using kinematic equations and extended Kalman filter. NASA TN D-8514.
35. KLEIN, V. (1977) Determination of aerodynamic derivatives from steady-state measurement of an aircraft. AIAA Paper No. 77-1123.
36. KLEIN, V. (1978) Aircraft parameter estimation in the frequency domain. AIAA Paper No. 78-1344.
37. KLEIN, V. (1979) Determination of stability and control parameters of a light airplane from flight data using two estimation methods. NASA TP-1306.
38. KLEIN, V. (1980) Maximum likelihood method for estimating airplane stability and control parameters from flight data in frequency domain. NASA TP-1637.
39. KLEIN, V., BATTERSON, J. G. and MURPHY, P. C. (1981) Determination of airplane model structure from flight data by using modified stepwise regression. NASA TP-1916.
40. KLEIN, V. and BATTERSON, J. G. (1983) Determination of airplane model structure from flight data using splines and stepwise regression. NASA TP-2126.
41. KLEIN, V. and BATTERSON, J. G. (1986) Aerodynamic parameters estimated from flight and wind tunnel data, *J. Aircr.* **23 (4)**, 306–312.
42. KLEIN, V. and MAYO, M. H. (1986) Estimation of aerodynamic parameters from flight data of a high incidence research model. ICAS Paper No. 86-5.5.2.
43. KLEIN, V. and MORGAN, D. R. (1987) Estimation of bias errors in measured airplane responses using maximum likelihood method. NASA TM-89059.
44. KOCKA, V. (1970) Downwash at unsteady motion of a small aeroplane at low airspeeds—flight investigation and analysis. ICAS Paper No. 70-25.

45. MAINE, R. E. and ILIFF, K. W. (1979) Maximum likelihood estimation of translational acceleration derivatives from flight data, *J. Aircr.* **16 (10)**, 674–679.
46. MAINE, R. E. and ILIFF, K. W. (1980) User's manual for MMLE 3. A general FORTRAN program for maximum likelihood parameter estimation. NASA TP-1563.
47. MAINE, R. E. and ILIFF, K. W. (1981) The theory and practice of estimating the accuracy of dynamic flight-determined coefficients. NASA RP-1077.
48. MAINE, R. E. (1980) Programmer's manual for MMLE 3. A general FORTRAN program for maximum likelihood parameter estimation. NASA TP-1690.
49. MAINE, R. E. and ILIFF, K. W. (1985) Identification of dynamic system; theory and formulation. NASA RP-1138.
50. MAINE, R. E. and ILIFF, K. W. (1986) Application of parameter estimation to aircraft stability and control. The output–error approach. NASA RP-1168.
51. MEHRA, R. K. (1970) Maximum Likelihood Identification of Aircraft Parameters. 1970 JACC, Atlanta, Georgia, USA.
52. MILLIKEN, W. F., JR. (1947) Progress in dynamic stability and control research, *J. Aero. Sci.* **14 (9)**, 493–519.
53. MONTGOMERY, D. C. and PECK, E. A. (1982) *Introduction to Linear Regression Analysis*, John Wiley and Sons, Inc.
54. MULDER, J. A. (1986) Design and evaluation of dynamic flight test maneuvers. Ph.D. Dissertation, Delft Univ. of Techn., Delft, The Netherlands.
55. MURPHY, P. C. (1986) A methodology for airplane parameter estimation and confidence interval determination in nonlinear estimation problems. NASA RP-1153.
56. MURPHY, P. C. (1987) Efficient computation of parameter confidence intervals. AIAA Paper No. 87-2624-CP.
57. PLAETSCHKE, E. and SCHULTZ, G. (1979) Practical input signal design in parameter identification, AGARD-LS-104, pp. 3–1 to 3–19.
58. QUEEN, E. M. (1987) Analysis of flight data of a highly augmented, unstable aircraft using frequency domain. M.S. Thesis, The George Washington University, Washington, D.C., USA.
59. QUEIJO, M. J., WELLS, W. R. and KESKAR, D. A. (1978) The influence of unsteady aerodynamics on extracted aircraft parameters. AIAA Paper No. 78-1343.
60. RANEY, D. (1987) Analysis of lateral stability for X-29 drop model using system identification methodology. AIAA Paper No. 87-2625-CP.
61. RINASKI, E. G., ANDRISANI, D., II and WEINGARTEN, N. C. (1978) Identification of the stability parameters of an aeroelastic airplane. AIAA Paper No. 78-1328.
62. ROSS, A. J. and FOSTER, G. W. (1976) Fortran programs for the determination of aerodynamic derivatives from transient longitudinal or lateral responses of aircraft. RAE ARC CP-1344.
63. SCHUMAKER, L. L. (1981) *Spline Functions: Basic Theory*, John Wiley and Sons, Inc.
64. SHINBROT, M. (1951) A least squares curve fitting method with applications to the calculation of stability coefficients from transient-response data. NACA TN-2341.
65. STEPHNER, D. E. and MEHRA, R. K. (1973) Maximum likelihood identification and optimal input design for identifying aircraft stability and control derivatives. NASA CR-2200.
66. TAYLOR, L. W., JR, ILIFF, K. W. and POWERS, B. G. (1969) A comparison of Newton–Raphson and other methods for determining stability derivatives from flight data. AIAA Paper No. 69-315.
67. TISCHLER, M. B. and KALETKA, J. (1986) Modeling XV-15 tilt-rotor aircraft dynamics by frequency and time domain identification techniques, In: *AGARD Flight Mech. Panel Symp. on Rotorcraft Design and Operation*, Amsterdam, Paper No. 9.
68. TOUTENBURG, H. (1982) *Prior Information in Linear Models*, John Wiley and Sons, Inc.
69. WINGROVE, R. C. (1973) Quasi-linearization technique for estimating aircraft states from flight data, *J. Aircr.* **10 (5)**, 303–307.
70. WOERKOM VAN, K. (1981) Design and evaluation of an instrumentation system for measurements in non-steady symmetrical flight conditions with the Hawker Hunter MK VII. Delft Univ. of Techn., Delft, The Netherlands, Rep. LR-308.
71. ZADEH, L. A. (1962) From circuit theory to system theory, In: *Proceedings of the IRE*, pp. 856–965.